Effect of temperature on growth, expression of growth regulating genes, and skeletal development of juvenile European plaice (*Pleuronectes platessa*)

Master of Science in Biology – Aquaculture Biology

by Malin Østervold

Department of Biological Sciences

University of Bergen

August 2023

Professor Albert Kjartan Dagbjartarson Imsland – Department of Biological Sciences – University of Bergen

Dr. Birgitta Norberg – Reproduction and Developmental Biology – Institute of Marine Research

Acknowledgements

I want to extend my gratitude to all the knowledgeable people who have helped me finish my master's. Thanks to you, I have delivered a product I am proud of.

First, I would like to thank my supervisors at University of Bergen; Albert Kjartan Dagbjartarson Imsland, and at the Institute of Marine Research; Birgitta Norberg, for giving me the opportunity to work on this project, being there for me, answering questions, guiding me, motivating me, and helping me reach my goals. You have devoted the school year and the summer to my work and helped me complete a thesis I can proudly show off.

Ozlem Yilmaz, thank you very much for always welcoming me into your office when I come slightly confused and need clarification. The way you convey knowledge has been essential to my understanding of gene expression. You have a work ethic and passion that I will strive for in my career. Cristos Siapazis, thank you for helping me optimizing the qPCR, you have been a great lab partner and have done a precise and good work.

Per Gunnar Fjelldal, I greatly appreciate your always being available on teams. All my questions about deformities in fish have been answered - whether they are complicated or easy questions or if it is something I have discovered that I found interesting and would like to discuss with someone. You have been a great help, and I am so grateful.

Anne-Hege Straume, thank you for helping me with isolating RNA and making cDNA at the Institute of Marine Research in Bergen. It was fun to learn how to operate a the Biomek 4000 automated workstation.

Margareth Møgster, Ragnfrid Mangor-Jensen, and Anders Mangor-Jensen, thank you for building up a biological material of excellent quality and for helping me with all the samplings. You have always greeted me with a good mood, knowledge, and practical solutions. We were a great team!

I would also like to thank my family, partner, and friends for always being there for me - even if they don't always fully understand what I'm talking about, they listen and motivate me to keep going. You have helped me balance the school stress with fun experiences, making these

five years at the University of Bergen perfect. I would also like to give an extra big thank you to my two favorite fellow students, Tora Lervik and Guro Berle Lokshall. You have made the study period fantastic.

Malin Østervold

Abstract

The flatfish European plaice (*Pleuronectes platessa*) is a demersal, temperate species and a candidate for marine aquaculture. At present, little is known about optimal rearing conditions for plaice. Accordingly, to better understand growth and the mechanisms involved in growth regulation, juvenile plaice (initial mean weight ±SEM, 10.4 ± 0.1 g) were reared in triplicate rearing tanks at three different temperature regimes, ambient (average of 8.6°C), 12° C and 16°C, for 100 days and the interaction between growth, expression of growth regulating genes, and skeletal development studied to determine optimal rearing conditions for juvenile plaice.

Juvenile plaice grew fastest at 16°C, followed by the 12°C group, and lastly, the 8.6°C, which had significantly lower mean weight compared to the two other groups. The condition factor was inversely correlated to increased temperatures and was highest in the 8.6°C group.

At the start of the experiment, 11% of the fish had skeletal deformities. Increasing temperature resulted in higher frequency and severity of malformations, and the 8.6°C group had 8% less skeletal deformities at the end of the experiment compared to the 12°C and the 16°C groups. The 12°C and 16°C groups had similar number of deformed fish in the tanks, however, the 16°C had more severe deformities.

Temperature affected gene transcript levels of *ghr*, *igf-1*, and *igf-1r* differently. The temperature did not affect *ghr* transcript levels in the liver and muscle tissue. Hepatic *igf-1* transcript levels increased with increased growth and temperature. Muscular *igf-1r* transcript levels increased with increasing temperature in each sampling, indicating that *igf-1r* corresponded with muscular growth.

Based on present findings, a rearing temperature of 12°C is recommended for on-growing of juvenile plaice.

Table of content

1 Introduction

1.1 Norwegian aquaculture

Norway has been a pioneer in the salmon farming industry since the beginning of the 1970s, and after a decade, the industry became commercial (Afewerki et al., 2022). The elongated coast with hundreds of fjords and the optimal water temperature has given good predictions of a low-cost production cycle. As the production volume rose, Norway started to export Atlantic salmon (*Salmo salar*) globally, and today 95% of the production is exported to more than 100 countries (Afewerki et al., 2022). In Norway, the farming of Atlantic halibut (*Hippoglossus hippoglossus*), Atlantic cod (*Gadus morhua*), and sugar kelp (*Saccharina latissima*) is evolving, and the interest in developing new species within the aquaculture industry is steadily increasing (Akvaplan Niva, 2019).

The family Pleuronectidae, the right-eye flounders, represents the best-studied group of flatfishes within the order Pleuronectiformes (Vinnikov et al., 2018). Many members of this family have a high commercial value and a relatively large size (Vinnikov et al., 2018). A greater quantity of the representatives in the list of "new marine species for aquaculture" belongs to the order *Pleuronectiformes*, and flatfish cultivation in the Atlantic region is increasing (Akvaplan Niva, 2019). In 2017, the aquaculture of Atlantic halibut, a species of the family *Plauronectidae*, was profitable and rearing of Atlantic Halibut now provides a high-quality product with good market value and has a constantly increasing survival rate (Hamre et al., 2020). The halibut has been challenging to breed (Hamre et al., 2020), but increased experience and knowledge have shown great progress. Another flatfish that has reached the commercialization phase is turbot (*Scophthalmus maximus L.)* (Akvaplan Niva, 2019). A key role of the aquaculture industry is to adapt its knowledge and technology to farm other aquaculture species (Afewerki et al., 2022), ensuring global development.

1.2 European plaice as a model species

1.2.1 Biology

The European plaice (*Pleuronectes platessa*) is a demersal fish (Kendler et al., 2023) characterized by its brown or grey-brown surface with irregularly distributed bright red, orange, or orange-yellow spots. The skin is smooth with small scales, and the underside is white. The right eye has migrated during metamorphosis; hence, the name righteye flounder. The species has a straight lateral line slightly curved above the pectoral fin. Compared to the more elongated halibut, the plaice is more oval-shaped. In nature, the detected max length is 100.0 cm (Nielsen, 1986), while the standard length is around 40.0 cm (Bauchot, 1987). It has been reported that the plaice can live up to 50 years and reach a weight of 7 kg (Muus & Dahlström, 1974). According to Albert et al. (1998), female plaice grow faster than male plaice.

1.2.2 Distribution

The European plaice is distributed along the Atlantic coast of Europe from Portugal to the eastern regions of the Barents Sea and around Iceland and the Faroe Islands (Jakobsen & Ozhigin, 2011). The species prefer temperatures between 2-15°C (Bristow, 1992). In warmer years, the distribution area expands compared to colder years, and the growth rate increases in warmer periods compared to colder (Jakobsen & Ozhigin, 2011). However, a high biomass stock can result in intraspecific competition, reducing the growth rate, even with an elevated temperature (Jakobsen & Ozhigin, 2011). In the study by Kuipers (1977) juvenile European plaice was captured at temperatures from 7.6 to 23.0°C on a tidal flat in the Wadden sea. The plaice inhabits seabeds at a depth range of 0-200m, although they are usually at a depth range of 10-50m (Muus & Nielsen, 1999). Although there is a distributional change with age, the species seeks deeper grounds as it ages (Albert et al., 1998). The plaice inhabits seabeds covered with sand or muddy areas (Kendler et al., 2023). Before winter approaches, the European plaice seeks muddy, or muddy and sandy, seabeds at depths of 160-250 m with temperatures of 1.6 - 4.0°C (Jakobsen & Ozhigin, 2011). The plaice has an upper lethal temperature limit of 26-27°C (Fonds et al., 1992).

1.2.3 Migration and reproduction

The European plaice is a stationary species for long periods but can migrate far when they go to spawn (Muus & Nielsen, 1999). The species matures between the length of 24-62 cm (Jakobsen & Ozhigin, 2011) and spawns in batches (Murua & Saborido-Rey, 2003) when the

temperature is around 6°C (Nielsen, 1986). Males mature at a younger age than females, and within the spawning population, there usually are four males per female (Jakobsen & Ozhigin, 2011). In the North Sea, climate change is leading to elevated sea temperatures; therefore, the European plaice is migrating further north (Kendler et al., 2023). In the Barents Sea, the plaice migrate from the Murmansk coast to the east during summer due to foraging areas and migrates back during autumn for wintering (Jakobsen & Ozhigin, 2011). In the fjords north of Lofoten, mature plaice tended to migrate towards Lofoten to spawn, and along the rest of the Norwegian coast, the mature plaice can migrate into fjords to spawn (Albert et al., 1998). Spawning areas in fjords, where there are beaches, also tend to be nursery areas (Albert et al., 1998). In the north part of the Norwegian Sea, the spawning season is from December to May, while in the south of the Norwegian Sea and the Northern Sea, the spawning season is from January to March (Kendler et al., 2023). After spawning, the pelagic eggs drift into shallow areas, where the eggs hatch and the larvae settle and metamorphose into juveniles (Jakobsen & Ozhigin, 2011). After metamorphosis, the plaice inhabits bays and inlets (Jakobsen & Ozhigin, 2011). Juvenile plaice perform tidal migrations connected to feeding (Kuipers, 1973).

1.2.4 Foraging

The European plaice has a seasonal cycle in feeding and growth; during summer months, it feeds, grows, and restore energy reserves (Dawson & Grimm, 1980). It uses energy reserves during winter for metabolism and gonad maturation (Dawson & Grimm, 1980). The European plaice is active in shallow water at night, while in the daytime, it is buried in the sand (Muus & Nielsen, 1999). The juvenile plaice migrate to intertidal zones (Kuipers, 1973, Gibson, 1999), as they are great for foraging on small invertebrates before returning to the sand-covered seabed to hide. It feeds on polychaetes, thin-shelled mollusks, small worms, crustaceans, small fish, and parts of other small benthic invertebrates (Kuipers, 1977, De Vlas, 1979; Eriksen et al., 2020), and as they grow, they choose larger prays (De Vlas, 1979).

1.2.5 Fisheries

The European plaice is an important flatfish for fisheries in Europe. The North Sea is a capture hotspot (Kendler et al., 2023), and the stock is within safe biological limits (Viðarsson et al., 2022). In 2020, 67 698 mt of plaice were captured in fisheries (FAO, 2022). The leading suppliers, in decreasing order, are the Netherlands, Denmark, the Russian Federation, and the United Kingdom, which caught approximately 75% of the total catch (FAO, 2022). The fishing gear used to catch plaice is bottom and beam trawl (Viðarsson et al., 2022), and it is possible to

fish plaice from depths of 25-200 m, but most of the catch is above 100 m depth (Albert et al., 1998). The greater part of the fish caught is between the length range of 30-50 cm (Albert et al., 1998). Today, Norwegian fisheries of European plaice are low, but due to increased migration north of the North Sea, it can be expected an increased capture in the future (Kendler et al., 2023).

1.3 European plaice as an aquaculture species

1.3.1 **The need for new species in aquaculture**

Capture fisheries in marine waters represent the primary source of seafood production (FAO, 2022). However, since the 1980s, aquaculture has been the leading driver of increased seafood production globally (FAO, 2022). A further expansion of the aquaculture industry is essential to generate jobs and meet the demand for food for a growing world population. In 2020, the global aquaculture production was 87.5 million tonnes, including 33.1 million tonnes from marine aquaculture and 54.4 million tonnes from inland aquaculture, excluding algae (FAO, 2022). Seafood contains high-quality protein, essential fatty acids, and micronutrients, which benefit human health (Kendler et al., 2023). The aquaculture industry needs new species to be more resilient to environmental change challenges and to increase total production.

1.3.2 **Suitability**

The European plaice is one of the species represented in the list of new marine species for aquaculture in a recent report commissioned by the Norwegian Ministries of Fisheries (Akvaplan Niva, 2019). The species was given high sustainability marks and as European plaice is expected to tolerate high densities, area usage will be low. In addition, closed facilities provide good control over the spread of infection, genetic influence, and the release of pharmaceuticals and environmental substances (Akvaplan Niva, 2019). In Norway, the plaice is sold as a whole fish and has a low commercial value (Tsoukalas et al., 2022). Consumers desire convenient seafood products and farming a thicker filet packed in modified atmosphere packaging (MAP) has the potential for increased value (Tsoukalas et al., 2022). The large-sized European plaices caught are high-value products sold to restaurants (Viðarsson et al., 2022). The countries that import the most European plaice are Italy, Germany, UK, and Belgium (Viðarsson et al., 2022). In 2018, landing prices were between 2.15–2.59 €/kg, depending on size, in the Netherlands, Denmark, and the UK, and the export raw material prices from the

Netherlands were 4.31 €/kg and for processed fillets 2.06 €/kg live weight (Viðarsson et al., 2022).

1.3.3 **Previous experiences with plaice aquaculture**

From 1936-1939, Rollefsen (1940) researched the effect of artificial hatching of European plaice fry and European flounder-European plaice hybrid fry and seawater fish farming. Rollefsen pointed to the fry phase as the flounder's life cycle bottleneck. He justified this by saying that the transparent and camouflaged egg, which is self-sufficient with a nutritious yolk sac, will not attract predators in the egg phase. The same applies to flounder that have settled; they bury themselves in the sand, feed near the bottom, and will most likely not be discovered by predators. On the other hand, the fry phase consists of movement in an open body of water and nutritional needs, and this can lead to the fry being discovered by predators in their search for food. He concluded that if farmers managed to develop a feed for the fry, which could be mass-produced and arouse the fry's appetite, European plaice could be reared past the critical fry phase. In 1938 and 1939, he successfully managed to feed *Artemia* nauplii to the fry and determined that the rearing of flounder fry now depended on the availability and price of *Artemia* eggs and facilities with access to seawater (Rollefsen, 1940).

What Rollefsen saw as challenges with aquaculture farming in 1940 is now the standard procedure for producing flounder fry, but since the early trials in the 1940s reasearh to develop plaice for aquaculture has been dormant. However, in 2020, the first time the Institute of Marine Research (IMR) in Austevoll farmed European plaice, the methods for fry production in cod and halibut formed the basis for larval and juvenile plaice farming in land-based facilities. Newly hatched plaice larvae depend on a live-feed phase before weaning to formulated feed. As for Atlantic cod and Atlantic halibut, enriched *Artemia* amplifies the growth and survival of fish larvae (Choi et al., 2021). As a result, the European plaice farmed at the IMR had an exceptionally high survival among the juveniles with good fish welfare. In February 2023, the biggest fish in the stock has reached 1.7 kg at three years old (Margareth Møgster, IMR, Austevoll, pers. comm.). The fish have mainly been fed a flavored lumpfish feed (Clean transfer) but not a growth feed, and was reared at a water temperature of 8°C. However, in February, the feed was replaced with a halibut feed on-growth feed (Hippo Express 203 25kg, 3 mm, Skretting, Averøy, Norway), hoping to induce faster growth. The mortality has been low; only eight out of 490 individuals have died, and five out of the eight died from February to March 2022 and were matured males, and the last three can be related to a sampling where some fish were lost on the floor (Margareth Møgster, IMR, Austevoll, pers. comm.).

1.4 Temperature effect on growth

1.4.1 **Growth-temperature relationship**

Temperature is an environmental factor that affects fish growth (Sheridan, 2021) and can limit growth by influencing the metabolic rate (Beuvard et al., 2022). The majority of fish species cannot regulate body temperature; therefore, the body temperature is determined by the surrounding water temperature (Little et al., 2020; Volkoff & Rønnestad, 2020). In ectotherms, the body temperature affects physiological processes such as muscle and cardiovascular function, metabolism, reproduction, survival, and growth (Little et al., 2020; Li et al., 2021). The aerobic scope (AS), which is the difference between the maximum aerobic metabolic rate (MMR) and standard metabolic rate (SMR), will reach its maximum at the temperature optimum for aerobic scope and decreases at supra-optimal temperatures (Beuvard et al., 2022). Common to many fish species is that the aerobic scope temperature optimum corresponds with the growth temperature optimum (Beuvard et al., 2022). Fish generally have an optimal temperature for growth and survival (Imsland et al., 1996; Li et al., 2021). The temperature-growth relationship has been studied in many fish species, such as Arctic charr (*Salvelinus alpinus*) (Beuvard et al., 2022), sea bass (*Dicentrarchus labrax*) (Claireaux & Lagardère, 1999), the Chinese cold-water fish *Schizothorax prenanti* (Li et al., 2021), and Northern pike (*Esox lucius*) (Fey & Greszkiewicz, 2021). However, the optimal temperature can change with age and size, and juveniles prefer higher temperatures than adults (Imsland et al., 1996; Li et al., 2021).

Growth is essential in deciding if a species will be economically suitable for commercial aquaculture. Therefore, the temperature will be crucial in finding the optimal conditions for rearing a new species (Burel et al., 1996). For example, the study by Burel et al. (1996) reported that the growth in juvenile turbot is depressed below 8°C and above 23°C. The optimal growth temperature for juvenile in the weight range 25-75 g turbot is between 16-19°C (Imsland et al., 1996), which is in the upper natural temperature range (Burel et al., 1996). After reaching a weight of 100 g the optimum temperature for growth decreased to 13-16°C, i. e. ontogenetic shift (Imsland et al., 1996). The European plaice has a natural temperature range of 2-15°C depending on life stage (Bristow, 1992). However, the optimal temperature range for growth in plaice juveniles is at present unknown and defining it will be necessary for establishing optimal rearing conditions for this species.

1.4.2 **Mechanisms involved in growth regulation**

The growth hormone (Gh)–Insuline-like growth factor (Igf) system regulates muscle growth in vertebrates (Fuentes et al., 2013; Sheridan, 2021). The pituitary gland produces growth hormone, and Gh is regulated by hypothalamic hormones (Triantaphyllopoulos et al., 2019; Canosa & Bertucci, 2020; Sheridan, 2021). Hypothalamic release of growth hormone releasing hormone (GhRH) stimulates the production of Gh (Figure 1a) while the release of somatostatin inhibits the production of Gh (Figure 1g) (Janssen, 2020). The Gh affects teleosts' skeletal and soft tissue development by controlling hypertrophy (Fuentes et al., 2013; Triantaphyllopoulos et al., 2019) and hyperplasia (Fuentes et al., 2013). In addition, it contributes to gonadal development, osmoregulation, metabolism, foraging and social behavior, and immune function (Reinecke et al., 2005; Canosa & Bertucci, 2020). The Gh enters the bloodstream (Figure 1c), is transported to the target organ, and binds to growth hormone receptors (GhR) present on cellular surfaces on target tissue (Janssen, 2020) (Figure 1d). GhR expression is the highest in the liver and muscle (Zhao et al., 2015), but it is also expressed in other tissues such as brain, kidney, stomach, and gonad (Zhao et al, 2015). Gh plays a crucial role in stimulating the liver to synthesize insulin-like growth factor 1 (Igf-1) (Figure 1e) (Triantaphyllopoulos et al., 2019), and the liver is the primary source of circulating Igf-1 (cIgf-1) (Lara-Diaz et al., 2017). cIgf-1 is mainly bound to Igf binding proteins (IgfBPs), which help to bind cIgf-1 to Igf-1 receptors (Igf-1r) (Figure 1f) (Lara-Diaz et al., 2017). In fish, muscle has a higher abundance of Igf-1 receptors than insulin receptors, indicating the importance of Igf-1 in regulation of muscle function (Reinecke et al., 2005). Like Gh, Igf-1 will also promote the growth and development of bones and tissues throughout the body (Triantaphyllopoulos et al., 2019). Igf-I produced in the liver inhibits Gh release via negative feedback on the pituitary and stimulation of somatostatin release in the hypothalamus (Janssen, 2020). In many fish species, tissue levels of Igf-I mRNA positively correlate with body growth rate (Reinecke et al., 2005). An elevated temperature causes an upregulated expression of Gh regardless of feed condition libitum (Triantaphyllopoulos et al., 2019; Li et al., 2021). On the other hand, elevated temperatures will only increase Igf-1 expression if the fish is fed ad libitum (Triantaphyllopoulos et al., 2019). In addition, environmental factors, such as water temperature, can affect the gene expression of *Gh* and *igf*-1 in cold-blooded fish (Triantaphyllopoulos et al., 2019).

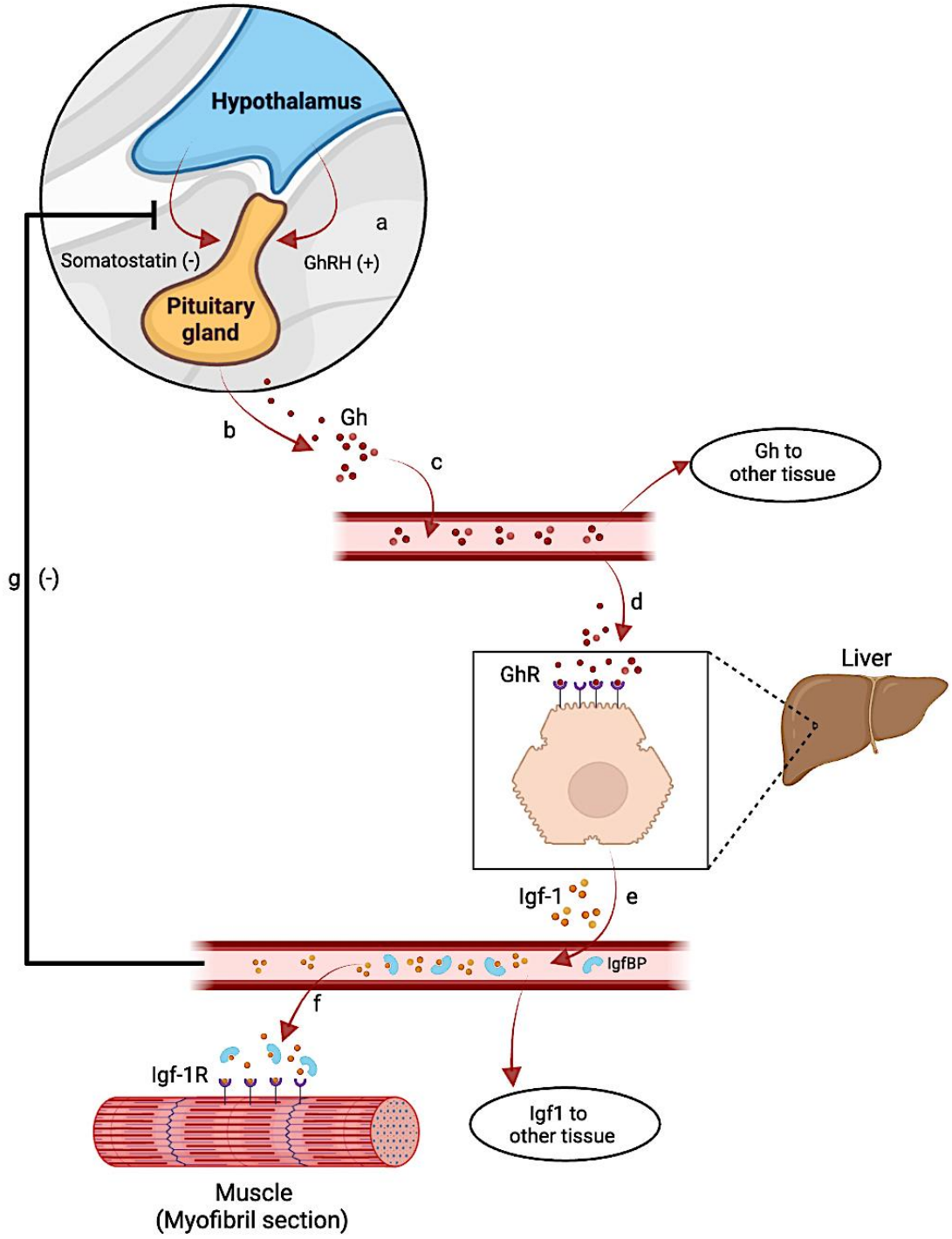

Figure 1 Mechanisms involved in growth regulation (a – growth hormone releasing hormone (GhRH) secretion from the hypothalamus, b – growth hormone (Gh) secretion from the pituitary gland, c – Gh entering the bloodstream, d - Gh binding to growth hormone receptors (GhR) in the liver, e – insulin like-growth factor 1 (Igf-1) produced and released from the liver and binding to Igf binding proteins (IgfBP), f – Igf1 binding to Igf-1 receptors (Igf-1r), g – Igf-1 establishing a negative feedback mechanism maintaining balanced GH/IGF levels by hypothalamus somatostatin release.) The arrows show the direction of the signal, and + and – indicate induction or reduction, respectively.

1.4.3 **Vertebrae deformities**

Skeletal deformities can be found in many teleost species (Witten et al., 2009) and are observed in both wild and farmed fish (Boglione et al., 2001; 2003; Fjelldal et al., 2009b; 2020). However, deformities are more frequently observed in farmed fish (Boglione et al., 2003; Fjelldal et al., 2020). Deformities that affect the vertebrae column are of interest as it is the structure that transmits muscular force to swimming activity (Webb, 1984; Wardle et al., 1995), and may compromise the swimming ability (Basaran et al., 2007). In addition, malformations of the vertebral column are of economic importance as they can lead to altered body shapes, behavioral changes connected to swimming and feeding, stress, and high susceptibility to disease (Eissa et al., 2021). Deformities of vertebrae in an early life stage can lead to reduced growth and survival (Han et al., 2020). Malformations are often caused by an interaction between several factors that can induce deformities in the vertebrae column, such as infections, vitamin C deficiency, elevated egg incubation temperatures, incorrect photoperiod, and water quality (Lall & Lewis., 2007; Witten et al., 2009; Fjelldal et al., 2012).

The teleost vertebral column is composed of vertebrae separated by notochordal tissue (Nordvik et al., 2005). Common spinal abnormalities are lordosis, kyphosis, and scoliosis, as well as vertebrae fusion, compression, and modified shape (Han et al., 2020). X-ray is an established tool for screening many individuals (Witten et al., 2009). Unfavorable temperatures have a negative effect on the development of the vertebrae column, as shown in studies on Japanese flounder (*Paralichthys olivaceus*) (Lü et al., 2015), golden pompano (*Trachinotus ovatus*) (Han et al., 2020), and Atlantic salmon (Fraser et al., 2019). Fish reared under high temperatures may have an increased growth rate but also show a greater abundance of deformities than those reared in lower temperatures (Grini et al., 2011; Árnason et al., 2019; Eissa et al., 2021). Deformed fish has low economic value and must be removed from production, and is therefore not cost-efficient (Han et al., 2020). Deformities in the vertebral column of European plaice has not yet been studied. By defining the optimum temperature conditions of European plaice, the occurrence of deformities can be reduced, production costs will be reduced, and it will lead to increased fish welfare and growth.

1.5 Aim of the study

The European plaice has been proposed as a possible new farming species and as a model species for studies of development and physiology in flatfish. Initial trials with fry production

have yielded good results, with high survival through early life stages and up to mature fish. This thesis aims to define optimal growth conditions for juvenile European plaice at different water temperatures; ambient temperature (range 7.9-9.5°C), 12°C, and 16°C. In addition, the aim was to increase knowledge about gene expression of growth and skeletal development in plaice at different water temperatures. This was done by looking at gene expression of relevant growth factors in fish and taking X-ray examinations of skeletal growth and development in the various experimental groups. Based on those aims, the null hypothesis of this study was:

H_0 Temperature does not affect growth, gene expression of growth-regulating factors, and deformities in juvenile plaice.

The alterative hypotheses of this study were as follows:

H_1 Temperature influences growth in juvenile plaice.

$H_{1.1}$ Juvenile plaice grow better at 16 degrees than at 8 degrees.

$H_{1.2}$ Juvenile plaice grow better at 12 degrees than at 8 degrees.

$H_{1.3}$ Juvenile plaice grow better at 16 degrees than at 12 degrees.

H_2 Gene expression of growth-regulating factors in juvenile plaice is influenced by temperature.

$H_{2.1}$ Juvenile plaice have higher gene expression of growth-regulating factors at 16 degrees than 8 degrees.

$H_{2.2}$ Juvenile plaice have higher gene expression of growth-regulating factors at 12 degrees than 8 degrees.

$H_{2.3}$ Juvenile plaice have higher gene expression of growth-regulating factors at 16 degrees than 12 degrees.

H_3 Temperature influences skeletal development in juvenile plaice.

$H_{3.1}$ Juvenile plaice have more deformities at 16 degrees than at 8 degrees.

$H_{3.2}$ Juvenile plaice have more deformities at 12 degrees than at 8 degrees.

$H_{3.3}$ Juvenile plaice have more deformities at 16 degrees than at 12 degrees.

2 Material and methods

2.1 European plaice juvenile production

2.1.1 **Broodstock, stripping, and fertilization of eggs**

Local fishermen caught sexually mature European plaice with fishing nets at the beginning of March 2022. The fish were transported to indoor rearing facilities, 2x2m rearing tanks with a depth of 60 cm, at the Institute of Marine Research (IMR), Austevoll. Among the ten fish captured, two females and three males were used for reproduction (Figure 2). The fish were inspected daily for gonadal growth, and at the presumed time of ovulation, the ripe individual fish was placed on a wet towel for stripping of eggs and sperm. Once successfully spawned, the fish was marked with an external floy tag. The eggs were retained in a plastic measuring cup, and the sperm were sampled with a pipette directly from the genital pore. Sea water contamination was restricted to avoid uncontrolled activation (Cosson et al., 2008). Shortly after stripping, approximately 0.5 ml sperm was mixed into 2-3 liters of seawater before adding 0.95-1.15 dl of eggs (Table 1). The eggs were gently mixed into the water/sperm solution and left stagnant for 10 minutes. The average fertilization rate between the groups was 87% (Table 1). The procedure for fertilization was identical to the methodology for Atlantic halibut (Norberg et al., 1991). In the experiment, four groups were implemented: group 2, group 3, group 4, and group 5.

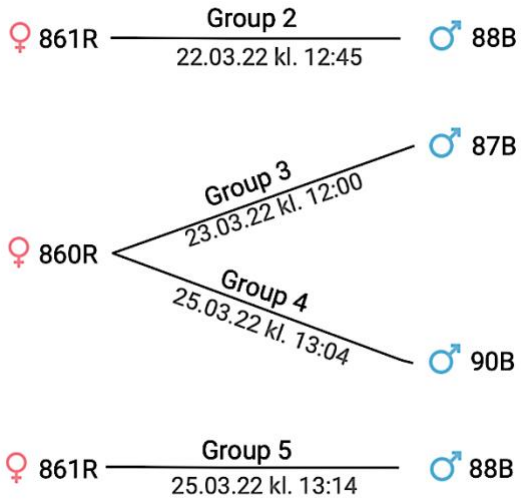

Figure 2 Overview of European plaice parental generation crosses and time of fertilization. The experiment consisted of these four groups: group 2, group 3, group 4, and group 5.

2.1.2 **Hatchery and incubation**

The fertilized egg batches were kept separately in 70 L incubators for embryonic development and subsequent larval hatching. The incubators were cylindrical with conic bottoms and supplied with a surface water inlet, and a central outlet through a standpipe covered with a 750 μm planktonic screen. The egg batches were kept at 6.2 – 6.6°C beyond the time of hatching at day 20 after fertilization (DPF) with 24 h light. The flow was 4 L/min, and a gentle air bubbling was used to secure necessary convection. For each incubator, the date, day number, mortality, and temperature were registered daily. Dead eggs were removed by shutting the water inlet and air bubbling for some minutes before draining the bottom water. Live eggs floated right below the surface and were not affected. All the eggs hatched 20 days post fertilization (DPF) and were carefully transferred to start-feeding rearing tanks.

Table 1 Egg quality of European plaice.

Date	Group	Volume of eggs (dl)	Amount of sperm (ml)	Total of dead eggs (ml)	Fertilization (%)
22.03.22	2	1.15	0.5	17	96
23.03.22	3	1.1	0.5	49	62
25.03.22	4	1.0	0.5	60	91
25.03.22	5	0.95	0.5	8	98

2.1.3 **Start-feeding and weaning**

The fiberglass rearing tanks used in the experiment were 1.5 m in diameter and 1.0 m in height (Figure 3). To ensure good water circulation, the tanks were arranged with a water supply pipe, positioned sidewards, with a flowmeter (Figure 3a). The drain was placed at the center of the rearing tank (Figure 3b), and the water level was determined by an external overflow pipe (Figure 3c). A plug with 5 mm holes, covered by a 750 μm planktonic screen, was placed in the drain, and a rotating windshield wiper (Figure 3d) was put over the plug to keep the tank bottom clean. In addition, aeration (Figure 3e) was arranged at the bottom around the center tube to ensure homogeneity. A lamp with two Philips master TL-D De Luxe 18W-965 fluorescent tubes was mounted 65 cm over the rearing tanks (Figure 3f), and the light condition was 16L:8D. Lastly, an automatic feeding machine was placed above the periphery of the tank (Figure 3g).

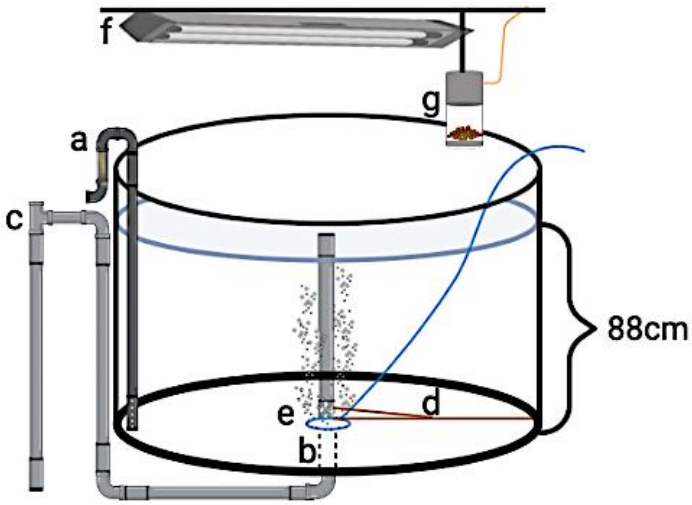

Figure 3 Start-feeding rearing tank (a – water supply pipe with flowmeter, b - drain, c- external overflow pipe, d – a rotating windshield wiper placed on a plug with 5 mm holes, e - aeration, f – lamp with two Philips master TL-D De Luxe 18W-965 fluorescent tubes, g –automatic feeding machine). Before the European plaice settled, the water level was 88 cm. After settling, the water level was reduced to 38 cm. The rotating windshield wiper was exchanged for a center tube in the experimental tanks, and the aeration was removed.

On the first day, the tank was prepared with 1.5 million *Artemia*, enriched with LARVIVA Multigrain (Biomar, France), in the water before the newly hatched larvae were transferred. The larvae were fed enriched Artemia 40 days after first feeding (AFF) by adding Artemia to the tank thrice daily to a concentration of 1000 Artemia/liter. In addition to Artemia, 80 grams of suspended clay was added to each tank to increase turbidity and enhance food ingestion. The meal size was adjusted according to appetite based on the remaining Artemia in the tank, and the amount of clay was adjusted visually according to turbidity. After the transfer, the larvae were temperature acclimated from 8°C ambient temperature to 12°C gradually over four days and kept at this temperature until the experiment started. Simultaneously, the flow was gradually increased from 1 L/min to 4 L/min. After that, the flow was increased according to the oxygen needed for the fish biomass and to ensure enough flow for self-cleaning in the tank. When the fish started settling, the water level was reduced from 88 cm to approximately 38 cm and kept at this level throughout the experiment. The rearing tanks were flushed for 3-4 sec daily until the experiment started. The fish were 45 days post first-feeding (dpff) when weaning from live feed to formulated feed started; 30 mL B2 Otohime (PTAqua, Dublin, Ireland) was put into the automatic feeding machine in addition to hand feeding. After the weaning period, the aeration was removed. Two tanks were initially used for the first feeding of the larvae, but

during the next three months, the fish were gradually distributed into more tanks, finally, nine tanks, to compensate for growth.

2.1.4 **Sorting and counting the fish**

The sorting station consisted of a tub filled with seawater, a tap counter, two buckets with seawater, and a bucket with deadly anesthesia (Finquel vet, 100g/L, MSD, Boxmeer, Netherlands). The tub filled with seawater was changed regularly. The two buckets with seawater separated the fish going back and those not returning to the experiment. The fish from each of the nine tanks were visually sorted based on size and exterior. Fish below 5.0 cm were transferred to a rearing tank not included in the experiment. To sort the fish from the nine rearing tanks, an extra clean rearing tank, with fresh 12°C seawater, was used. The fish from one of the nine rearing tanks was transferred to the sorting station, and fish over 5.0 cm were counted and transferred back into the experimental tank. The tank emptied of fish was cleaned with Jif Cream cleaner (Orkla, Oslo, Norway) and a mop before it was filled with fresh 12°C seawater, ready to start sorting the following fish tank. This procedure was repeated until all the fish were sorted. After sorting, the total number of fish was 2448 remained. The experiment material consisted of 2407 fish: 250 fish per tank, 145 for initial x-ray samples, and 12 fish for initial muscle and liver sampling. Therefore, 41 fish were transferred to another rearing tank and not included in the experiment.

2.1.5 **Distribution of fish**

The produced juvenile plaice (n=2407) from all nine sorted tanks were randomly distributed into three empty holding tanks. From these tanks, 145 fish were put into a lethal concentration of anesthetic (Finquel vet, 100g/l, MSD, Boxmeer, Netherlands) for later X-ray analysis: 48 from the first and the second tank and 49 from the third tank. Next, 160 fish were distributed into each of the nine rearing tanks by distributing ten fish from each of the three tanks at the time. The weight and length of 450 randomly collected fish from the three holding tanks were measured and distributed to each rearing tank. Lastly, 40 fish were supplemented to each of the nine rearing tanks to give 250 fish per tank. The remaining 12 fish were put into deadly anesthetic (Finquel vet, 100g/l, MSD, Boxmeer, Netherlands) and were used as the baseline for muscle and liver gene expression.

2.2 Experimental design

2.2.1 **Ethical statement**

Austevoll Research Station is approved as a laboratory animal department (Appendix 2) and all handling of the experimental fish was carried out according to the station's ethical guidelines. The fish did not undergo treatment that is outside of what the fish can experience naturally, and thus there was no need to apply for separate Norwegian Food Safety Authority (FOTS) approval for the experiment.

2.2.2 **Rearing conditions**

Juvenile European Plaice (n=2250) were distributed to nine rearing tanks, 250 fish per tank, and kept in triplicate at three different temperatures: ambient water temperature (an average of 8.6°C), 12°C, and 16°C. In addition, 145 fish were killed by overdose anesthesia (Finquel vet, 100g/l, MSD, Boxmeer, Netherlands) and frozen for later x-ray analysis. If the fish were handled, they were transferred with a hand net and buckets with seawater. On the 5 of September 2022, the three different experimental temperature regimes were initiated. The experiment was terminated 13 December 2022.

The rearing tanks used in the experiment were the same as the start-feeding rearing tanks. Except, the rotating windshield wiper had been exchanged for a center tube with 5 mm holes at the bottom of the center tube. When the experiment was initiated, the flow was at 9 L/min. Oxygen saturation and temperature were measured daily in the drain with a YSI ProSolo handheld digital water quality meter, and the flow was increased if the oxygen level went below 80%. The tanks were flushed every day for 10 seconds.

2.2.3 **Water quality and temperature measurement**

Seawater was pumped through a 2 km long intake pipe, which was 710 mm in diameter, from a depth of 160 m with a submersible pump. The water quality from 160 m depth includes stable parameters, such as temperature, oxygen, and salinity, and few to no bacteria and viruses (Mohd Nani, 2016). The water was then pumped through a 120 m^3 sand filter with aeration, which filters particles down to 20 µm, before it was sent to pressure booster pumps. The aeration process was used to increase dissolved oxygen concentration and decrease the concentration of CO_2 and H_2S in the water (Roy et al., 2021). From there, the water passed through an Arkal filter. Raw water went straight to aeration before arriving at the rearing tanks. In contrast, the

tempered water, 12°C and 16°C, was first transferred through a heat pump before it was aerated and distributed into the rearing tanks (Jorunn Sanden, IMR, Austevoll, pers comm).

To measure the temperature, a Web Sensor - four channels remote thermometer hygrometer (Comet system s.r.o, Roznov pod Radhostem, Czech Republic) was used. The temperature logger measured the temperature, in Celsius degrees, in one rearing tank from each temperature every 15 minutes around the clock. In addition, hand measurements were taken once a day with a YSI ProSolo handheld digital water quality meter.

2.2.4 **Feed and feed size**

In addition to hand-feeding, a Sterner MicroFeeder (Sterner FishTech AS, Ski, Norway) was used to feed the fish. In the morning, the fish were fed to satiation, and then the feed container was filled with 150 mL of feed twice a day, at 08:00 and 14:00. The automatic feeding machine fed the fish between 07:30 and 20:30 and was active for 30 min every two hours. During the 30 minutes, the fish were fed for 0,8 sec every minute. The fish were fed Skretting Clean Assist CF 1.0 mm when the experiment was initiated. There was a transition phase when changing between two feed types, where the two feeds were mixed 50/50 for 3-4 days (Table 2).

Table 2 Feed and feed size

Date	Feed	The mix of feed (ml/day)	Weight of feed (g)
05.09.22	Clean Assist CF (Skretting AS, Averøy, Norway) 1.0 mm	300	100mL = 55g
12.09.22	Skretting Clean Assist CF 1.0 mm and Skretting Clean Transfer 1.5 mm	150+150	
15.09.22	Clean Transfer (Skretting AS, Averøy, Norway) 1.5 mm	300	100mL = 61g
21.10.22	Skretting Clean Transfer 1.5 mm and Skretting Clean Transfer 2.0 mm	150+150	
25.10.22	Clean Transfer (Skretting AS, Averøy, Norway) 2.0 mm	300	100mL = 68 g
27.10.22	Trofi Aglonorse Berggylt (Tromsø Fiskeindustri AS, Tromsø, Norway) 1.2-1.6 mm	300	100mL = 62g
01.11.22	Trofi Aglonorse 1.4-1.6 mm and Skretting clean transfer 2 mm	150+150	

24.11.22	Trofi Aglonorse (Tromsø Fiskeindustri AS, Tromsø, Norway) 1.4-1.6 mm	300	100mL = 59 g

2.3 Weight and length measurements of European plaice

In the first sampling, the fork length (to nearest 0.1 cm) and weight (to nearest 0.1 g) of 50 fish from each rearing tank were measured alive with a laminated 1-millimeter graph paper and a Sartorius CP323P balance (Sartorius AG, Göttingen, Germany). The fish were transferred from the rearing tanks to a tub with seawater, measured, and transferred back to the rearing tank. In the second and third sampling, the length of 50 fish per rearing tank was measured similarly, but the weighing scale was exchanged for a Stainless-steel platform scale KERN FES 17K0.1IPM (Kern & Sohn GmbH, Balingen, Germany).

At the end of the experiment, a Scaleit W30S15 Stainless Check Scale (Scale it AS, China) was used to weigh (g) the fish. To measure the length (mm), a ruler was printed on a sheet, the ratio of the ruler corresponded with the printed ruler, and the sheet was laminated. After sampling the fish needed for RNA extraction, x-ray, and parasites, the remaining fish of every rearing tank were weighed and measured. One rearing tank was measured at the time. The fish were measured and weighed alive before they were transferred to an empty rearing tank. This cycle was repeated until the fish length and weight were measured. The weight and length of the fish was used to find the condition factor by following formula (Froese, 2006):

$$Condition\ factor = \frac{weight(g)*100}{(length(mm)*0.1)^3}$$

2.4 Detection and relative quantification of gene expression of growth-regulating factors

PCR (Polymerase Chain Reaction) is a laboratory technique to amplify small amounts of DNA or RNA sequences to produce millions of copies (Lafrance et al, 2021). qPCR (quantitative Polymerase Chain Reaction), also known as Real-Time PCR, is a variation of PCR that allows for the detection and quantification of DNA in real-time during the amplification process (Purohit et al., 2016). The main difference between PCR and qPCR is that PCR only amplifies the target DNA, while qPCR amplifies and quantifies the amount of amplified DNA. In qPCR,

the amount of DNA being amplified is measured during each amplification cycle, allowing for the estimation of how much DNA was present in the initial sample (Valasek & Repa, 2005). Furthermore, qPCR allows for detecting the amplification process earlier than regular PCR, which can help detect low concentrations of DNA or RNA (Purohit et al., 2016). As a result, qPCR is widely used for quantifying gene expression, identifying viral and bacterial infections, and genotyping (Valasek & Repa, 2005). Therefore, conventional PCR was used to detect and prove the functionality of growth-regulating factor genes such as the *ghr*, *igf-1* and *igf-1r* and TaqMan based qPCR was utilized to quantify their mRNA levels as indicator of their active expression in the muscle of fish from each treatment group. Four fish per replicate tank of each temperature treatment group were sampled for liver and muscle tissue as target tissues in this study as indicated below.

2.4.1. **Collection of biological samples**

Liver and muscle were sampled three times during the experiment: at the beginning, middle, and end of the experiment. In the first sampling, a part of the liver and muscle from 12 fish were retrieved, giving 24 samples. In the following samplings, a liver and muscle sample from 12 fish from each temperature were retrieved, equaling 72 samples per sampling.

2.4.2 **Preparing the tubes for the liver and muscle sampling**

Two freestanding 2 mL microtubes with caps and graduations were used for each fish sampled. In addition, 1 mL of Sigma Life Science RNAlater^{TM} (LabMal, Puchong, Malaysia) was pipetted into each micro tube and stored in a refrigerator before sampling. The microtubes were marked with species, the date of sampling, and the material retrieved from the fish. The cap was also marked with the material that was retrieved.

2.4.3 **Dissection of the fish and retrieving of liver and muscle sample**

The fish were transferred from the rearing tank to a bucket of lethal anesthetic (Finquel vet, 100g/L, MSD, Boxmeer, Netherlands) with a hand net. Weight and length measurements of the fish were collected. An incision with a scalpel was made across the brain to ensure the fish was dead before the dissection. The liver was sampled by cutting open the abdominal cavity with a sterile scalpel and forceps and retrieving a piece of the liver (Appendix 3). The liver sample was put into the prepared microtube. The muscle was sampled by cutting a section dorsally, removing the skin, retrieving a sample, and putting it into a microtube with 1 mL RNAlater (Appendix 3). The scalpel and forceps used in the dissection were cleaned between each fish sampled, first in distilled water, then 70% ethanol, and wiped with paper towels. Regularly the

equipment was sprayed with RNaseZap. The liver and muscle samples were stored for one day in the fridge before freezing the sample at –20°C.

2.4.4 **RNA Isolation**

The RNA was isolated using the Promega simplyRNA kit (Promega corporation, Madison, USA) and the Biomek 4000 automated workstation (Beckman Coulter INC, California, USA). First, the samples were homogenized. A mix of 1-thioglycerol and homogenization solution (HS) at a 1:50 ratio was made. Two sample boxes were used, with room for 96 homogenization tubes in each box. 400 µl of the HS mix was pipetted into the homogenization tubes (Appendix 4). Next, the tissue was cut to an appropriate size and added to the HS. Lastly, the caps were put back on the homogenization tubes, and the sample box was put into the shaker, SPEX™ SamplePrep 1600 MiniG™ (SPEX SamplePrep, USA), at max speed for 3 minutes. The homogenized samples were stored at -80°C. On the day of RNA isolation, the homogenized samples had to be transferred manually, in the same order as the sample box (Appendix 4), to a deep well plate. The sample box was transferred from the -80°C freezer and immersed in cold water to thaw. A multichannel (8) pipette with 300 µl tips pipetted 200 µl lysate to the 96 deep well plate for later use during the RNA isolation.

The RNA was isolated using the Biomek 4000 automated workstation (Beckman Coulter INC, California, USA). An excel workbook was used to calculate the volumes of the solutions needed for the RNA isolation according to the number of samples. The Biomek 4000 automated workstation operates with columns. Therefore, the sample number was rounded up to a complete column of samples, eight samples per column. Two vessel adaptors with reservoirs were used, and each reservoir contained a different reagent. The first vessel contained two quarter reservoirs, with reagents 1 and 2, and two quarter reservoirs divided by length, with reagents 3-6 (Table 3). The second vessel contained three quarter reservoirs with reagents 7-9 (Table 4). A pipetboy with glass serological pipettes, 10, 25, and 50 mL depending on volume, dispersed the different solutions. DNase 1 lyophilized was dissolved in 1.1 ml water and mixed into the RNA DNase wash. The resin was mixed by vortexing before aspiration. When all the reagents were prepared in the vessels, they were transferred to the Biomek 4000 automated workstation. Once the Biomek layout was set, according to the manufactured protocol of the biomek software (Figure 4), the biomek 4000 automated workstation started isolating the RNA. After the isolation of RNA, the 96 well PCR plate was concealed with an AlumaSeal CS sealing foil for freezing at -80°C.

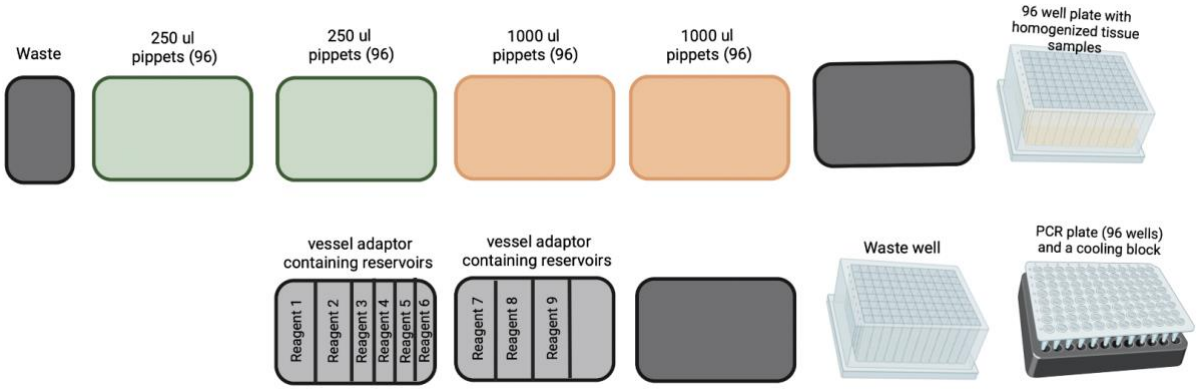

Figure 4 Setup for Biomek 4000 automated workstation.

Table 3 The first vessel adaptor containing reservoirs with the volume of different reagents needed for RNA isolation of 96 samples.

Reag 1	**Reag 2**	**Reag 3**	**Reag 4**	**Reag 5**	**Reag 6**
Cell lysis Buffer (CLD)	**Binding Buffer III, Custom**	**DNase I (Lyophilized) with added RNA DNase wash, custom**	**Protein-ase K (PK) solution**	**Simply-RNA Resin, Custom**	**Nuclease-Free Water**
32.4 mL	47.1 mL	1.1 mL DNase + 21,6 mL RNA DNase wash	5,2 mL	5.2 mL	9.2 mL

Table 4 The second vessel adaptor containing reservoirs with the volume of different reagents needed for RNA isolation of 96 samples.

Reag 7	**Reag 8**	**Reag 9**	**-**
Binding Solution 2, Custom	**Wash Buffer**	**80% Ethanol**	**-**
22.4 mL	42.9 mL	12.4 mL	-

The isolated RNA concentrations were measured by first centrifuging the samples for 10 seconds with a mini plate spinner centrifuge (Labnet Inc, USA). Next, a water sample was added to initialize the instrument. Thereafter, 1.5 μL of each RNA sample was added to the ND-1000 UV/Vis Spectrophotometer (NanoDrop Technologies, USA) to receive the RNA

concentrations (ng/µL) (Appendix 5). The RNA concentrations in the samples were diluted with nuclease free water to 50 ng/µL using Biomek 4000 (Beckman Coulter INC, California, USA) (Appendix 6). The diluted samples were put in the -80°C freezer for storage.

Some samples (n=23) had low concentrations of RNA when measured in the Nanodrop. Therefore, RNA was extracted again using the TriReagent (Invitrogen™). To isolate RNA, the tissue was first weighted in mg with a Radwag model AS 220 X2 (Radwag wagi Electoniczne, Radom, Poland). The tissue was between 40-100 mg. Tissue bigger than 100 mg is cut in half. Next, the tissue is put into 2 mL tubes containing approximately 365 mg Ceramic beads 1.4 mm (GIAGEN, Hilden, Germany). After that, 1 mL of TriReagent reagent was added to each tube and homogenized for 20 sec in a FastPrep FP120-230 (Thermo Savant, New York, USA). After the homogenization, 200 µL of chloroform was added to each tube. The tubes were shaken vigorously for 15 sec before letting the samples stand for 15 min at room temperature (RT). Next, the samples were centrifuged at 12 000 x g for 15 min at 4°C. Then, the aqueous phase was transferred into a new tube. Next, 500 µL 2-propanol was added, and the sample rested for 10 min at room temperature. After that, the samples were centrifuged at 12 000 x g for 15 min at 4°C, and the supernatant was removed. Next, the RNA pellet in each sample was washed with 1 mL of 75% ethanol. Then the sample was vortexed and centrifuged at 7500 x g for 5 min at 4°C. Once more, the supernatant was removed, and the pellets were left to air-dry. The pellet was dissolved in 20 µL water, and the concentration was read in a Nanodrop (Thermo Fisher Scientific, USA) and further diluted to 400-1000 ng/µL (Appendix 7). The RNA samples that were manually extracted were treated with DNase1 (Invitrogen™) prior cDNA synthesis. For that 1 µL DNase buffer and 1 µL DNase1 (1 U/µl) were added, and samples were incubated for 15 min at RT. Enzyme activity was stopped by adding 1 µL EDTA (25 mM, pH 8.0) and incubation for 10 min at 65°C.

2.4.5 **cDNA synthesis**

700 ng of DNase1 treated RNA was used to generate the cDNA from each sample using the SuperScript™ VILO™ cDNA Synthesis Kit. For that 4 µL 5X VILO Reaction Mix and 2 µL 10X SuperScript Enzyme Mix was added to 10 µL DNAse1 treated RNA before adding 4 µL DEPC-treated water to get a total of 20 µL in the tube. The tube content was genteelly mixed and incubated at 25°C for 10 minutes, followed by 42°C for 60 min, and the reaction was terminated at 85°C for 5 min. Half of the cDNA samples was diluted 1:10 (10 µL cDNA + 90 µL H_2O). The cDNA was stored in the -20°C freezer.

2.4.6 **Conventional PCR**

A conventional PCR was used to test the functionality of the genes in the experimental tissues. A 2720 Thermal Cycler (Applied Biosystems, Singapore) was used to run the PCR. PCR reaction and cycling conditions are as below (Table 5). The concentrations were compared to the Promega Usage information.

Table 5 PCR reaction and cycling conditions. mM6 = master-mix for 6 samples. Master-mix for each gene was added to the tubes before adding 2 µL of cDNA.

PCR reaction						**Cycling conditions**	
	Amount per sample (µL)	**Concentrations**	**eef1a mM6 (µL)**	**gapdh1 mM6 (µL)**	**gapdh2 mM6 (µL)**	**Temp (°C)**	**Time**
Gotag Bf. 5x 5 µL	5	0.2	30	30	30	95	10 minutes
$MgCl_2$ [25 mM]	2	0.08	12	12	12	95	30 seconds
dNTPs [1.25 mM]	2	0.08	12	12	12	60	30 seconds
Fw [10 µM]	0.5	0.02	3	3	3	70	20 seconds
Rv [10 µM]	0.5	0.02	3	3	3	72	7 minutes
cDNA [1:10]	2	0.08	-	-	-	4	∞
Enzyme	0.25	0.01	1.5	1.5	1.5		
H_2O	12.75	0.51	76.5	76.5	76.5		
Total	**25**		138µL/6 = **23 µL**	138µL/6 = **23 µL**	138µL/6 = **23 µL**		

Electrophoresis was used to separate DNA molecules based on size and electrical charge. First, the gel was prepared by heating a mix of 4 g Electran® Agarose DNA Grade (VWR International BVBA, Ecuador) and 100 mL of 50x TAE Electrophoresis Buffer diluted to 1x. Next, 4 µL of SYBR® Safe DNA gel stain (Invitrogen, USA) was added to the gel solution and mixed before pouring it onto a glass plate and letting it sit for 20 min. When the gel had solidified, the comb was removed, and each gene was loaded into the sample wells; Eukaryotic translation elongation factor 1 alpha (*eef1a*), glyceraldehyde-3-phosphate dehydrogenase (*gapdh*), insulin-like growth factor 1 (*igf-1*), insulin like growth factor 1 receptor (*igf-1r*), and growth hormone receptor (*ghr*). Next, the gel plate was immersed in charged buffer solution,

and the DNA fragments moved through the gel toward the positive electrode. After approximately 30 min, the size of the amplicon in base pairs was determined by an iBrigth imaging system model CL1500 (Life technologies, Singapore).

2.4.7 **Relative quantification of gene expression using qPCR**

As indicated above, *igf-1*, *igf-1r*, and *ghr* were chosen to be tested as growth indicators target genes, and their mRNA levels were quantified relatively to *eef1a* and *gapdh* as housekeeping genes. Gene specific primers and dual labeled probes (labelled with 6-carboxyfluorescein and BHQ-1, Black Hole Quencher 1 on 5′ and 3′ terminus, respectively) for each gene were designed using Integrated DNA Technologies PrimerQuest™ and OligoAnalyzer™ tools available online at https://eu.idtdna.com and produced by Eurofins Genomics (Germany GmbH). The name, sequence, sense, annealing temperature, and GC content along with the amplicon size to be generated by these primers are given in Appendix 8. qPCR reactions for each gene, including housekeeping genes, were optimized for best efficiency using the standard curve method. The optimalization process covered three main elements: cDNA concentration, primer/probe annealing temperature, and primer/probe ratio/concentration (Taylor et al., 2010). Five times serial dilutions were prepared from mix of cDNA samples at each treatment group (for example Muscle 12°C October; n=12). Parameters for qPCR reaction efficiencies for all tested genes were as shown in Appendix 8. The optimal reaction cycling conditions for the genes are shown below (Table 6), and 1:100 dilution of cDNA was the optimal dilution to use (Appendix 9).

Table 6 The optimal reaction cycling conditions for the genes.

eef1a*, *igf-1*, *igf-1r*, and *ghr			***gapdh***		
Temp (°C)	**Time**	**Cycles**	**Temp (°C)**	**Time**	**Cycles**
50	2 minutes	-	50	2 minutes	-
95	10 minutes	-	95	10 minutes	-
95	15 seconds	40	95	15 seconds	40
60	30 seconds		55	30 seconds	

2.4.8 Calculating the fold gene expression ($2^{-\Delta\Delta CT}$)

The delta delta CT method of real time PCR quantification was used for calculating the fold gene expression (Wang et al., 2007). From the raw data output of the qPCR machine, the cycle threshold (CT) means of the housekeeping genes and the CT mean of the target genes were

gathered. The first thing that was calculated was the average CT of the housekeeping genes, which was the average of the *eef1a* CT mean and the *gapdh* CT mean of each sample, as shown below.

$$CT\ mean\ (\ housekeeping\ genes) = \frac{eef1a\ CT\ mean + gapdh\ CT\ mean}{2}$$

Thereafter, the delta CT (ΔCT) was found by subtracting the average of the housekeeping genes from the CT mean of the gene of interest.

$$\Delta CT_{Control} = CT\ mean\ (target\ gene) - \ CT\ mean\ (housekeeping\ genes)$$

The $\Delta\ CT_{Calibrator}$ was calculated by the difference between the average CT mean of the zero sample of the gene of interest and the average CT mean of the zero samples of the (housekeeping genes).

$$\Delta\ CT_{Calibrator}\ =$$
$$average\ of\ CT\ mean\ (gene\ of\ interest)\ zero\ sample\ values\ (n = 12) -$$
$$average\ of\ \ CT\ mean\ (housekeeping\ genes)\ zero\ sample\ values\ (n = 12)$$

The difference between $\Delta CT_{Control}$ and $\Delta\ CT_{Calibrator}$ was used to calculate the delta delta CT (ΔΔCT).

$$\Delta\Delta CT = \ \Delta CT_{Control} - \ \Delta\ CT_{Calibrator}$$

Finally, the fold gene expression ($2^{-\Delta\Delta CT}$) for each sample was calculated, as shown below.

$$Fold\ gene\ expression = \ 2^{-\Delta\Delta CT}$$

The mean of the $2^{-\Delta\Delta CT}$ values from each temperature at each sampling, including the zero sample, was used to do statistical analysis and to create the graphs.

2.5 X-ray samples

2.5.1 **Sampling the fish**

Two x-ray samples were taken, at the experiment's beginning and end. In the first x-ray sampling, 145 fish, with an average weight of 10.7 g, were collected from 12°C seawater and transferred from the rearing tank into a lethal dose of anesthetic (Finquel vet, 100g/l, MSD, Boxmeer, Netherlands). In the final x-ray sampling, 450 fish were collected, 150 from each temperature, with an average weight of 38.5 g. From each tank, 50 fish were transferred into seawater with a lethal dose of anesthesia (Finquel vet, 100g/l, MSD, Boxmeer, Netherlands). First, the weight and length were measured from both samplings before the fish were sorted into Styrofoam boxes. Inside each Styrofoam box, a cardboard plate was layered, followed by paper towels, the fish, and plastic on top of the fish before the next layer was started. Next, the boxes were marked with the number of the rearing tanks, the temperature, and the date. Then, they were put into -20°C freezers at the IMR in Austevoll until the x-rays were taken.

2.5.2 **Collecting the x-ray data**

The X-rays of the fish were taken at the Institute of Marine Research in Matre, Norway, with a Portable X-Ray unit Hiray plus model porta 100 HF (Job corporation, Yokohama, Japan). The tube voltage was set to 40 kV, and the tube current in milliamps with exposure time in seconds was 4.0 mAs. The frozen fish were placed on a square styrofoam lid, without any overlapping fish, and photographed on the Canon CXDI-410C Wireless plate. The distance between the Canon plate and the x-ray apparatus was 73.6 cm. MicroDicom viewer was used to converting the Dicom format to TIFF pictures.

2.5.3 **Analyzing the x-ray data**

The methodology of Witten et al. (2009) was used to examine the x-rays and determine the European plaice's vertebral column deformities. The pictures were taken from a laterolateral view of the animal and alterations of ribs, inter-muscular spines, and haemal and neural arches were excluded from the determination (Witten et al., 2009). Vertebra number and deformity type was recorded (Witten et al., 2009).

2.5.4 **Meristic characters - vertebral column**

The number of vertebrae was counted in 50 fish, and the average was used to state the number of vertebrae. The vertebrae ranged from 41 to 44, but mainly the fish had 43 vertebrae.

2.5.5 **Deciding the percent frequency of deformities per vertebrae**

The sum of deformities found per vertebrae was divided by the total number of fish per group and multiplied by 100 to determine the percent frequency of deformities per vertebrae for each of the three groups.

2.6 Statistical analyses

All the data for growth, gene expression, and deformities were expressed as mean values ± SEM. For most of the data, including growth and gene expression, statistical analyses were carried out using R-studio (R Core Team, 2023, Vienna, Austria). A Grubbs Outlier test was performed to detect outliers within the data set. A two-way nested ANOVA followed by Tukey HSD post-hoc test was used to determine the differences between temperatures at each sampling point. The graphs and bar-plots were made in R-studio (R Core Team, 2023, Vienna, Austria).

For changes of gene expression in time per temperature, a t-test was done using IBM SPSS Statistics (IBM Corp., 2020, New York, United States), and the figure was made in power point. For the deformity data a one-way ANOVA followed by Tukey HSD post-hoc test was used to determine the differences between temperatures at each sampling point. The deformity data were carried out using R-studio (R Core Team, 2023, Vienna, Austria).

A significance level of $\alpha < 0.05$ was chosen for all statistical tests.
Details of statistical test results can be found in Appendix 10.

3 Results

The fish were reared at three different water temperatures during the experiment: ambient water temperature (average ± SD, of 8.6°C ± 0.4, range 7.9-9.5°C), 12.2°C ± 0.1 (range (min-max) 12.0-12.5°C), and 16.0°C ± 0.2 (range (min-max) 15.5-16.4°C). The temperatures were automatically measured every 15 minutes each day during the experiment (Figure 5).

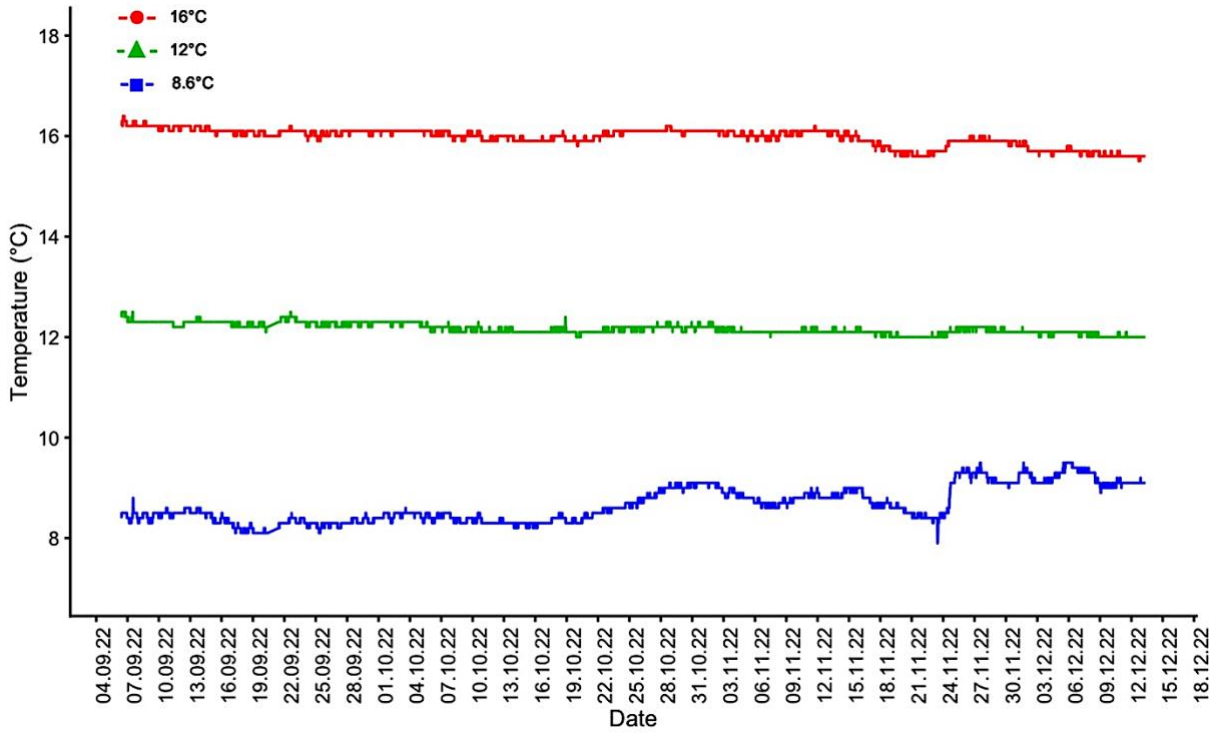

Figure 5 Water temperature (°C) in European plaice rearing tanks. The plaice were reared at three different temperatures: ambient water temperature (average of 8.6°C ± SD of 0.4, range (min-max) 7.9-9.5°C), 12.2°C ± SD of 0.1 (range (min-max) 12.0-12.5°C), and 16.0°C ± SD of 0.2 (range (min-max) 15.5-16.4°C).

3.1 Growth of European plaice at different temperatures

The three different temperatures affected the mean weight changes of the plaice differently (Figure 6). The experimental fish had a mean weight of 10.41 g (SEM = 0.14) at start of the experiment in September (Figure 6). All the following samplings, i.e., October, November, and December, had a significant difference in temperature (two-way nested ANOVA, $P < 0.05$). In the two samplings in the middle, i.e., October and November, the fish at 12°C and 16°C had a similar body weight (Tukey post hoc test October, $P > 0.13$ and Tukey post hoc test November, $P > 0.45$). However, in the final sampling of the experiment, the fish in 16°C water grew faster

(Tukey post hoc test December, $P < 0.05$, Figure 6) than the fish in 12°C. The 8.6°C was significant different from 12°C and 16°C in all samplings (Tukey post hoc test October, November and December, $P < 0.05$). The final body weight differed between the three rearing temperatures (two-way nested ANOVA, $P < 0.05$, Figure 6). The fish in ambient water temperature had the lowest (Tukey post hoc test, $P < 0.05$, Figure 6) final body weight (29.00 g ± 0.33), followed by the 12°C group (Tukey post hoc test, $P < 0.05$, 41.01 g ± 0.44), and with the 16°C group displaying the highest final mean body weight (Tukey post hoc test, $P < 0.05$, 48.78 g ± 0.50).

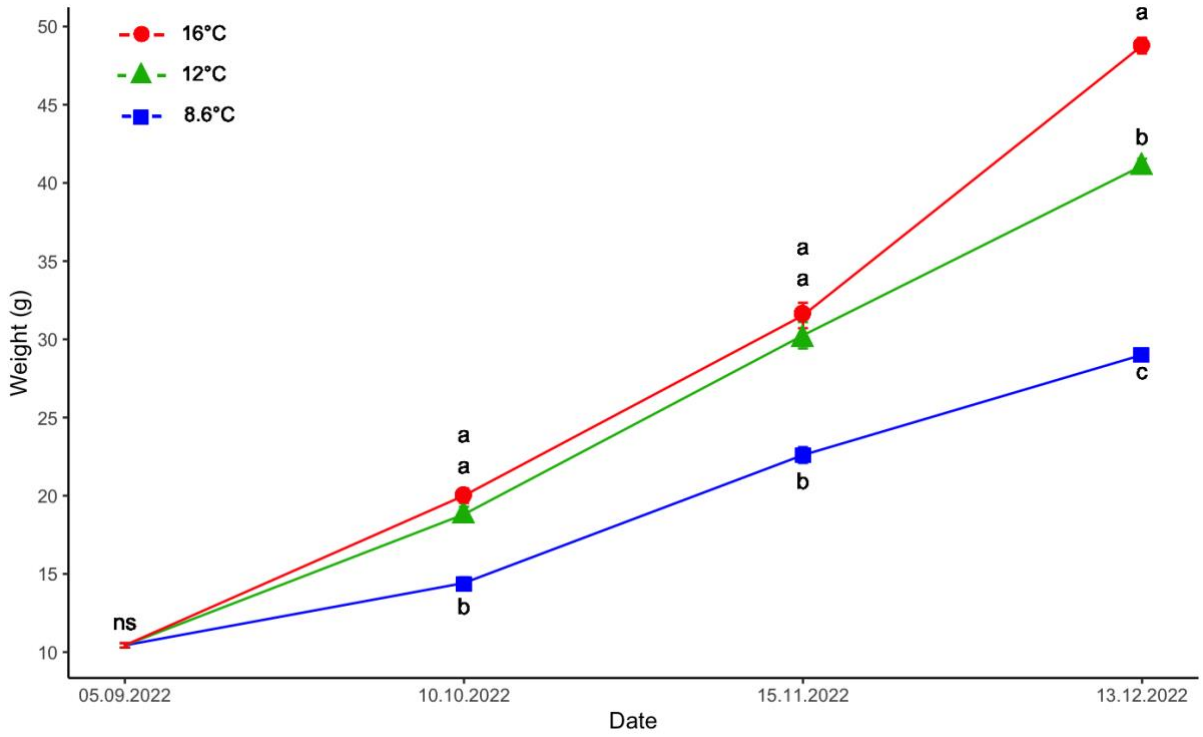

Figure 6 Mean weight (g) of European plaice at ambient water temperature (average of 8.6°C), 12°C, and 16°C water temperature. Vertical lines indicate standard errors. Different letters indicate statistical differences (Tukey post-hoc test, $p < 0.05$) between the experimental groups.

In all samplings, the temperatures were significantly different when measuring the mean length of the fish (two-way nested ANOVA, $P < 0.05$, Figure 7). At the experiment's beginning, the fish's average length was 8.40 cm (SEM = 0.04). In the three following samplings, the fish in 16°C water was the longest (Tukey post hoc test, $P < 0.05$, Figure 7), followed by 12°C (Tukey post hoc test, $P < 0.05$, Figure 7), and lastly, the ambient temperature water (Tukey post hoc

test, P < 0.05, Figure 7). In December, the final length of the 16°C fish was 14.48 cm ± 0.05, the 12°C fish was 13.49 cm ± 0.05, and the 8.6°C fish was 11.94 cm ± 0.04.

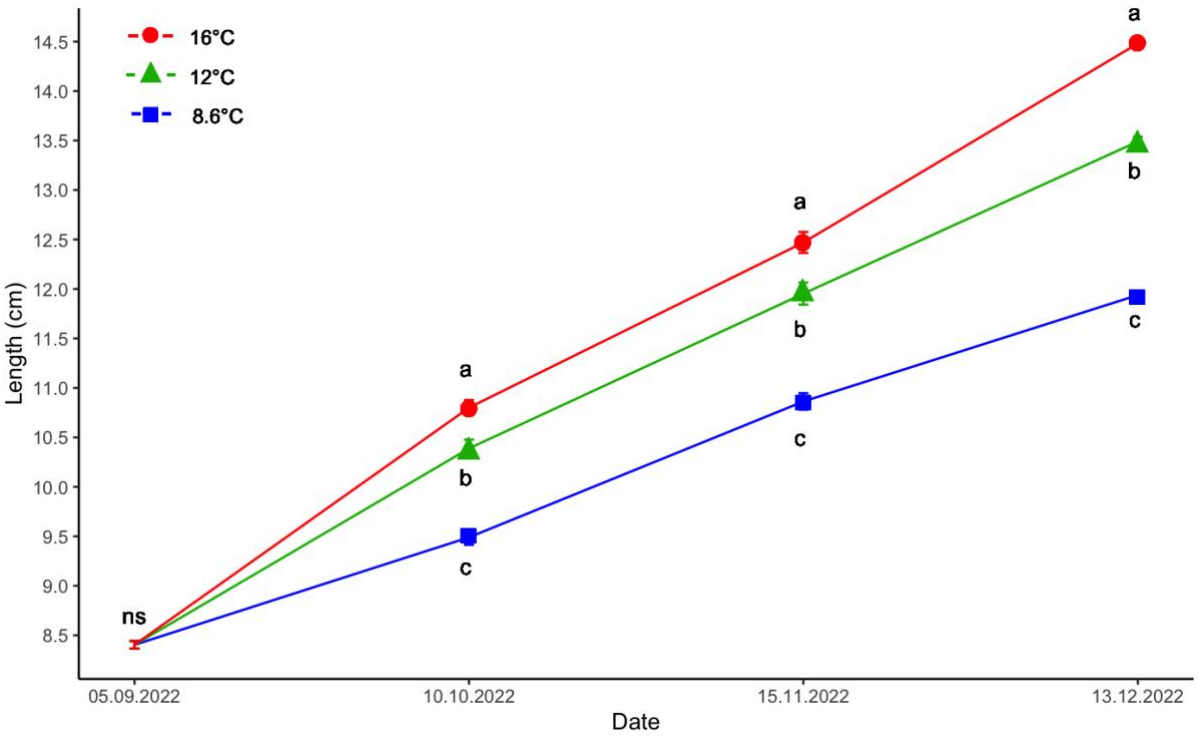

Figure 7 Mean length (cm) of European plaice at ambient water temperature (average of 8.6°C), 12 °C, and 16 °C water temperature. Vertical lines indicate standard errors. Different letters indicate statistical differences (Tukey post-hoc test, p < 0.05) between the experimental groups.

The temperature affected the condition factor of the fish (two-way nested ANOVA, P < 0.05, Figure 8). The fish at 12°C and 8.6°C had similar condition factors in the two middle samplings (Tukey post hoc test October, P > 0.73, Tukey post hoc test November, P > 0.68, Figure 8). On the other hand, the fish at 16°C water had a significantly lower condition factor (Tukey post hoc test, P < 0.05, Figure 8) from October onwards. In the final sampling, all the temperatures were significantly different (Tukey post hoc test, P < 0.05, Figure 8), and the three groups' condition factors were 1.57 ± 0.01, 1.64 ± 0.01, and 1.66 ± 0.01 for 16°C, 12°C, and 8°C respectively.

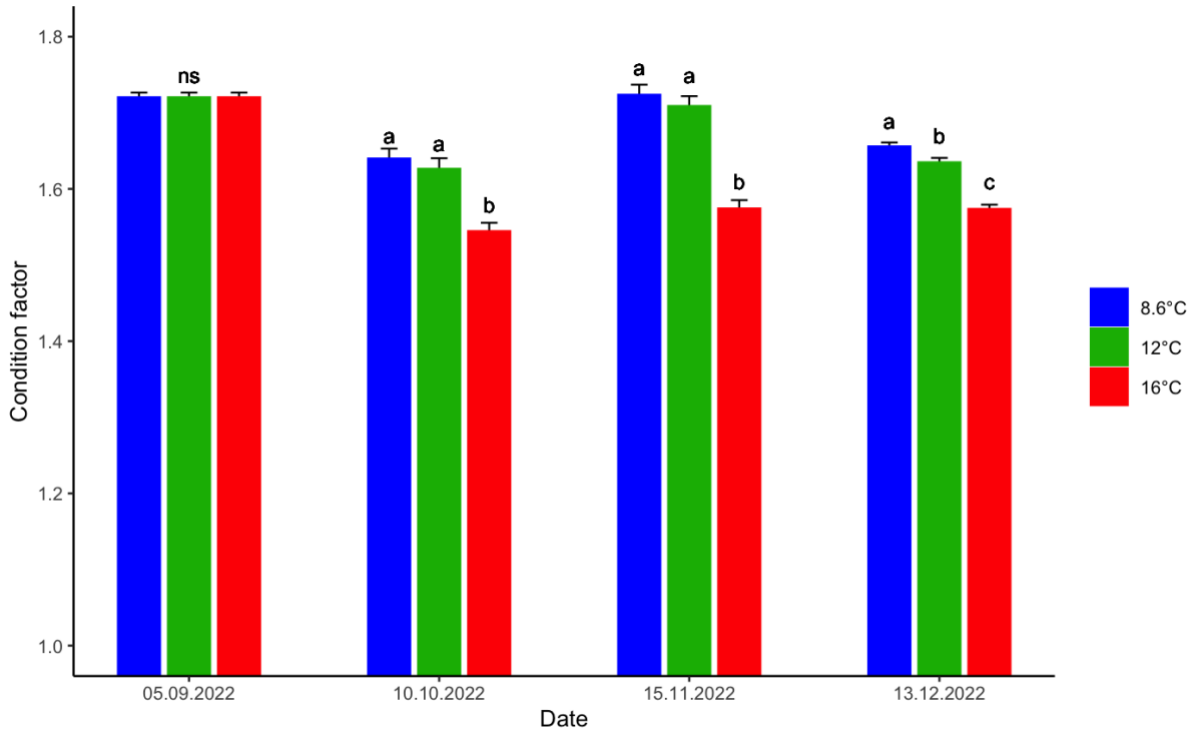

Figure 8 Condition factor of European plaice at ambient water temperature (average of 8.6°C), 12 ℃, and 16 ℃ water temperature. Vertical lines indicate standard errors. Different letters indicate statistical differences (Tukey post-hoc test, $p < 0.05$) between the experimental groups.

3.2 Gene expression in European plaice at different temperatures

The relative gene expression of growth hormone receptor (*ghr*) in the liver of European plaice was 1.12 (SEM = 0.164) at the beginning of the experiment (Figure 9). In the second and final sampling of the *ghr*, in October and December, there were significant differences in temperature (two-way nested ANOVA, $P < 0.05$ in October, two-way nested ANOVA, $P < 0.05$ in December). In October, 8.6°C was significantly different from both 12°C and 16°C (Tukey post hoc test, $P < 0.05$). In December, 8.6°C was significantly different from 16°C (Tukey post hoc test, $P < 0.05$). Final *ghr* transcript levels in December were 0.47 ± 0.05, 0.70 ± 0.06 and 0.92 ± 0.12 for the 16°C, 12°C and 8.6°C groups respectively.

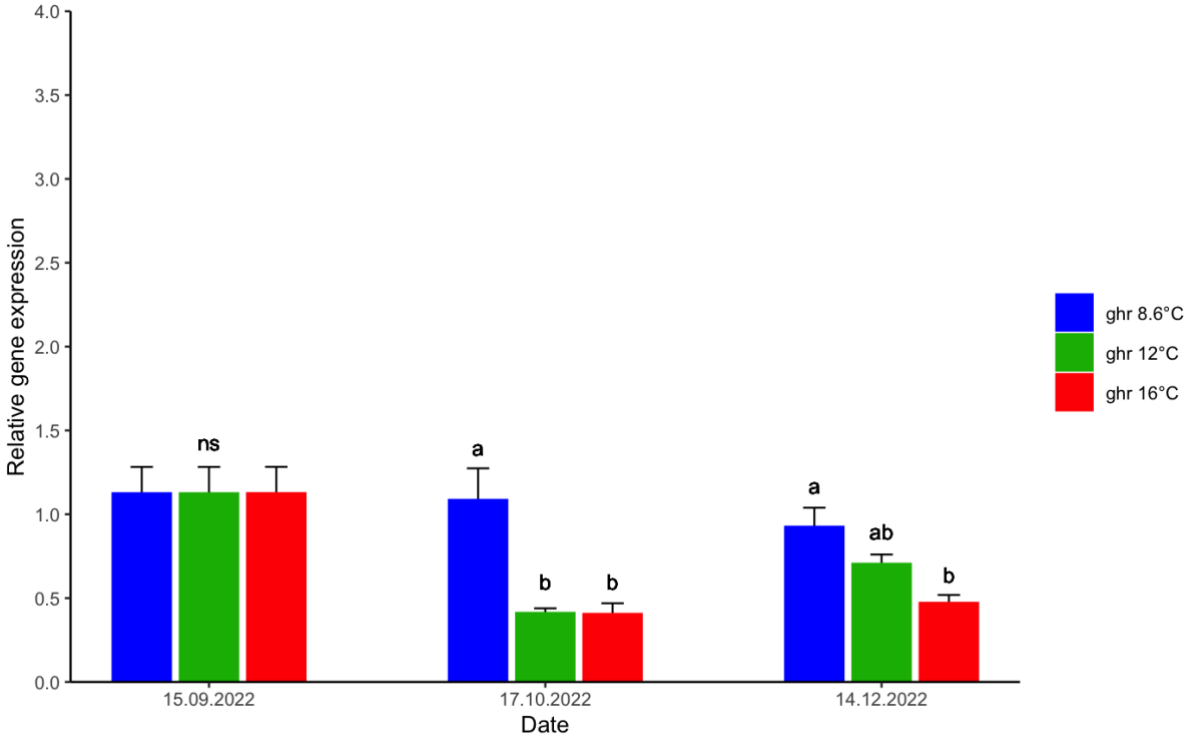

Figure 9 Relative gene expression of growth hormone receptor (ghr) in liver of fish reared at 8.6℃, 12℃, and 16℃ water temperature. Vertical lines indicate standard errors. Different letters indicate statistical differences (Tukey post-hoc test, p < 0.05) between the experimental groups.

The relative gene expression of insulin-like growth factor 1 (*igf-1*) in the liver of European plaice was 1.08 (SEM = 0.13) at the beginning of the experiment (Figure 10). In the second and third sampling of the *igf-1*, in October and December, there was a significant difference in temperature (two-way ANOVA, $P < 0.05$ in October, two-way ANOVA, $P < 0.05$ in December). In October, 16°C was significantly different than 8°C and 16°C (Tukey post hoc test, $P < 0.05$). In December, a Tukey post hoc test showed a significant difference between 8.6°C and 12°C ($P < 0.05$, Figure 10). Final *igf-1* transcript levels in December were 2.27 ± 0.14, 2.33 ± 0.09 and 1.85 ± 0.17 for the 16°C, 12°C and 8.6°C groups respectively.

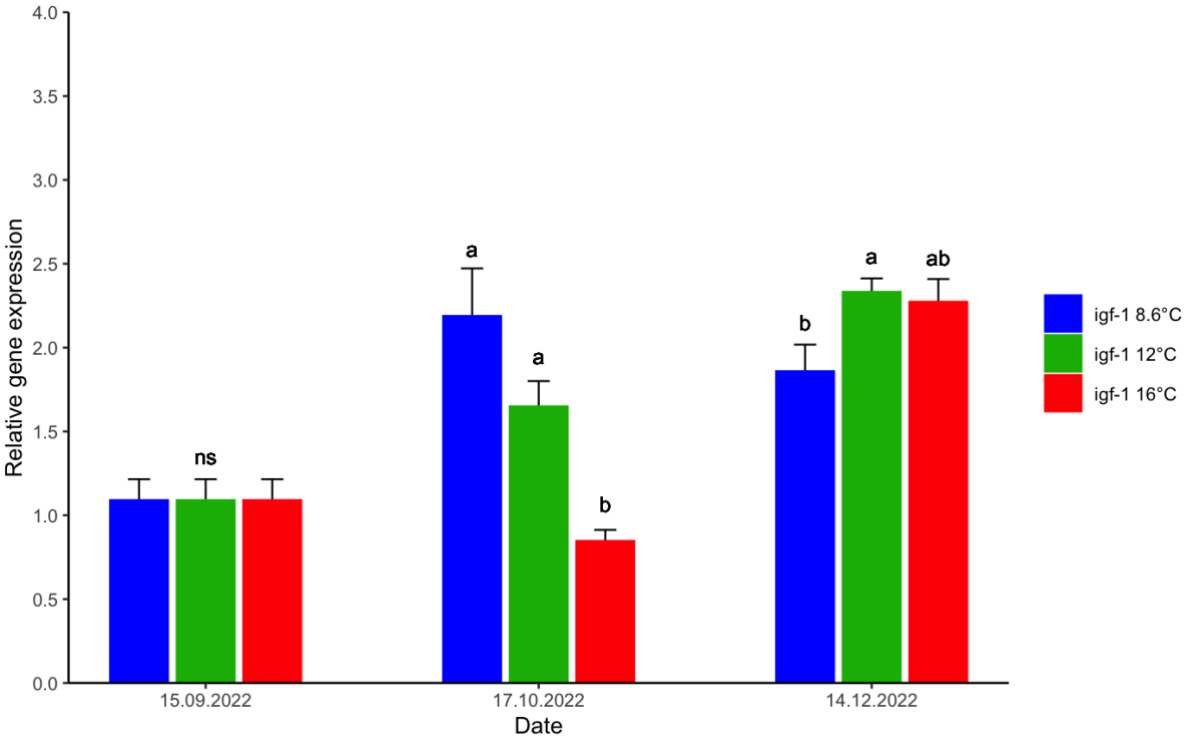

Figure 10 Relative gene expression of insulin-like growth factor 1 (igf-1) in liver of fish reared at 8.6 ℃, 12 ℃, and 16 ℃ water temperature. Vertical lines indicate standard errors, ns indicates no statistical differences between the experimental groups.

The relative gene expression of growth hormone receptor (*ghr*) in the muscle of European plaice was 1.11 (SEM = 0.18) at the beginning of the experiment (Figure 11). In the second and third sampling of the *ghr*, i.e., October and December, there was not a significant difference in temperature (two-way ANOVA, $P > 0.05$ in October, two-way ANOVA, $P > 0.06$ in December). Final *ghr* transcript levels in December were 2.35 ± 0.86, 0.95 ± 0.12 and 1.45 ± 0.29 for the 16°C, 12°C and 8.6°C groups respectively.

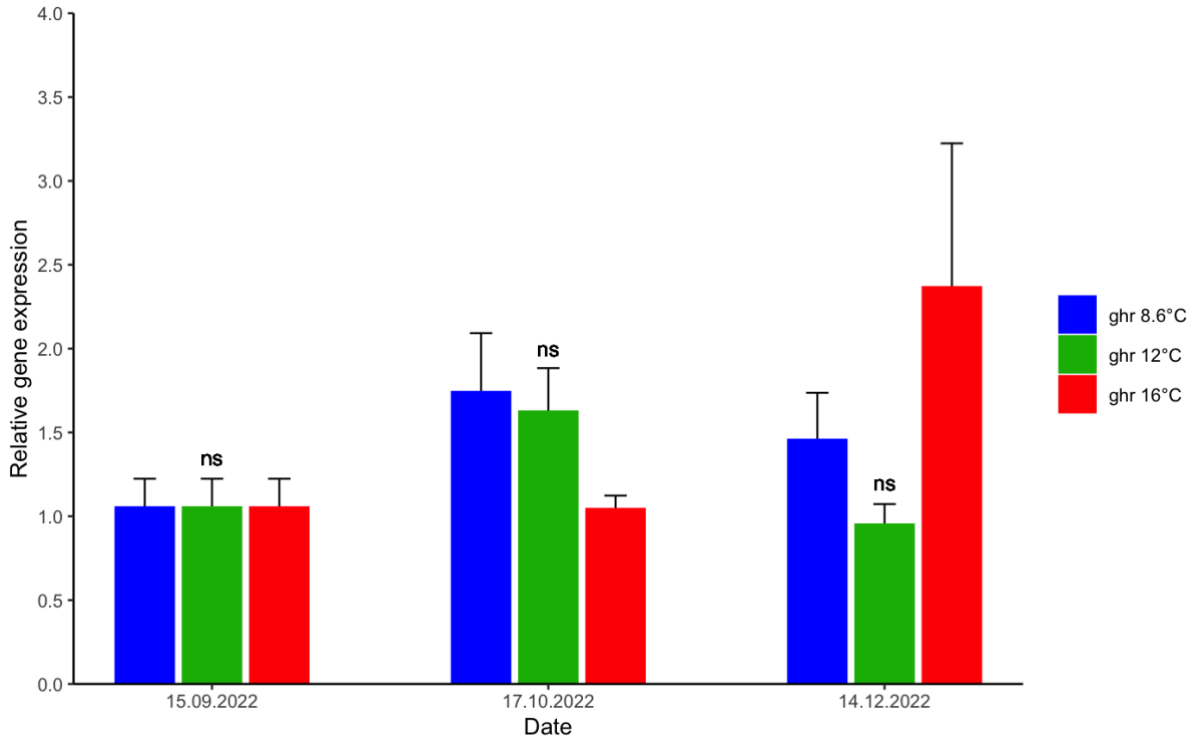

Figure 11 Relative gene expression of growth hormone receptor (ghr) in muscle of fish reared at 8 ℃, 12 ℃, and 16 ℃ water temperature. Vertical lines indicate standard errors. Different letters indicate statistical differences (Tukey post-hoc test, p < 0.05) between the experimental groups.

The temperature did not affect the regulation of insulin-like growth factor 1 receptor (*igf-1r*, Figure 12) in the muscle. The relative gene expression of *igf-1r* in the muscle of European plaice was 1.12 (SEM = 0.20) at the beginning of the experiment (Figure 12). In the second sampling, October, there was a significant difference in temperature (two-way nested ANOVA, $P < 0.05$). The fish reared at 8.6°C and 16°C were significantly different (Tukey post hoc test October, $P < 0.05$, Figure 12). In the final sampling, December, there was no significant difference between the temperatures (two-way nested ANOVA, $P > 0.90$ in December, Figure

12). Final *igf-1r* transcript levels in December were 2.56 ± 0.42, 2.86 ± 0.41 and 2.42 ± 0.29 for the 16°C, 12°C and 8.6°C groups respectively.

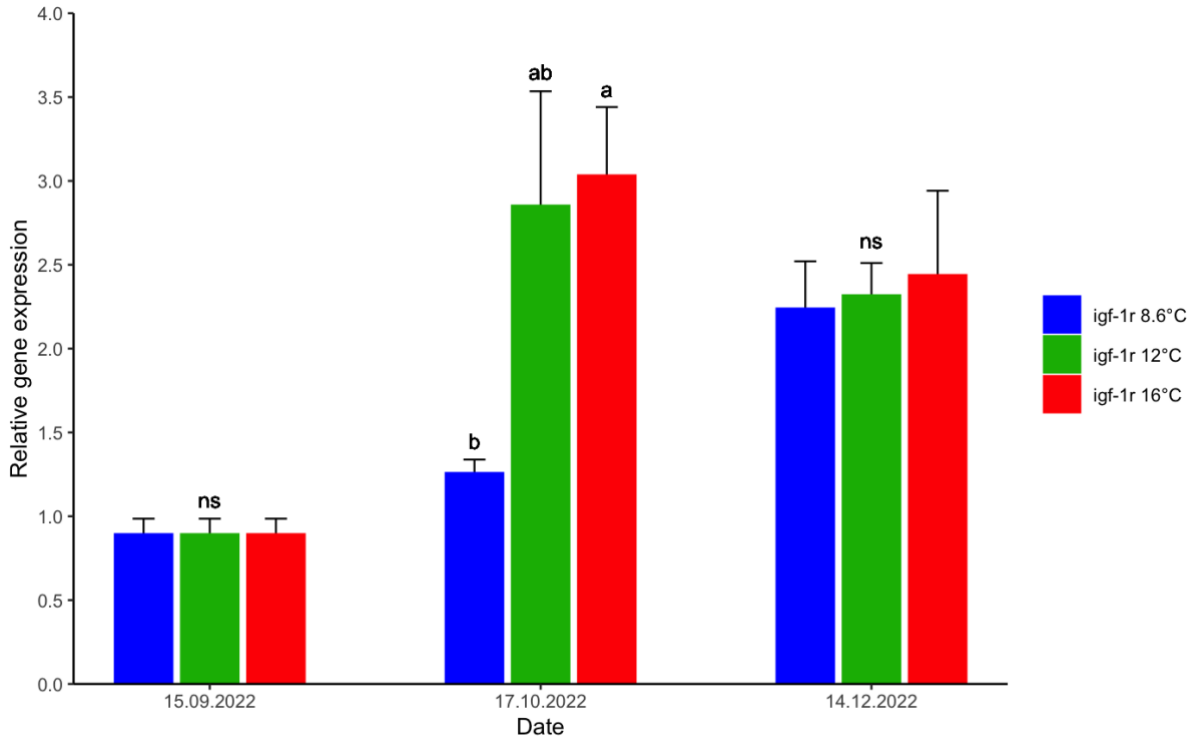

Figure 12 Relative gene expression of insulin-like growth factor 1 receptor (igf-1r) in muscle of fish reared at 8 ℃, 12 ℃, and 16 ℃ water temperature. Vertical lines indicate standard errors, ns indicates no statistical differences between the experimental groups.

The change of growth and gene transcript levels with time per temperature is shown in Figure 13. The European plaice had significant growth between each sampling at each temperature (Tukey post hoc test, $P < 0.05$, Figure 13). In muscle, *ghr* had a significant difference in time in 12°C and 16°C (t-test, $p < 0.05$), while in 8°C there were no significant difference in time (t-test, $p > 0.27$). *igf-1r* had a significant difference in 8°C and in between September and October in the 12°C group (t-test, $p < 0.05$). In liver, only 12°C had a significant difference of gene expression of *ghr* in time (t-test, $p < 0.05$). Hepatic *igf-1* had a significant difference in time in 12°C and 16°C (t-test, $p < 0.05$).

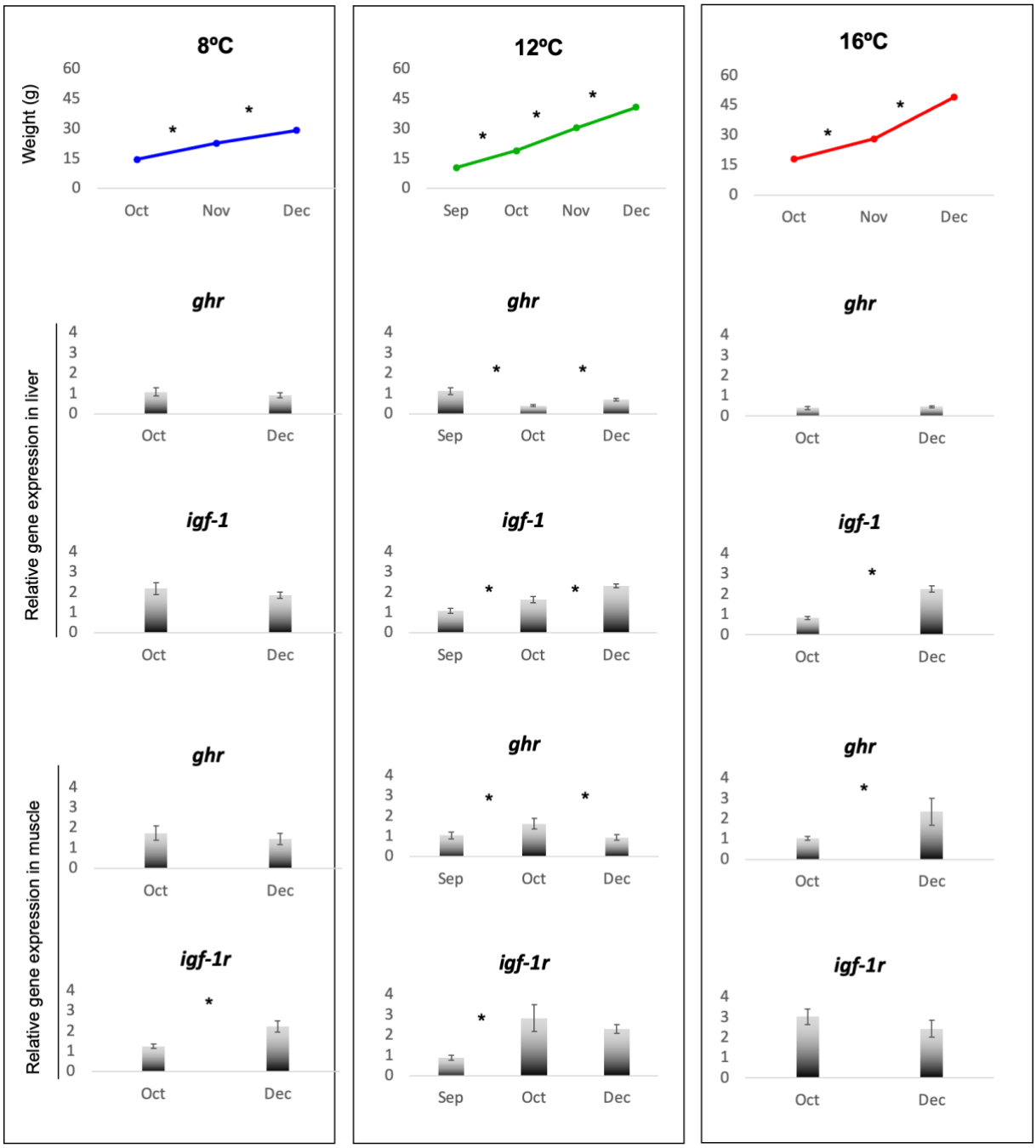

*Figure 13 Changes of growth and gene expression of ghr and igf-1r in muscle and ghr and igf1 in liver with time per temperature. * was used to show significant differences.*

3.3 X-ray analysis of European plaice at different temperatures

The European plaice has 43 (SEM = 0.08, range 41-44) vertebrae in the vertebral column, and deformities were most frequently formed in vertebrae 13-16 (Figure 14). Externally, the fish looked normal. Out of the 43 vertebrae in the vertebral column, the maximum of deformed vertebrae in one fish was 22 vertebrae at 8.6°C, 30 vertebrae at 12°C, and 28 vertebrae at 16°C. The mean number of deformed vertebrae per fish increase with temperature. The severity of

number of deformed vertebrae in the vertebral column was categorized in ranges, of five vertebra per range, per temperature (Figure 15). Out of 150 fish sampled per temperature, 8.6°C had 103 fish without deformities, 16°C had 92 fish without deformities, and 12°C had 91 fish without deformities. Only 12°C and 16°C had fish within the 26-30 deformed vertebrae range. Statistical analysis showed no significant difference in the vertebral column of fish with at least one deformity between the rearing temperatures in the final x-ray sampling (one-way ANOVA, $P > 0.38$). However, fish with more than five deformed vertebrae showed a significant difference in temperature in the final sampling (one-way ANOVA, $P < 0.05$), and the 16 °C is significantly different than the two other groups (Tukey post hoc test, $P < 0.05$).

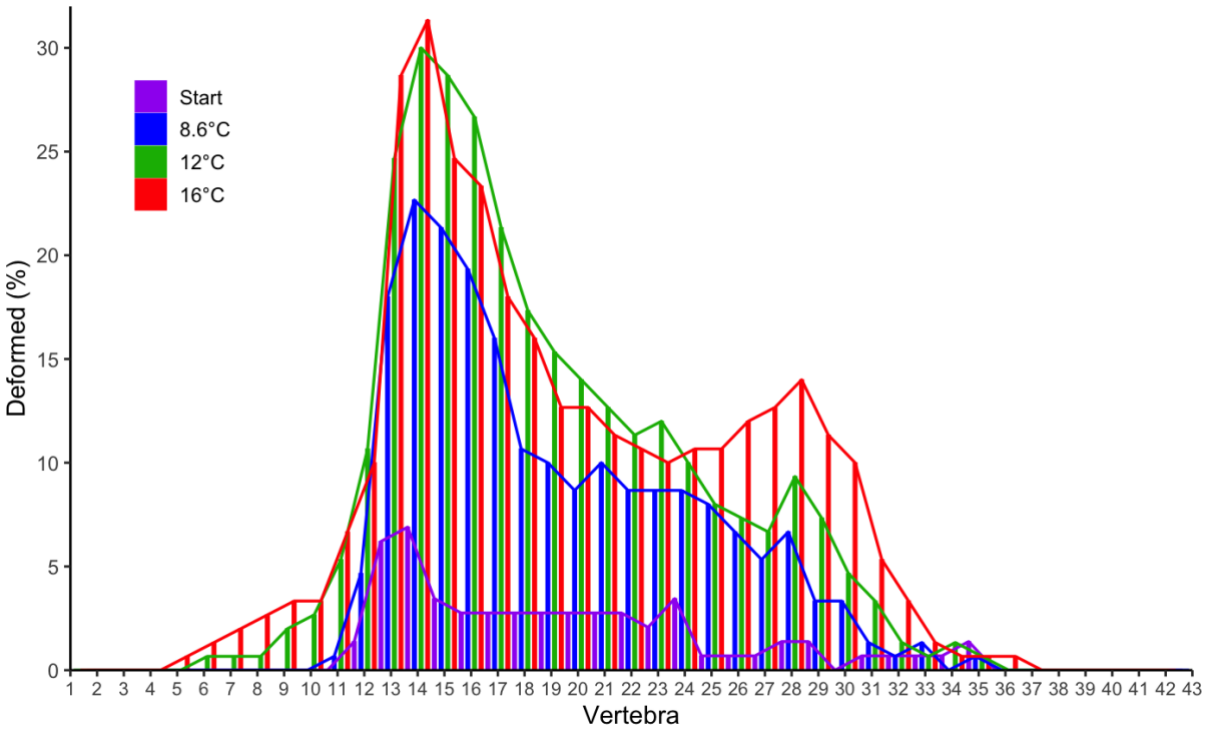

Figure 14 Deformities (%) connected to vertebrae in the vertebral column of European plaice at the end of the temperature experiment. The Start group describes deformities of the zero sample before the three temperatures (8.6 ℃, 12 ℃, and 16 ℃) was initiated. The plaice has 43 vertebrae, and the vertebrae with the most deformities are nr 13-16, which is at the posterior part) of the abdominal cavity.

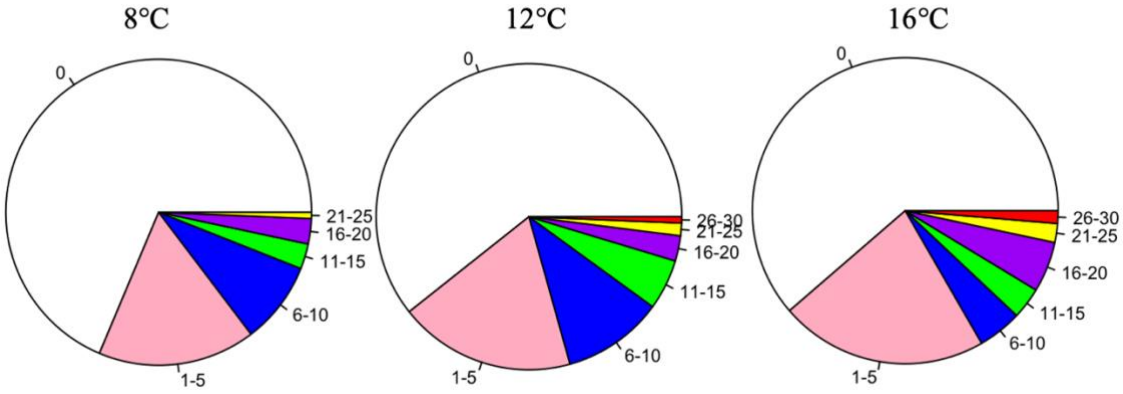

Figure 15 Number of deformed vertebrae per fish, divided into ranges of five deformed vertebrae per range, per temperature (8.6 ℃, 12 ℃, and 16 ℃).

A plaice without deformities is shown in Figure 16. Witten et al. (2009) have classified different types of deformities, and out of the 20 types of deformities described in the article (Appendix 11), type 1, 2, 3, 4, 5, 6, 8, 17, and 19 was found in the plaice. Figure 17 and Figure 18 show the hotspot of deformities found in the present study in the vertebral column, where the vertebrae were categorized in the type of deformity (Appendix 11). There was a significant difference between the start point and the final sampling (one-way ANOVA, $P < 0.05$). The fish reared at 12°C and 16°C had a significantly higher proportion of vertebral deformity in the final sampling than the start point (Tukey post hoc test, $P < 0.05$). While the fish reared at ambient temperature were not significantly different from the start point (Tukey post hoc test, $P > 0.08$). At the start point, 11.0% of the fish, in all the groups, had at least one deformity in the vertebral column. At the end of the experiment, the 8.6°C had the lowest rate of deformities, with 30.0% of the fish having at least one deformity in the vertebral column, followed by 12°C and 16°C with 38.0% and 38.7% vertebral deformities respectively.

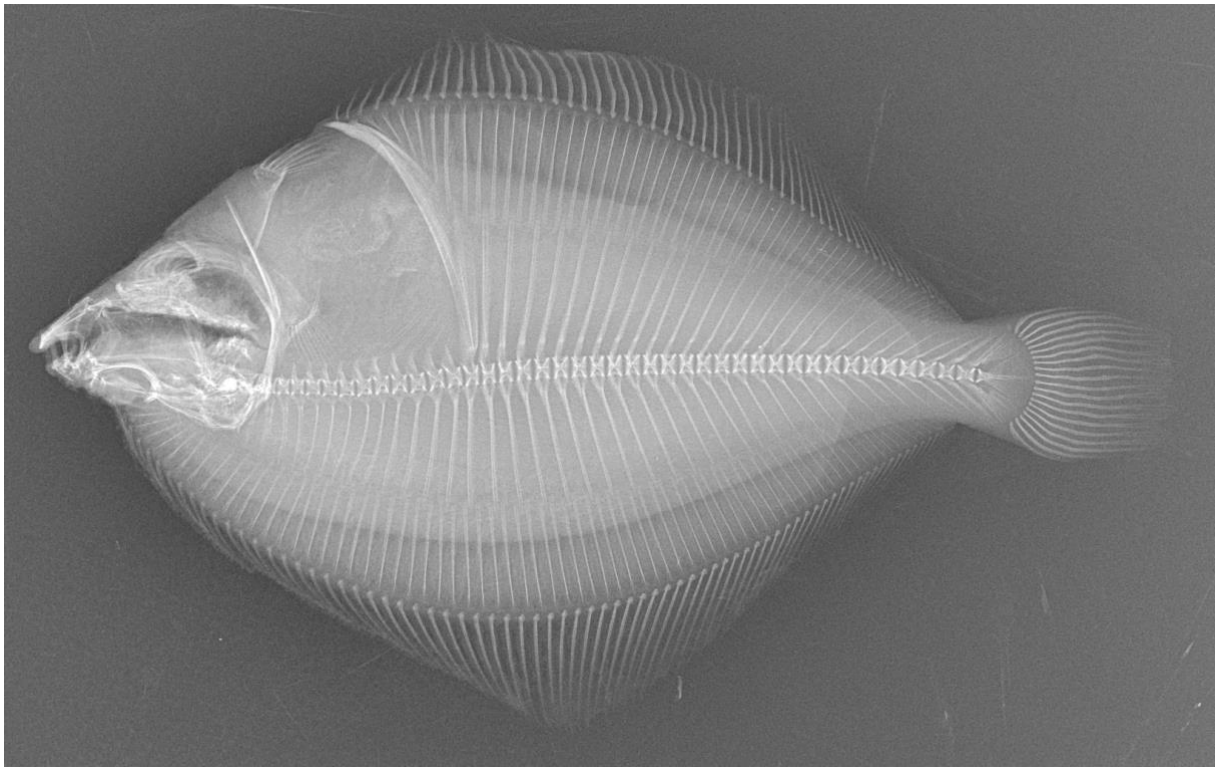

Figure 16 X-ray of a European plaice without deformities.

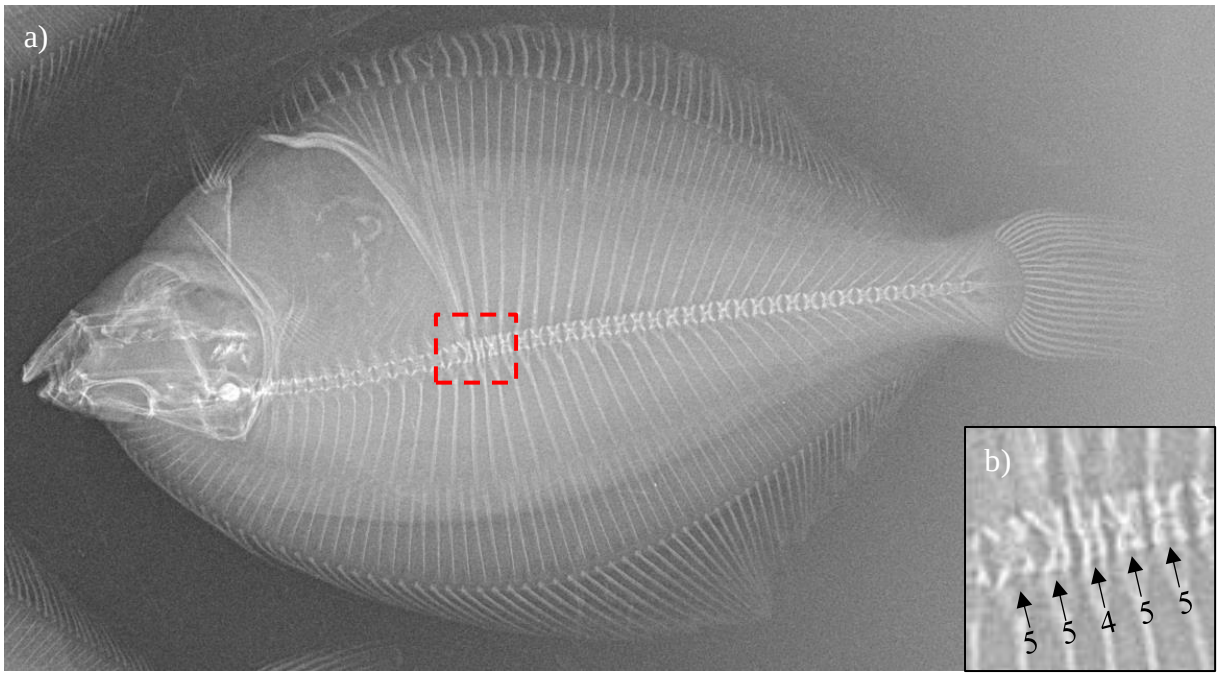

Figure 17 a) X-ray of juvenile European plaice reared at 16°C with an average weight of 48.7 g ±0.5 and average length of 14.9 cm ± 0.1. The area marked with dashed red outline is an example of a hotspot with deformities, in the vertebral column of the fish; vertebrae 13-17. b) The arrows point at the deformed vertebrae and the numbers indicate the type of deformities, as explained in Witten et al. (2009).

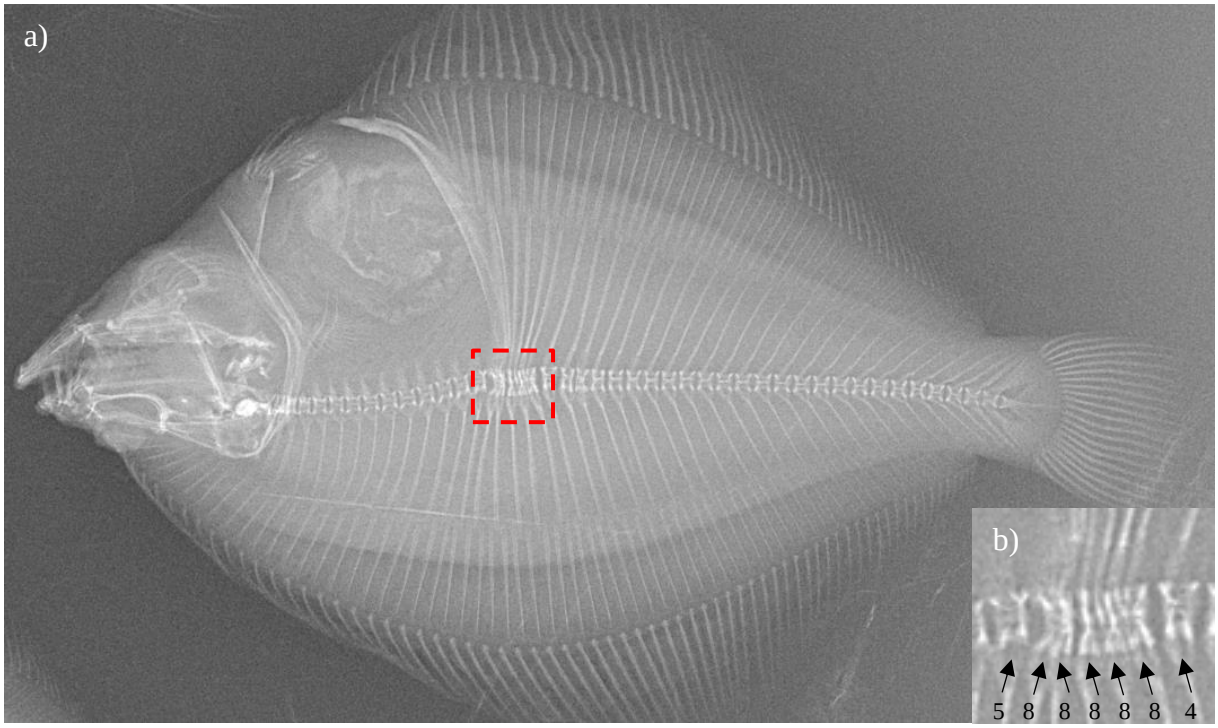

Figure 18 a) X-ray of the vertebral column of juvenile European plaice reared at 8 ℃ with an average weight of 29.0 g ± 0.3 and average length of 11.9 cm ± 0.1. Within the area marked with *dashed red outline* there is a fusion center. b) Zoomed in on the fusion center. The arrows point at the deformed vertebras and the numbers indicate the type of deformities, as explained in *Witten et al.* (*2009*).

4 Discussion

4.1 Temperature effect on growth

In the present trial, juvenile plaice were reared at three different temperatures, ambient water temperature (8.6°C), 12°C, and 16°C, over 100 days. In nature, many teleost species, including plaice, can be observed outside the optimal temperature range due to limited food resources, interspecific competition, and predators that force the species to migrate from its preferred thermal niche (Kuipers, 1977; Jakobsen & Ozhigin, 2011). The growth of juvenile European plaice, considering both weight and length, was influenced by temperature. The growth of plaice increased with increasing temperature. Fonds et al. (1992) found similar results; juvenile plaice had increased growth with increased temperature up to 16 cm long. After reaching 16 cm, the European plaice fed better at 5°C than the smaller ones (Fonds et al., 1992). A similar temperature effect on growth, increased growth with increased temperature, was found in juvenile Atlantic halibut by Jonassen et al. (1999), juvenile Japanese flounder by Fonds et al. (1995), and in juvenile turbot by Burel et al. (1996) and Imsland et al. (1996). However, in turbot, the temperature ranged from 8-20°C, where the fish reared at 8-17°C had a growth that increased with temperature, but the fish at 20°C had a lower growth rate (Burel et al., 1996). Deviations from the optimal temperature range can lead to reduced growth rates.

As expected, the temperature affected growth, and in the final sampling, the fish reared at 16°C were both heavier and longer compared to the two other temperature groups, followed by the 12°C group and then the 8.6°C. Fonds et al. (1992) already demonstrated that European plaice and European flounder (*Platichthys flesus*) have a maximum growth rate at 18-20°C in the size range of 2-22°C, after that the growth rate stagnated. The European flounder has a higher growth rate than European plaice at high temperatures (Fonds et al., 1992). The condition factor of the plaice decreased with increasing temperature. Even though the growth was highest at 16°C, the condition factor of the fish reared at 16°C was the lowest. Low condition faction indicates thinner fish, which is not optimal for fillet production in aquaculture. A study done in Denmark by Solgaard et al. (2023) showed that 60.4% of consumers preferred fish fillets over whole fish. The 8°C group had the lowest growth, 41% and 29% lower than 16°C and 12°C, respectively, but the highest condition factor. Wild-caught plaice have a seasonal cycle with a condition factor between 0.9-1.2 (De Vlas, 1979), and the plaice reared at three different

temperatures had a condition factor of 1.6-1.7. Even though the plaice reared at 16°C had the lowest condition factor (range 1.2 to 2.4), it is still at least 0.3 higher than the wild-caught plaice. The condition factor of Japanese flounder showed the opposite effect; the condition factor was higher at increased temperatures than colder ones (Fonds et al., 1995).

In this current study, increased temperature led to increased growth, but increased temperature is also known to increase bacterial growth (Markošová & Jeźek, 1994) and thermal stress (Triantaphyllopoulos et al., 2019). The tanks had to be cleaned more frequently with increased temperature. A pink coating appeared more frequently in the 16°C rearing tanks, followed by 12°C, and lastly, 8°C. A flapping behavior was observed when cleaning the tank, indicating that the fish was stressed. Stress can lead to reduced immune defenses in the fish (Nardocci et al., 2014), causing the fish to be more susceptible to bacteria, and consequently, the survival rate may be reduced.

Growth, condition factor, and bacterial growth are all important factors in evaluating the rearing conditions of a new species. The European plaice grew faster with higher temperatures, but the condition factor is inversely correlated. The 16°C group had the highest growth but also had the lowest condition factor and the most observed bacterial growth. The 12°C group had high growth, a high condition factor, and less bacterial growth than 16°C. The 8°C group had the highest condition factor and little bacterial growth in the rearing tank but significantly lower growth. Based on those findings, a rearing temperature of 12°C is recommended for the on-growing of juvenile plaice.

4.2 Temperature effect on gene expression

4.2.1 Gene expression of *ghr* and *igf-1* in liver

Age, season, environment, and nutritional status can affect the gene expression and tissue distribution of *ghr* (Zhao et al., 2015). In teleost fish, the expression of g*hr* in the liver was reduced during fasting (Triantaphyllopoulos et al., 2019). *ghr* transcript levels in the liver of European plaice reared at 12°C and 16°C decreased from first to second sampling, then increased in final sampling, but only the 12°C had a significant increase in final sampling. Since the fish reared at 12°C and 16°C has the most remarkable growth despite low hepatic *ghr* transcript levels, it suggests that there may be other growth regulatory mechanisms at play.

While *ghr* is important for growth, it is not the sole determinant (Vélez et al., 2017). Other factors, such as hormone signaling pathways or environmental conditions (Vélez et al., 2017), could compensate for the low *ghr* transcript levels and promote fish growth.

Nutritional condition and growth rate are correlated with circulating levels of *gh*, *igf-1*, and their respective binding proteins (GhBP, IgfBP) and cell membrane receptors (Pérez-Sánchez et al., 2002; Imsland et al., 2007; Hagen et al., 2009). In turbot, plasma Igf-1 concentrations were three times higher in fast- than slow-growing individuals (Imsland et al., 2007). In the current study, the *igf-1* transcript levels of 12°C and 16°C significantly increased from second to final sampling, and 8°C did not significantly increase in this period. This corresponds to the growth curve in Figure 13, where 12°C and 16°C degrees had steeper growth curves in this period, indicating temperature and growth have affected the *igf-1* transcript levels.

4.2.2 Gene expression of *ghr* and *igf-1r* in muscle

Muscle tissue in fish has been found to have increased *ghr* levels during fasting and returning to normal levels after the fish feeds again (Triantaphyllopoulos et al., 2019). There was no clear connection between temperature and gene transcript levels of *ghr* in the muscle. Fish reared at 16°C displayed the best growth and the highest gene transcript levels of muscular *ghr*. On the other hand, the fish reared at 8°C had the lowest growth, but moderate gene transcript levels. Lastly, the fish reared at 12°C displayed medium growth, but the lowest *ghr* gene transcript levels. This suggests that other factors may influence the growth of plaice at different temperatures, apart from the gene transcript levels of muscular *ghr* alone. The endogenous proteolytic systems are also essential in controlling growth (Vélez et al., 2017).

The gene transcript levels of *igf-1r* in the muscle increased with increased temperature, indicating that higher temperatures may enhance the signaling pathway of *igf-1r*. The upregulation of *igf-1r* expression in warmer temperatures may indicate an adaptive mechanism to support growth in a thermally favorable environment. Studies on Senegalese sole (*Solea senegalensis*) (Campos et al., 2013) and rainbow trout (*Oncorhynchus mykiss*) (Gabillard et al., 2003) have found the opposite results, i.e., gene transcript levels of *igf-1r* did not correspond with temperature and indicating that muscular growth is not affected by temperature.

4.3 Temperature effect on deformities

The number of deformed vertebrae in the vertebral column of the European plaice increased with increased temperature. The 8°C group had the lowest percentage of deformed fish in the tank (30.0%). The degree of deformities was highest at 12°C (38.0%) and 16°C (38.7%). Increased deformity with increasing temperature aligns with studies on juvenile Atlantic cod (Imsland et al., 2006) and Atlantic wolffish (*Anarhichas lupus*) (Árnason et al., 2019). Combining all three rearing temperatures, the frequency of deformed plaice ranged from 30-38.7%. Deformities in the vertebral column are found in many reared fish species; 61.3-80.0% in Atlantic halibut (Lewis & Lall, 2006), 20-75% in Atlantic cod (Fjelldal et al., 2009b), 4.8-27.6% in turbot (Tong et al., 2012), and 9-32% in Japanese flounder (Lü et al., 2015). In the present experiment, deformities in European plaice were most frequently formed in vertebrae 13-16 – located in the trunk-tail junctional region – which is within the same region Lewis et al. (2004) found the most deformities in Atlantic halibut, Andrades et al. (1996) and Boglione et al. (2001) primarily found lordosis in gilthead sea bream (*Sparus aurata L.*), and one of the regions where Ferreri et al. (2000) found a high percent of frequency of deformities in zebrafish (*Danio rerio*).

The severity of deformities increased with increasing temperature. The fish reared at 16°C and 12° had at least one fish within the range of 26-30 deformed vertebrae out of the total of 43 vertebrae in the vertebral column. Deformities can lead to altered swimming and feeding behavior, stress, and higher disease susceptibility (Fjelldal et al., 2020; Eissa et al., 2021). Severe deformities can consequently lead to fish with reduced growth and welfare, which are two important parameters for high-quality fish in aquaculture. The present results from skeletal deformities in plaice showed that within fish with more than five deformed vertebrae, 16°C had a significantly higher proportion than 12°C and 8°C. Considering deformities, rearing plaice at 16°C is not optimal for farming this species.

Wild-caught fish have fewer deformities than reared fish (Boglione et al., 2001; Fjelldal et al., 2009a, 2009b). Today, there are no studies on the extent of deformities in wild plaice. Vertebral deformities were not found in juvenile wild-caught Japanese flounder (Lü et al., 2015) or in Atlantic salmon (Fjelldal et al., 2006), and only 4% of wild-caught gilthead sea bream have one or two vertebral deformities (Boglione et al., 2001), and 6% of wild-caught Atlantic cod (Fjelldal et al., 2009b). Increased frequency of deformities in wild fish can be observed, often

in conjunction with pollution (Barahona-Fernandes, 1982) and significant variations in environmental parameters such as temperature (Hubbs, 1959). In nature, European plaice is vulnerable to predation, in addition, tidal migrations involve swimming long distances to increase food availability (Raffaelli et al., 1990). Consequently, a deformed wild fish will have a low probability of surviving. Cushing (1975) showed that European plaice's natural mortality would be 80%/month during the first three months, then it will have a mortality of 40%/month for 4-5 months, and 10%/month during their first winter. After that, it will have a mortality rate of 10%/year (Cushing, 1975). The plaice in this study had an 86% fertilization and low mortality before and during the experiment. Only three fish died in total while rearing the plaice at three different temperatures for 100 days. A cultured fish will not face the same natural environmental challenges as a wild fish and will, therefore, have a higher survival rate, including the deformed fish. This can be one of the explanatory reasons for the increased proportion of deformed fish in aquaculture compared to nature.

Although survival is much higher in aquaculture than in the wild, and the fish have a greater chance of surviving with deformities in rearing tanks, the proportion of deformities in all temperatures is still high, indicating that it is not only temperature affecting deformities. Diet (Pérez-Sánchez et al., 2002; Imsland et al., 2007; Hagen et al., 2009; Zhao et al., 2015), genetic factors (Ishikawa, 1990), epigenetic factors (Fjelldal et al., 2009a), and other environmental factors, such as light, flow, and pH (Gavaia et al., 2009) may be one of the reasons that deformities have occurred. Deformities can be formed by the interaction between deformity-promoting factors (Jawad et al., 2018). For future aquaculture farming, factors causing deformities in the vertebral column must be minimized to ensure good growth and welfare.

Overall, this study shows that higher temperatures led to both increased deformities and increased severity of deformities in European plaice. The 8°C had the lowest number of deformed vertebrae in the vertebral column, and the deformities were less severe, followed by 12°C, and lastly, 16°C. 30.0-38.7% of the fish was deformed in all three temperatures. Generally, there are very few fish with deformities in nature, but no comparative studies have been done on wild European plaice. However, most wild fish, especially weakened fish, will not survive to become adults. Considering both deformities and growth, the optimal temperature for rearing European plaice is 12°C.

4.4 Synopsis: Optimal rearing conditions for European plaice

In aquaculture, many factors influence the rearing conditions of a species, and economy is a driving factor. The size of the fish plays a huge role in the industry, and bigger fish are more valuable. Temperature influenced growth in juvenile European plaice. The plaice grew fastest at 16°C, followed by the 12°C group, and lastly, the 8°C, which had significantly lower growth than the others. It is not economically beneficial to rear juvenile plaice at 8°C due to the slow growth. Considering only the weight, the fish reared at 16°C would have been the preferred group. As mentioned, the consumer prefers to buy fish filets (Tsoukalas et al., 2022; Solgaard et al., 2023), and fish with higher condition factor gives larger and more valuable filets. Considering this, 12°C is a good candidate due to the high condition factor and high growth.

Vertebral deformities can lead to economic losses because of increased mortality, limited swimming and feeding behavior, and reduced growth (Fjelldal et al., 2020; Han et al., 2020; Eissa et al., 2021). The present results revealed that increased temperature accelerated growth, but it also accelerated the deformities in European plaice. The 8°C group had approximately 8% less deformities than 12°C and 16°C, but it had 41% and 29% lower growth than 16°C and 12°C, respectively. The 12°C and 16°C had approximately the same number of deformed fish in the tanks, however, the 16°C had more severe deformities. Due to the low growth of the 8°C group and the more severe deformities in the 16°C, the 12°C group will be the best temperature to adapt to aquaculture.

4.5 Summary of hypothesis

The H_0 was rejected because temperature did affect growth, gene expression of growth-regulating factors, and deformities in juvenile plaice.

The H_1, with subhypoteses, was accepted because temperature influenced growth in juvenile plaice. Increased temperature led to increased growth.

The H_2 was accepted because gene expression of growth-regulating factors in juvenile plaice was influenced by temperature. However, the subhypotheses are not accepted because juvenile

plaice do not have higher gene expression of growth-regulating factors with increased temperature.

The H_3, with subhypothesis, was accepted because temperature influenced skeletal development in juvenile plaice. Increased temperature led to increased vertebral deformities.

5 Conclusion

To conclude, growth and deformities of European plaice increased with increasing temperature, but the condition factor was inversely correlated to temperature. In aquaculture, a fish with a high condition factor, good growth, and minimal deformities is preferred, and therefore, 12°C is recommended for rearing juvenile European plaice.

References

Afewerki, S., Asche, F., Misund, B., Thorvaldsen, T., & Tveteras, R. (2022). Innovation in the Norwegian aquaculture industry. *Reviews in Aquaculture*. https://doi.org/10.1111/raq.12755

Akvaplan niva. (2019). *Kunnskapsgrunnlag for nye arter i oppdrett*.

Albert, O. T., Eliassen, J.-E., & Høines, Å. (1998). Flatfishes of Norwegian coasts and fjords. *Journal of Sea Research*, *40*(1–2), 153–171. https://doi.org/10.1016/S1385-1101(98)00013-6

Andrades, J. A., Becerra, J., & Fernández-Llebrez, P. (1996). Skeletal deformities in larval, juvenile and adult stages of cultured gilthead sea bream (*Sparus aurata* L.). *Aquaculture*, *141*(1–2), 1–11. https://doi.org/10.1016/0044-8486(95)01226-5

Árnason, T., Gunnarsson, Á., Steinarsson, A., Daníelsdóttir, A. K., & Björnsson, B. T. (2019). Impact of temperature and growth hormone on growth physiology of juvenile Atlantic wolffish (*Anarhichas lupus*). *Aquaculture*, *504*, 404–413. https://doi.org/10.1016/j.aquaculture.2019.02.025

Barahona-Fernandes, M. H. (1982). Body deformation in hatchery reared European sea bass *Dicentrarchus labrax* (L). Types, prevalence and effect on fish survival. *Journal of Fish Biology*, *21*(3), 239–249. https://doi.org/10.1111/j.1095-8649.1982.tb02830.x

Basaran, F., Ozbilgin, H., & Ozbilgin, Y. D. (2007). Comparison of the swimming performance of farmed and wild gilthead sea bream, *Sparus aurata*. *Aquaculture Research*, *38*(5), 452–456. https://doi.org/10.1111/j.1365-2109.2007.01670.x

Bauchot, M.-L. (1987). Poissons osseux. In W. Fischer, M.L. Bauchot and M. Schneider (Eds.). *Fiches FAO d'identification pour les besoins de la pêche. (rev. 1). Méditerranée et mer Noire. Zone de pêche 37*. (Vol. II. pp. 891-1421.). Commission des Communautés Européennes and FAO.

Beuvard, C., Imsland, A. K. D., & Thorarensen, H. (2022). The effect of temperature on growth performance and aerobic metabolic scope in Arctic charr, *Salvelinus alpinus* (L.). *Journal of Thermal Biology*, *104*, 103117. https://doi.org/10.1016/j.jtherbio.2021.103117

Blum, J. R., Chernoff, H., Rosenblatt, M., & Teicher, H. (1958). Central Limit Theorems for Interchangeable Processes. *Canadian Journal of Mathematics*, *10*, 222–229. https://doi.org/10.4153/CJM-1958-026-0

Boglione, C., Costa, C., di Dato, P., Ferzini, G., Scardi, M., & Cataudella, S. (2003). Skeletal quality assessment of reared and wild sharpsnout sea bream and pandora juveniles. *Aquaculture*, *227*(1–4), 373–394. https://doi.org/10.1016/S0044-8486(03)00515-5

Boglione, C., Gagliardi, F., Scardi, M., & Cataudella, S. (2001). Skeletal descriptors and quality assessment in larvae and post-larvae of wild-caught and hatchery-reared gilthead sea bream (*Sparus aurata* L. 1758). *Aquaculture*, *192*(1), 1–22. https://doi.org/10.1016/S0044-8486(00)00446-4

Bristow, P. (1992). *The illustrated encyclopedia of fishes*. Chancellor Press.

Burel, C., Person-Le Ruyet, J., Gaumet, F., le Roux, A., Severe, A., & Boeuf, G. (1996). Effects of temperature on growth and metabolism in juvenile turbot. *Journal of Fish Biology*, *49*(4), 678–692. https://doi.org/10.1111/j.1095-8649.1996.tb00064.x

Campos, C., Valente, L. M. P., Conceição, L. E. C., Engrola, S., Sousa, V., Rocha, E., & Fernandes, J. M. O. (2013). Incubation temperature induces changes in muscle cellularity and gene expression in Senegalese sole (*Solea senegalensis*). *Gene*, *516*(2), 209–217. https://doi.org/10.1016/j.gene.2012.12.074

Canosa, L. F., & Bertucci, J. I. (2020). Nutrient regulation of somatic growth in teleost fish. The interaction between somatic growth, feeding and metabolism. *Molecular and Cellular Endocrinology*, *518*, 111029. https://doi.org/10.1016/j.mce.2020.111029

Claireaux, G., & Lagardère, J.-P. (1999). Influence of temperature, oxygen and salinity on the metabolism of the European sea bass. *Journal of Sea Research*, *42*(2), 157–168. https://doi.org/10.1016/S1385-1101(99)00019-2

Choi, J., Han, G. S., Lee, K. W., Byun, S.-G., Lim, H. J., Lee, C.-H., Lee, D.-Y., & Kim, H. S. (2021). Effects of feeding differentially enriched Artemia nauplii on the survival, growth, fatty acid composition, and air exposure stress response of Pacific cod (*Gadus macrocephalus*) larvae. *Aquaculture Reports*, *21*, 100829. https://doi.org/10.1016/j.aqrep.2021.100829

Cosson, J., Groison, A.-L., Suquet, M., Fauvel, C., Dreanno, C., & Billard, R. (2008). Studying sperm motility in marine fish: an overview on the state of the art. *Journal of Applied Ichthyology*, *24*(4), 460–486. https://doi.org/10.1111/j.1439-0426.2008.01151.x

Cushing, D. H. (1975). The natural mortality of the plaice. *ICES Journal of Marine Science*, *36*(2), 150–157. https://doi.org/10.1093/icesjms/36.2.150

Dawson, A. S., & Grimm, A. S. (1980). Quantitative seasonal changes in the protein, lipid and energy content of the carcass, ovaries and liver of adult female plaice, *Pleuronectes*

platessa L. *Journal of Fish Biology*, *16*(5), 493–504. https://doi.org/10.1111/j.1095-8649.1980.tb03729.x

De Vlas, J. (1979). Annual food intake by plaice and flounder in a tidal flat area in the dutch wadden sea, with special reference to consumption of regenerating parts of macrobenthic prey. *Netherlands Journal of Sea Research*, *13*(1), 117–153. https://doi.org/10.1016/0077-7579(79)90037-1

Eissa, A. E., Abu-Seida, A. M., Ismail, M. M., Abu-Elala, N. M., & Abdelsalam, M. (2021). A comprehensive overview of the most common skeletal deformities in fish. *Aquaculture Research*, *52*(6), 2391–2402. https://doi.org/10.1111/are.15125

Eriksen, E., Benzik, A. N., Dolgov, A. v., Skjoldal, H. R., Vihtakari, M., Johannesen, E., Prokhorova, T. A., Keulder-Stenevik, F., Prokopchuk, I., & Strand, E. (2020). Diet and trophic structure of fishes in the Barents Sea: The Norwegian-Russian program "Year of stomachs" 2015 – Establishing a baseline. *Progress in Oceanography*, *183*, 102262. https://doi.org/10.1016/j.pocean.2019.102262

FAO. (2022). *The State of World Fisheries and Aquaculture 2022*. FAO. https://doi.org/10.4060/cc0461en

Ferreri, F., Nicolais, C., Boglione, C., & Bmertoline, B. (2000). Skeletal characterization of wild and reared zebrafish: anomalies and meristic characters. *Journal of Fish Biology*, *56*(5), 1115–1128. https://doi.org/10.1111/j.1095-8649.2000.tb02127.x

Fey, D. P., & Greszkiewicz, M. (2021). Effects of temperature on somatic growth, otolith growth, and uncoupling in the otolith to fish size relationship of larval northern pike, *Esox lucius* L. *Fisheries Research*, *236*, 105843. https://doi.org/10.1016/j.fishres.2020.105843

Fjelldal, P. G., Glover, K. A., Skaala, Ø., Imsland, A., & Hansen, T. J. (2009a). Vertebral body mineralization and deformities in cultured Atlantic salmon (*Salmo salar* L.): Effects of genetics and off-season smolt production. *Aquaculture*, *296*(1–2), 36–44. https://doi.org/10.1016/j.aquaculture.2009.08.020

Fjelldal, P. G., Lock, E.-J., Grotmol, S., Totland, G. K., Nordgarden, U., Flik, G., & Hansen, T. (2006). Impact of smolt production strategy on vertebral growth and mineralisation during smoltification and the early seawater phase in Atlantic salmon (*Salmo salar*, L.). *Aquaculture*, *261*(2), 715–728. https://doi.org/10.1016/j.aquaculture.2006.08.008

Fjelldal, P. G., Madaro, A., Hvas, M., Stien, L. H., Oppedal, F., & Fraser, T. W. (2020). Skeletal deformities in wild and farmed cleaner fish species used in Atlantic salmon *Salmo salar*

aquaculture. *Journal of Fish Biology*, *98*(4), 1049–1058. https://doi.org/10.1111/jfb.14337

Fjelldal, P. G., van der Meeren, T., Jørstad, K. E., & Hansen, T. J. (2009b). A radiological study on vertebral deformities in cultured and wild Atlantic cod (*Gadus morhua*, L.). *Aquaculture*, *289*(1–2), 6–12. https://doi.org/10.1016/j.aquaculture.2008.12.025

Fonds, M., Cronie, R., Vethaak, A. D., & van der Puyl, P. (1992). Metabolism, food consumption and growth of plaice (*Pleuronectes platessa*) and flounder (*Platichthys flesus*) in relation to fish size and temperature. *Netherlands Journal of Sea Research*, *29*(1–3), 127–143. https://doi.org/10.1016/0077-7579(92)90014-6

Fonds, M., Tanaka, M., & van der Veer, H. W. (1995). Feeding and growth of juvenile Japanese flounder *Paralichthys olivaceus* in relation to temperature and food supply. *Netherlands Journal of Sea Research*, *34*(1–3), 111–118. https://doi.org/10.1016/0077-7579(95)90019-5

Fraser, T. W. K., Witten, P. E., Albrektsen, S., Breck, O., Fontanillas, R., Nankervis, L., Thomsen, T. H., Koppe, W., Sambraus, F., & Fjelldal, P. G. (2019). Phosphorus nutrition in farmed Atlantic salmon (*Salmo salar*): Life stage and temperature effects on bone pathologies. *Aquaculture*, *511*, 734246. https://doi.org/10.1016/j.aquaculture.2019.734246

Froese, R. (2006). Cube law, condition factor and weight-length relationships: history, meta-analysis and recommendations. *Journal of Applied Ichthyology*, *22*(4), 241–253. https://doi.org/10.1111/j.1439-0426.2006.00805.x

Fuentes, E. N., Valdés, J. A., Molina, A., & Björnsson, B. T. (2013). Regulation of skeletal muscle growth in fish by the growth hormone – Insulin-like growth factor system. *General and Comparative Endocrinology*, *192*, 136–148. https://doi.org/10.1016/j.ygcen.2013.06.009

Gabillard, J.-C., Weil, C., Rescan, P.-Y., Navarro, I., Gutiérrez, J., & le Bail, P.-Y. (2003). Effects of environmental temperature on IGF1, IGF2, and IGF type I receptor expression in rainbow trout (*Oncorhynchus mykiss*). *General and Comparative Endocrinology*, *133*(2), 233–242. https://doi.org/10.1016/S0016-6480(03)00167-9

Gavaia, P. J., Domingues, S., Engrola, S., Drake, P., Sarasquete, C., Dinis, M. T., & Cancela, M. L. (2009). Comparing skeletal development of wild and hatchery-reared Senegalese sole (*Solea senegalensis*, Kaup 1858): evaluation in larval and postlarval stages. *Aquaculture Research*, *40*(14), 1585–1593. https://doi.org/10.1111/j.1365-2109.2009.02258.x

Gibson, R. N (1999) Movement and homing in intertidal fishes. In M.H. Horn, K.L.M. Martin and M.A. Chotkowski (eds.) *Intertidal fishes. Life in two worlds.* (p. 97-125, p 399) Academic Press.

Gjerde, B., Pante, Ma. J. R., & Baeverfjord, G. (2005). Genetic variation for a vertebral deformity in Atlantic salmon (*Salmo salar*). *Aquaculture*, *244*(1–4), 77–87. https://doi.org/10.1016/j.aquaculture.2004.12.002

Grini, A., Hansen, T., Berg, A., Wargelius, A., & Fjelldal, P. G. (2011). The effect of water temperature on vertebral deformities and vaccine-induced abdominal lesions in Atlantic salmon, *Salmo salar* L. *Journal of Fish Diseases*, *34*(7), 531–546. https://doi.org/10.1111/j.1365-2761.2011.01265.x

Hagen, Ø., Fernandes, J. M. O., Solberg, C., & Johnston, I. A. (2009). Expression of growth-related genes in muscle during fasting and refeeding of juvenile Atlantic halibut, *Hippoglossus hippoglossus* L. *Comparative Biochemistry and Physiology Part B: Biochemistry and Molecular Biology*, *152*(1), 47–53. https://doi.org/10.1016/j.cbpb.2008.09.083

Hamidoghli, A., Won, S., Lee, S., Lee, S., Farris, N. W., & Bai, S. C. (2020). Nutrition and Feeding of Olive Flounder *Paralichthys olivaceus*: A Review. *Reviews in Fisheries Science & Aquaculture*, *28*(3), 340–357. https://doi.org/10.1080/23308249.2020.1740166

Hamre, K., Erstad, B., Kok, J., Norberg, B., & Harboe, T. (2020). Change in nutrient composition of *Artemia* grown for 3–4 days and effects of feeding on-grown *Artemia* on performance of Atlantic halibut (*Hippoglossus hippoglossus* , L.) larvae. *Aquaculture Nutrition*, *26*(5), 1542–1554. https://doi.org/10.1111/anu.13101

Han, M., Luo, M., Yang, R., Qin, J. G., & Ma, Z. (2020). Impact of temperature on survival and spinal development of golden pompano *Trachinotus ovatus* (Linnaeus 1758). *Aquaculture Reports*, *18*, 100556. https://doi.org/10.1016/j.aqrep.2020.100556

Hubbs, C. (1959). High incidence of vertebral deformities in two natural populations of fishes inhabiting warm springs. Ecology, 40 (1): 154-155.

IBM Corp. (2020). IBM SPSS Statistics for Macintosh (Version 28.0). Armonk, NY, United States. IBM Corp

Imsland, A. K., Björnsson, B. T., Gunnarsson, S., Foss, A., & Stefansson, S. O. (2007). Temperature and salinity effects on plasma insulin-like growth factor-I concentrations and growth in juvenile turbot (*Scophthalmus maximus*). *Aquaculture*, *271*(1–4), 546–552. https://doi.org/10.1016/j.aquaculture.2007.07.007

Imsland, A. K., Foss, A., Koedijk, R., Folkvord, A., Stefansson, S. O., & Jonassen, T. M. (2006). Short- and long-term differences in growth, feed conversion efficiency and deformities in juvenile Atlantic cod (*Gadus morhua*) startfed on rotifers or zooplankton. *Aquaculture Research*, *37*(10), 1015–1027. https://doi.org/10.1111/j.1365-2109.2006.01523.x

Imsland, A. K., Sunde, L. M., Folkvord, A., & Stefansson, S. O. (1996). The interaction of temperature and fish size on growth of juvenile turbot. *Journal of Fish Biology*, *49*(5), 926–940. https://doi.org/10.1111/j.1095-8649.1996.tb00090.x

Ishikawa, Y. (1990). Development of caudal structures of a morphogenetic mutant (Da) in the teleost fish, medaka (*Oryzias latipes*). *Journal of Morphology*, *205*(2), 219–232. https://doi.org/10.1002/jmor.1052050209

Jakobsen, T., & Ozhigin, V. K. (2011). *The Barents Sea - ecosystem, resources, management, half a century of Russian - Norwegian cooperation* (L. Postmyr, Ed.). Tapir academic press.

Janssen, J. A. M. J. L. (2020). Mechanisms of putative IGF-I receptor resistance in active acromegaly. *Growth Hormone & IGF Research*, *52*, 101319. https://doi.org/10.1016/j.ghir.2020.101319

Jawad, L. A., Fjelldal, P. G., & Hansen, T. (2018). First report on vertebral abnormality in the fivebeard rockling *Ciliata mustela* (Linnaeus, 1758) (Osteichthyes: Lotidae) from Masfjorden, Western Norway. *Marine Biodiversity*, *48*(2), 957–961. https://doi.org/10.1007/s12526-016-0545-7

Jonassen, T. M., Imsland, A. K., & Stefansson, S. O. (1999). The interaction of temperature and fish size on growth of juvenile halibut. *Journal of Fish Biology*, *54*(3), 556–572. https://doi.org/10.1111/j.1095-8649.1999.tb00635.x

Kendler, S., Tsoukalas, D., Jakobsen, A. N., Zhang, J., Asimakopoulos, A. G., & Lerfall, J. (2023). Seasonal variation in chemical composition and contaminants in European plaice (*Pleuronectes Platessa*) originated from the west-coast of Norway. *Food Chemistry*, *401*, 134155. https://doi.org/10.1016/j.foodchem.2022.134155

Kuipers, B. (1973). On the tidal migration of young plaice (*Pleuronectes platessa*) in the Wadden Sea. *Netherlands Journal of Sea Research*, *6*(3), 376–388. https://doi.org/10.1016/0077-7579(73)90023-9

Kuipers, B. R. (1977). On the ecology of juvenile plaice on a tidal flat in the Wadden Sea. *Netherlands Journal of Sea Research*, *11*(1), 56–91. https://doi.org/10.1016/0077-7579(77)90021-7

Lafrance, R., Villicaña, C., Valdéz-Torres, J. B., Martínez-Montoya, H., Castillo-Ruiz, O., Alemán-Castillo, S. E., Esparza-Araiza, M. J., & León-Félix, J. (2021). Optimization of PCR-based TYLCV molecular markers by response surface methodology. *Gene*, *785*, 145606. https://doi.org/10.1016/j.gene.2021.145606

Lall, S. P., & Lewis-McCrea, L. M. (2007). Role of nutrients in skeletal metabolism and pathology in fish — An overview. *Aquaculture*, *267*(1–4), 3–19. https://doi.org/10.1016/j.aquaculture.2007.02.053

Lara-Diaz, V., Castilla-Cortazar, I., Martín-Estal, I., García-Magariño, M., Aguirre, G., Puche, J., de la Garza, R., Morales, L., & Muñoz, U. (2017). IGF-1 modulates gene expression of proteins involved in inflammation, cytoskeleton, and liver architecture. *Journal of Physiology and Biochemistry*, *73*(2), 245–258. https://doi.org/10.1007/s13105-016-0545-x

Lewis, L. M., & Lall, S. P. (2006). Development of the axial skeleton and skeletal abnormalities of Atlantic halibut (*Hippoglossus hippoglossus*) from first feeding through metamorphosis. *Aquaculture*, *257*(1–4), 124–135. https://doi.org/10.1016/j.aquaculture.2006.02.067

Lewis, L. M., Lall, S. P., & Eckhard Witten, P. (2004). Morphological descriptions of the early stages of spine and vertebral development in hatchery-reared larval and juvenile Atlantic halibut (*Hippoglossus hippoglossus*). *Aquaculture*, *241*(1–4), 47–59. https://doi.org/10.1016/j.aquaculture.2004.08.018

Li, S., Guo, H., Chen, Z., Jiang, Y., Shen, J., Pang, X., & Li, Y. (2021). Effects of acclimation temperature regime on the thermal tolerance, growth performance and gene expression of a cold-water fish, *Schizothorax prenanti*. *Journal of Thermal Biology*, *98*, 102918. https://doi.org/10.1016/j.jtherbio.2021.102918

Little, A. G., Loughland, I., & Seebacher, F. (2020). What do warming waters mean for fish physiology and fisheries? *Journal of Fish Biology*, *97*(2), 328–340. https://doi.org/10.1111/jfb.14402

Lü, H., Zhang, X., Fu, M., Xi, D., Su, S., & Yao, W. (2015). Vertebral deformities in hatchery-reared and wild-caught juvenile Japanese flounder, *Paralichthys olivaceus*. *Chinese Journal of Oceanology and Limnology*, *33*(1), 84–91. https://doi.org/10.1007/s00343-015-4041-x

Markošová, R., & Ježek, J. (1994). Indicator bacteria and limnological parameters in fish ponds. *Water Research*, *28*(12), 2477–2485. https://doi.org/10.1016/0043-1354(94)90066-3

Mohd Nani, S. Z., Majid, F. A. A., Jaafar, A. B., Mahdzir, A., & Musa, M. N. (2016). Potential Health Benefits of Deep Sea Water: A Review. *Evidence-Based Complementary and Alternative Medicine*, *2016*, 1–18. https://doi.org/10.1155/2016/6520475

Muus, B. J., & Dahlström, P. (1974). *Collins guide to the sea fishes of Britain and North-Western Europe*. Collins.

Muus, B. J., & Nielsen, J. G. (1999). *Sea fish*. Scandinavian Fishing Year Book.

Nardocci, G., Navarro, C., Cortés, P. P., Imarai, M., Montoya, M., Valenzuela, B., Jara, P., Acuña-Castillo, C., & Fernández, R. (2014). Neuroendocrine mechanisms for immune system regulation during stress in fish. *Fish & Shellfish Immunology*, *40*(2), 531–538. https://doi.org/10.1016/j.fsi.2014.08.001

Nielsen, J. G. (1986). Pleuronectidae. In P.J.P. Whitehead, M.-L. Bauchot, J.-C. Hureau, J. Nielsen, & E. Tortonese (Eds.), *Fishes of the North-eastern Atlantic and the Mediterranean* (Vol. 3, pp. 1299–1307). UNESCO.

Norberg, B., Valkner, V., Huse, J., Karlsen, I., & Grung, G. L. (1991). Ovulatory rhythms and egg viability in the Atlantic halibut (*Hippoglossus hippoglossus*). *Aquaculture*, *97*(4), 365–371. https://doi.org/10.1016/0044-8486(91)90328-5

Nordvik, K., Kryvi, H., Totland, G. K., & Grotmol, S. (2005). The salmon vertebral body develops through mineralization of two preformed tissues that are encompassed by two layers of bone. *Journal of Anatomy*, *206*(2), 103–114. https://doi.org/10.1111/j.1469-7580.2005.00372.x

Pérez-Sánchez, J., Calduch-Giner, J. A., Mingarro, M., Vega-Rubín de Celis, S., Gómez-Requeni, P., Saera-Vila, A., Astola, A., & Valdivia, M. M. (2002). Overview of Fish Growth Hormone Family. New Insights in Genomic Organization and Heterogeneity of Growth Hormone Receptors. *Fish Physiology and Biochemistry*, *27*(3/4), 243–258. https://doi.org/10.1023/B:FISH.0000032729.72746.c8

Purohit, G. K., Mahanty, A., Mohanty, B. P., & Mohanty, S. (2016). Evaluation of housekeeping genes as references for quantitative real-time PCR analysis of gene expression in the murrel *Channa striatus* under high-temperature stress. *Fish Physiology and Biochemistry*, *42*(1), 125–135. https://doi.org/10.1007/s10695-015-0123-0

R Core Team (2023). R: A language and environment for statistical computing. R Foundation for Statistical Computing, Vienna, Austria. https://www.R-project.org/

Raffaelli, D., Richner, H., Summers, R., & Northcott, S. (1990). Tidal migrations in the flounder *(Platichthys flesus)*. *Marine Behaviour and Physiology*, *16*(4), 249–260. https://doi.org/10.1080/10236249009378753

Reinecke, M., Björnsson, B. T., Dickhoff, W. W., McCormick, S. D., Navarro, I., Power, D. M., & Gutiérrez, J. (2005). Growth hormone and insulin-like growth factors in fish: Where we are and where to go. *General and Comparative Endocrinology*, *142*(1–2), 20–24. https://doi.org/10.1016/j.ygcen.2005.01.016

Rollefsen, G. (1940) Utklekking og oppdretting av saltvannsfisk

Sheridan, M. A. (2021). Coordinate regulation of feeding, metabolism, and growth: Perspectives from studies in fish. *General and Comparative Endocrinology*, *312*, 113873. https://doi.org/10.1016/j.ygcen.2021.113873

Roy, S. M., P, J., Machavaram, R., Pareek, C. M., & Mal, B. C. (2021). Diversified aeration facilities for effective aquaculture systems—a comprehensive review. *Aquaculture International*, *29*(3), 1181–1217. https://doi.org/10.1007/s10499-021-00685-7

Solgaard, H. S., Yang, Y., & Nguyen, T. T. (2023). An investigation of consumers' preference and willingness to pay for fish welfare in Denmark: A discrete choice modeling approach. *Aquaculture*, *574*, 739652. https://doi.org/10.1016/j.aquaculture.2023.739652

Ståhle, L., & Wold, S. (1989). Analysis of variance (ANOVA). *Chemometrics and Intelligent Laboratory Systems*, *6*(4), 259–272. https://doi.org/10.1016/0169-7439(89)80095-4

Taylor, S., Wakem, M., Dijkman, G., Alsarraj, M., & Nguyen, M. (2010). A practical approach to RT-qPCR—Publishing data that conform to the MIQE guidelines. *Methods*, *50*(4), S1–S5. https://doi.org/10.1016/j.ymeth.2010.01.005

Tong, X. H., Liu, Q. H., Xu, S. H., Ma, D. Y., Xiao, Z. Z., Xiao, Y. S., & Li, J. (2012). Skeletal development and abnormalities of the vertebral column and of the fins in hatchery-reared turbot *Scophthalmus maximus*. *Journal of Fish Biology*, *80*(3), 486–502. https://doi.org/10.1111/j.1095-8649.2011.03173.x

Triantaphyllopoulos, K. A., Cartas, D., & Miliou, H. (2019). Factors influencing *GH* and *IGF-I* gene expression on growth in teleost fish: how can aquaculture industry benefit? *Reviews in Aquaculture*, raq.12402. https://doi.org/10.1111/raq.12402

Tsoukalas, D., Kendler, S., Lerfall, J., & Jakobsen, A. N. (2022). The effect of fishing season and storage conditions on the quality of European plaice (*Pleuronectes platessa*). *LWT*, *170*, 114083. https://doi.org/10.1016/j.lwt.2022.114083

Valasek, M. A., & Repa, J. J. (2005). The power of real-time PCR. *Advances in Physiology Education*, *29*(3), 151–159. https://doi.org/10.1152/advan.00019.2005

Vélez, E. J., Lutfi, E., Azizi, Sh., Perelló, M., Salmerón, C., Riera-Codina, M., Ibarz, A., Fernández-Borràs, J., Blasco, J., Capilla, E., Navarro, I., & Gutiérrez, J. (2017).

Understanding fish muscle growth regulation to optimize aquaculture production. *Aquaculture*, *467*, 28–40. https://doi.org/10.1016/j.aquaculture.2016.07.004

Vinnikov, K. A., Thomson, R. C., & Munroe, T. A. (2018). Revised classification of the righteye flounders (Teleostei: Pleuronectidae) based on multilocus phylogeny with complete taxon sampling. *Molecular Phylogenetics and Evolution*, *125*, 147–162. https://doi.org/10.1016/j.ympev.2018.03.014

Viðarsson, J. R., Nielsen, M., Þórðarson, G., Stefansson, G., & Salz, P. (2022). *Nordic and North European Flatfish Value Chains*. Nordisk Ministerråd. https://doi.org/10.6027/temanord2022-559

Volkoff, H., & Rønnestad, I. (2020). Effects of temperature on feeding and digestive processes in fish. *Temperature*, *7*(4), 307–320. https://doi.org/10.1080/23328940.2020.1765950

Wang, X., Hsu, M.-Y., Steinbacher, T. E., Monticello, T. M., & Schumacher, W. A. (2007). Quantification of platelet composition in experimental venous thrombosis by real-time polymerase chain reaction. *Thrombosis Research*, *119*(5), 593–600. https://doi.org/10.1016/j.thromres.2006.04.011

Wardle, C. S., Videler, J. J., & Altringham, J. D. (1995). Tuning In To Fish Swimming Waves: Body Form, Swimming Mode And Muscle Function. *Journal of Experimental Biology*, *198*(8), 1629–1636. https://doi.org/10.1242/jeb.198.8.1629

Webb, P. W. (1984). Form and Function in Fish Swimming. *Scientific American*, *251*(1), 72–83. https://doi.org/10.1038/scientificamerican0784-72

Witten, P. E., Gil-Martens, L., Huysseune, A., Takle, H., & Hjelde, K. (2009). Towards a classification and an understanding of developmental relationships of vertebral body malformations in Atlantic salmon (*Salmo salar* L.). *Aquaculture*, *295*(1–2), 6–14. https://doi.org/10.1016/j.aquaculture.2009.06.037

Zhao, J. L., Si, Y. F., He, F., Wen, H. S., Li, J. F., Ren, Y. Y., Zhao, M. L., Huang, Z. J., & Chen, S. L. (2015). Polymorphisms and DNA methylation level in the CpG site of the GHR1 gene associated with mRNA expression, growth traits and hormone level of half-smooth tongue sole (Cynoglossus semilaevis). *Fish Physiology and Biochemistry*, *41*(4), 853–865. https://doi.org/10.1007/s10695-015-0052-y

Appendix 1 – Discussion of materials and methods

Examination of parental generation

Deformities in fish can be caused by genetic abnormalities or mutations, therefore it is not recommended to select breeders with high prevalence of deformities (Gjerde et al., 2005). Genetic screening of the parental generation used for this experiment was not carried out. The parental generation may have deformities. There were four groups included in the experiment, and if deformities are genetically predisposed, then the fish could inherit them. For future aquaculture farming, fish will be selected from various criteria, we did not have the opportunity to do that. This means that it is possible that the fish used in this experiment have genetic deformities. However, this may explain that there are deformities in the fish at the beginning of the experiment, but it will not explain the difference between temperature in the final sampling. Flow, temperature (Gavaia et al., 2009), and nutritional status (Pérez-Sánchez et al., 2002; Imsland et al., 2007; Hagen et al., 2009; Zhao et al., 2015) are some factors that can influence deformities in fish.

Flow

The experiment was carried out in a start feeding locality with flowmeters limited to measuring waterflow more than of 9 L/min. Once the flow was above 9 L/min, it was registered as 9 + L/min, and not the actual flow. In retrospect, I see that it would have been beneficial to take manual measurements of flow to determine whether flow affected deformities. The flow was regulated considering the oxygen levels, and the flow was more frequently increased in the tanks with 12°C and 16°C water, and these two temperature groups also had more deformities.

Diet

Poor diet or an inadequate supply of essential nutrients can lead to developmental issues in all living organisms (Hamidoghli et al., 2020). European plaice is represented in the list of new marine species for aquaculture, and optimal feed has not yet been developed. Therefore, experience and knowledge from the feeding protocol of Atlantic halibut were adapted into rearing the plaice. It is, however, possible that poor nutritional status may have affected both growth and the results for gene expression (Pérez-Sánchez et al., 2002; Imsland et al., 2007; Hagen et al., 2009; Zhao et al., 2015), further investigation should be made on the role of nutritional status.

Use of ANOVA with significant differences in normal distribution of the data

There are some criteria to use ANOVA (Analysis of variance); the data should have a normal distribution, homogeneity of variance, and the data should be independent (Ståhle & Wold, 1989). In this study, the Shapiro-Wilk normality test showed that many of the datasets were not normally distributed. However, the central limit theorem (Blum et al., 1958) can defend that the data are normally distributed. The central limit theorem asserts that if the random variables are independent and identically distributed it approaches a normal distribution as the number approaches infinity (Blum et al., 1958), which is the case in this study.

Microscopic and molecular examination for parasites

At the end of the experiment, five fish from each temperature were given to another master's student, Georg Jarand Aleksander Remme Hollevik, for microscopic and molecular examination for parasites on the gills. The length and weigh of the fish were measured before the fish was killed by cutting a section over the head, and thereafter delivered for a microscopic examination. The microscopic examination took place at the Marine institute of Research in Austevoll, while the molecular examination took place at the University of Bergen. The microscopic examination of the gills did not result in any findings of trichodinids or costia in the European plaice, and the PCR test looking for Ichthyobodo sp. (costia) also gave negative results.

Appendix 2 – Legal approval of laboratory animal facility 2022-26

Havforskningsinstituttet Forskningsstasjonen Austevoll
Sauganeset 16
5392 STOREBØ

Att. Stig Ove Utskot

Fakturaref: Stig Ove Utskot
Vår ref: 22/75946
Dato: 09.06.2022
Org.nr: 971349077

Statens tilsyn for planter, fisk, dyr og næringsmidler

Mattilsynet

VEDTAK OM VIRKSOMHET - VSID 3127
Virksomhetsnummer 093: Havforskningsinstituttet Forskningsstasjonen Austevoll

Behandlet av Mattilsynet, 09.06.2022.

Saken gjelder
Havforskningsinstituttet søker om regodkjenning av sin forsøksdyrvirksomhet ved stasjonen i Austevoll (avd. 093). Virksomheten utfører forsøk med fisk og krepsdyr både i laboratorium og i felt. Vedlagt søknaden er SSD for Havforskningsinstituttet generelt og for forskningsstasjonen på Austevoll spesielt.

Dokumenter i saken:
Søknad om regodkjenning, VSID 3127, datert 08.06.2022.

Vedtak
Vi regodkjenner Havforskningsinstituttet Forskningsstasjonen Austevoll (avd. 093) som omsøkt. Godkjenningen gjelder fra 17.09.2022 til 16.09.2026. Godkjenningen er gitt på bakgrunn av opplysninger i vedlagte system- og styringsdokumenter.

Godkjenningen er fattet med hjemmel i forskrift 18. juni 2015 nr. 761 om bruk av dyr i forsøk § 37, ref. § 5.

Begrunnelse
For å kunne regodkjenne en forsøksdyrvirksomhet må dere sannsynliggjøre at kravene til forsøksdyrvirksomheter fremdeles er oppfylt. Disse kravene er beskrevet i forsøksdyrforskriften §§ 5 (Godkjenning av oppdrettere, formidlere, brukere og lokaler), 24-27 (Personell og kompetanse, Personell med særskilt kontrollansvar, Dyrevelferdsenhet og Navngitt veterinær eller fiskehelsebiolog), 29-31 (Levemiljø og stell, Innredning og utstyr og Dyrejournal) og 35-36 (Dokumentasjon og Årsrapport). Dyrevelferdsenheten skal bl.a. utarbeide og revidere interne driftsrutiner for å overvåke, dokumentere og følge opp velferden hos dyrene, jf. forsøksdyrforskriften § 26, femte ledd, a). Et system- og styringsdokument (SSD) skal vise at forsøksdyrvirksomheten har tilstrekkelige rutiner for å oppfylle kravene i forsøksdyrforskriften.

Dere har gitt tilfredsstillende informasjon om hvordan disse kravene skal oppfylles.

Vi gjør oppmerksom på at dyrearter med mangelfull kunnskap om ikke skal holdes oppstallet i en forsøksdyravdeling uten at de inngår eller skal inngå i et planlagt forsøk.

Dersom det skjer endringer i virksomheten må dette sendes til Mattilsynets forsøksdyrenhet via FOTS som søknad/melding om endring.

Denne godkjenningen kan trekkes tilbake dersom regelverket ikke følges.

Det vil bli innkrevd et gebyr på 6665 NOK (+100 NOK i administrasjonsgebyr) for behandling av søknad om godkjenning av oppdrettere, brukere og formidlere og lokaler i forbindelse med dyreforsøk, jf. forskrift 13. februar 2004 nr. 406 om betaling av gebyrer for særskilte ytelser fra Mattilsynet § 5.

www.mattilsynet.no

Mattilsynet
Avdeling nasjonale oppgaver

Saksbehandler: Dag Atle Tuft
Tlf.: 22 40 00 00
E-post: postmottak@mattilsynet.no
(Husk mottakers navn)

Postadresse:
Felles postmottak, Postboks 383
2381 Brumunddal
Telefaks: 23 21 68 01

Type virksomhet
Bruker (lab.): Ja
Bruker (felt): Ja
Avl/oppdrett: Nei
Formidler: Nei

Godkjente dyrearter
Fisk og krepsdyr

Vedtak kan påklages til Mattilsynet, jfr. lov 10 feb 1967 om behandlingsmåten i forvaltningssaker(forvaltningsloven) § 28. Klagefristen er 3 uker fra mottak av dette brev, jfr.forvaltningsloven § 29. Klagen stiles til Mattilsynet, Hovedkontoret, men sendes via avdeling nasjonale oppgaver.

Med hilsen

Ole Aarnodt
avdelingssjef

Med hilsen

Dag Atle Tuft
seniorrådgiver

Kopi:
personell med særskilt kontrollansvar
postmottak@mattilsynet.no

Appendix 3 – Dissection of liver and muscle tissue sample

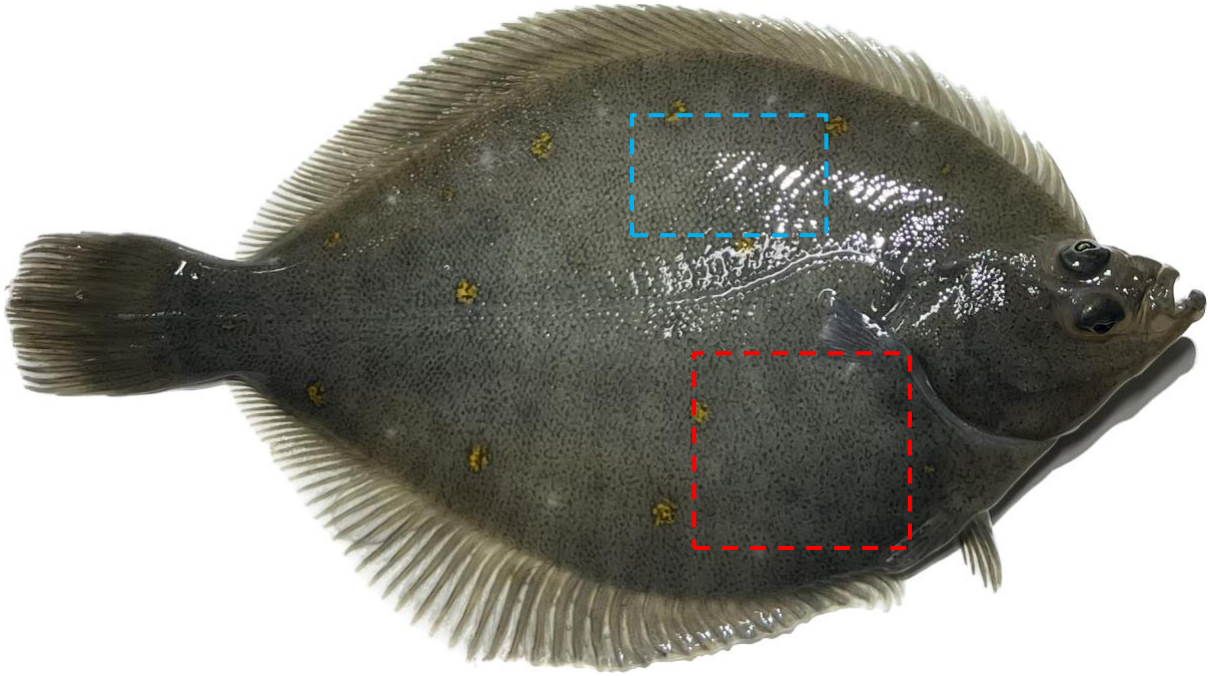

Appendix 3 Figure 1 The area for dissection and retrieving the muscle and liver sample from European plaice. The area marked with dashed blue outline indicates the area the muscle sample was retrieved, and the area marked with dashed red outline indicates the area the liver sample was retrieved.

Appendix 4 – Homogenized muscle and liver in the sample boxes

Appendix 4 Table 1 Homogenized piece of muscle (M) and liver (L) tissue in a sample box with room for 96 samples. Purple: tissue from fish in 12 ℃ water; Red: tissue from fish in 16 ℃ water; Blue: tissue from fish in raw water.

M1 15.09.22	M9 15.09.22	**L5** 15.09.22	M1 17.10.22	M9 17.10.22	M17 17.10.22	M25 17.10.22	M33 17.10.22	M5 14.12.22	M13 14.12.22	M21 14.12.22	M29 14.12.22
M2 15.09.22	M10 15.09.22	**L6** 15.09.22	M2 17.10.22	M10 17.10.22	M18 17.10.22	M26 17.10.22	M34 17.10.22	M6 14.12.22	M14 14.12.22	M22 14.12.22	M30 14.12.22
M3 15.09.22	M11 15.09.22	**L7** 15.09.22	M3 17.10.22	M11 17.10.22	M19 17.10.22	M27 17.10.22	M35 17.10.22	M7 14.12.22	M15 14.12.22	M23 14.12.22	M31 14.12.22
M4 15.09.22	M12 15.09.22	**L8** 15.09.22	M4 17.10.22	M12 17.10.22	M20 17.10.22	M28 17.10.22	M36 17.10.22	M8 14.12.22	M16 14.12.22	M24 14.12.22	M32 14.12.22
M5 15.09.22	**L1** 15.09.22	**L9** 15.09.22	M5 17.10.22	M13 17.10.22	M21 17.10.22	M29 17.10.22	M1 14.12.22	M9 14.12.22	M17 14.12.22	M25 14.12.22	M33 14.12.22
M6 15.09.22	**L2** 15.09.22	**L10** 15.09.22	M6 17.10.22	M14 17.10.22	M22 17.10.22	M30 17.10.22	M2 14.12.22	M10 14.12.22	M18 14.12.22	M26 14.12.22	M34 14.12.22
M7 15.09.22	**L3** 15.09.22	**L11** 15.09.22	M7 17.10.22	M15 17.10.22	M23 17.10.22	M31 17.10.22	M3 14.12.22	M11 14.12.22	M19 14.12.22	M27 14.12.22	M35 14.12.22
M8 15.09.22	**L4** 15.09.22	**L12** 15.09.22	M8 17.10.22	M16 17.10.22	M24 17.10.22	M32 17.10.22	M4 14.12.22	M12 14.12.22	M20 14.12.22	M28 14.12.22	M36 14.12.22

Appendix 4 Table 2 Homogenized piece of liver (L) tissue in a sample box with room for 96 samples. Purple: tissue from fish in 12 ℃ water; Red: tissue from fish in 16 ℃ water; Blue: tissue from fish in raw water.

L1 17.10.22	L9 17.10.22	L17 17.10.22	L25 17.10.22	L33 17.10.22	L5 14.12.22	L13 14.12.22	L21 14.12.22	L29 14.12.22			
L2 17.10.22	L10 17.10.22	L18 17.10.22	L26 17.10.22	L34 17.10.22	L6 14.12.22	L14 14.12.22	L22 14.12.22	L30 14.12.22			
L3 17.10.22	L11 17.10.22	L19 17.10.22	L27 17.10.22	L35 17.10.22	L7 14.12.22	L15 14.12.22	L23 14.12.22	L31 14.12.22			
L4 17.10.22	L12 17.10.22	L20 17.10.22	L28 17.10.22	L36 17.10.22	L8 14.12.22	L16 14.12.22	L24 14.12.22	L32 14.12.22			
L5 17.10.22	L13 17.10.22	L21 17.10.22	L29 17.10.22	L1 14.12.22	L9 14.12.22	L17 14.12.22	L25 14.12.22	L33 14.12.22			
L6 17.10.22	L14 17.10.22	L22 17.10.22	L30 17.10.22	L2 14.12.22	L10 14.12.22	L18 14.12.22	L26 14.12.22	L34 14.12.22			
L7 17.10.22	L15 17.10.22	L23 17.10.22	L31 17.10.22	L3 14.12.22	L11 14.12.22	L19 14.12.22	L27 14.12.22	L35 14.12.22			
L8 17.10.22	L16 17.10.22	L24 17.10.22	L32 17.10.22	L4 14.12.22	L12 14.12.22	L20 14.12.22	L28 14.12.22	L36 14.12.22			

Appendix 5 – Nanodrop measurements of RNA concentrations

Appendix 1 Tabell 1 Nanodrop measurements of RNA concentrations. Tissue sample market with yellow had to low RNA concentration, therefore, new RNA was made for these samples (n = 23). The stage abbreviation for Tissue, degree_sampling_sample.nr (A stage example for muscle; M0_3 is muscle, first sampling, and the third fish sampled. A stage example for liver: L16_3_12 is liver tissue, 16°C, third sampling, fish nr 12 sampled).

Stage	**Sample ID**	**Date**	**260/2280**	**260/230**	**ng/µL**	**µL RNA**	**H_2O to 50 ng**
M0_1	M1	15.03.2023	2.09	2.15	352.62	2.8	17.2
M0_2	M2	15.03.2023	2.08	2.13	418.48	2.4	17.6
M0_3	M3	15.03.2023	2.08	1.88	298.83	3.3	16.7
M0_4	M4	15.03.2023	2.06	2.08	363.63	2.8	17.2
M0_5	M5	15.03.2023	2.07	2.09	437.21	2.3	17.7
M0_6	M6	15.03.2023	2.11	2.04	294.87	3.4	16.6
M0_7	M7	15.03.2023	2.03	2.04	413.57	2.4	17.6
M0_8	M8	15.03.2023	2.06	2.17	408.67	2.4	17.6
M0_9	M9	15.03.2023	2.04	2.01	437.45	2.3	17.7
M0_10	M10	15.03.2023	2.12	2.29	458.71	2.2	17.8
M0_11	M11	15.03.2023	2.06	2.06	442.8	2.3	17.7
M0_12	M12	15.03.2023	2.08	1.98	402.5	2.5	17.5
M12_2_1	M13	15.03.2023	2.13	1.82	178.14	5.6	14.4
M12_2_2	M14	15.03.2023	2.13	1.83	160.97	6.2	13.8
M12_2_3	M15	15.03.2023	2.16	2.06	274.14	3.6	16.4
M12_2_4	M16	15.03.2023	2.16	1.78	130.7	7.7	12.3
M12_2_5	M17	15.03.2023	2.16	1.7	128.77	7.8	12.2
M12_2_6	M18	15.03.2023	2.11	1.49	135.94	7.4	12.6
M12_2_7	M19	15.03.2023	2.16	1.55	153.16	6.5	13.5
M12_2_8	M20	15.03.2023	2.1	1.55	112.89	8.9	11.1
M12_2_9	M21	15.03.2023	2.13	1.9	169.58	5.9	14.1
M12_2_10	M22	15.03.2023	2.13	1.65	145.47	6.9	13.1
M12_2_11	M23	15.03.2023	2.16	1.56	159.34	6.3	13.7
M12_2_12	M24	15.03.2023	2.1	1.6	119.52	8.4	11.6
M16_2_1	M25	15.03.2023	2.12	1.75	116.86	8.6	11.4
M16_2_2	M26	15.03.2023	2.13	1.79	110.04	9.1	10.9
M16_2_3	M27	15.03.2023	2.12	1.52	85.46	11.7	8.3
M16_2_4	M28	15.03.2023	2.14	1.68	101.22	9.9	10.1
M16_2_5	M29	15.03.2023	2.11	1.76	156.15	6.4	13.6
M16_2_6	M30	15.03.2023	2.15	1.7	137.95	7.2	12.8
M16_2_7	M31	15.03.2023	2.17	1.66	128.9	7.8	12.2
M16_2_8	M32	15.03.2023	2.13	1.76	166.37	6	14

M16_2_9	M33	15.03.2023	2.14	1.67	129.05	7.7	12.3
M16_2_10	M34	15.03.2023	2.13	1.57	183.23	5.5	14.5
M16_2_11	M35	15.03.2023	2.14	1.84	153.95	6.5	13.5
M16_2_12	M36	15.03.2023	2.06	1.35	67.1	-	-
M8_2_1	M37	15.03.2023	2.11	1.83	187.13	5.3	14.7
M8_2_2	M38	15.03.2023	2.11	1.91	200.27	5	15
M8_2_3	M39	15.03.2023	2.07	1.28	74.36	-	-
M8_2_4	M40	15.03.2023	2.09	1.55	67.74	-	-
M8_2_5	M41	15.03.2023	2.13	1.75	139.32	7.2	12.8
M8_2_6	M42	15.03.2023	2.1	1.87	162.35	6.2	13.8
M8_2_7	M43	15.03.2023	2.06	1.15	49.39	-	-
M8_2_8	M44	15.03.2023	2.1	1.67	141.22	7.1	12.9
M8_2_9	M45	15.03.2023	2.09	1.76	145.95	6.9	13.1
M8_2_10	M46	15.03.2023	2.1	1.55	108.99	9.2	10.8
M8_2_11	M47	15.03.2023	2.11	1.74	174.38	5.7	14.3
M8_2_12	M48	15.03.2023	2.09	1.71	138.06	7.2	12.8
M16_3_1	M49	15.03.2023	2.09	1.94	207.62	4.8	15.2
M16_3_2	M50	15.03.2023	2.09	1.67	123.72	8.1	11.9
M16_3_3	M51	15.03.2023	2.01	0.17	55.32	-	-
M16_3_4	M52	15.03.2023	2.13	1.23	170.07	5.9	14.1
M16_3_5	M53	15.03.2023	2.09	1.82	135.68	7.4	12.6
M16_3_6	M54	15.03.2023	2.11	2.04	167.38	6	14
M16_3_7	M55	15.03.2023	2.1	1.55	109.72	9.1	10.9
M16_3_8	M56	15.03.2023	2.14	1.58	176.62	5.7	14.3
M16_3_9	M57	15.03.2023	2.12	1.6	112.1	8.9	11.1
M16_3_10	M58	15.03.2023	2.16	1.77	202.57	4.9	15.1
M16_3_11	M59	15.03.2023	2.1	1.69	120.35	8.3	11.7
M16_3_12	M60	15.03.2023	2.07	1.61	114.02	8.8	11.2
M12_3_1	M61	15.03.2023	2.11	1.66	100.99	9.9	10.1
M12_3_2	M62	15.03.2023	2.12	1.93	207.73	4.8	15.2
M12_3_3	M63	15.03.2023	2.09	1.81	237.72	4.2	15.8
M12_3_4	M64	15.03.2023	2.09	1.62	108.92	9.2	10.8
M12_3_5	M65	15.03.2023	2.13	1.66	152.61	6.6	13.4
M12_3_6	M66	15.03.2023	2.08	1.39	105.6	9.5	10.5
M12_3_7	M67	15.03.2023	2.09	1.55	131.98	7.6	12.4
M12_3_8	M68	15.03.2023	2.08	1.45	63.29	-	-
M12_3_9	M69	15.03.2023	2.1	1.79	157.82	6.3	13.7
M12_3_10	M70	15.03.2023	2.07	1.36	91.17	11	9
M12_3_11	M71	15.03.2023	2.08	1.52	129.59	7.7	12.3

M12_3_12	M72	15.03.2023	2.11	1.81	109.62	9.1	10.9
M8_3_1	M73	15.03.2023	2.09	1.7	144.95	6.9	13.1
M8_3_2	M74	15.03.2023	2.09	1.47	163.21	6.1	13.9
M8_3_3	M75	15.03.2023	2.07	1.48	137.04	7.3	12.7
M8_3_4	M76	15.03.2023	2.11	1.78	144.34	6.9	13.1
M8_3_5	M77	15.03.2023	2.12	1.98	256.1	3.9	16.1
M8_3_6	M78	15.03.2023	2.08	1.2	243.85	4.1	15.9
M8_3_7	M79	15.03.2023	2.12	1.67	152.94	6.5	13.5
M8_3_8	M80	15.03.2023	2.08	1.35	87.86	11.4	8.6
M8_3_9	M81	15.03.2023	2.08	1.6	130.17	7.7	12.3
M8_3_10	M82	15.03.2023	2.11	2.02	232.24	4.3	15.7
M8_3_11	M83	15.03.2023	2.11	1.37	130.8	7.6	12.4
M8_3_12	M84	15.03.2023	2.07	1.68	96.18	10.4	9.6
L0_1	L1	15.03.2023	2.05	1.29	87.08	11.5	8.5
L0_2	L2	15.03.2023	2.08	2.16	463.38	2.2	17.8
L0_3	L3	15.03.2023	2.07	1.59	86.52	11.6	8.4
L0_4	L4	15.03.2023	2.07	0.91	45.29	-	-
L0_5	L5	15.03.2023	2.14	1.86	175.56	5.7	14.3
L0_6	L6	15.03.2023	2.1	1.83	95.62	10.5	9.5
L0_7	L7	15.03.2023	2.09	1.44	117.94	8.5	11.5
L0_8	L8	15.03.2023	2.07	1.22	58.99	-	-
L0_9	L9	15.03.2023	2.12	1.54	102.84	9.7	10.3
L0_10	L10	15.03.2023	2.04	1.51	55.75	-	-
L0_11	L11	15.03.2023	2.07	1.43	56.77	-	-
L0_12	L12	15.03.2023	2.04	0.86	33.59	-	-
L12_2_1	L1	14.03.2023	2.09	1.57	130.98	7.6	12.4
L12_2_2	L2	14.03.2023	2.13	1.36	134.29	7.4	12.6
L12_2_3	L3	14.03.2023	2.15	1.36	90.93	11	9
L12_2_4	L4	14.03.2023	2.08	1.98	337.8	3	17
L12_2_5	L5	14.03.2023	2.11	1.68	262.29	3.8	16.2
L12_2_6	L6	14.03.2023	2.13	1.31	77.92	-	-
L12_2_7	L7	14.03.2023	2.11	1.31	77.11	-	-
L12_2_8	L8	14.03.2023	2.14	1.83	141.19	7.1	12.9
L12_2_9	L9	14.03.2023	2.12	1.58	82.79	12.1	7.9
L12_2_10	L10	14.03.2023	2.11	1.95	514.03	1.9	18.1
L12_2_11	L11	14.03.2023	2.09	1.74	187.43	5.3	14.7
L12_2_12	L12	14.03.2023	2.05	1.77	398.31	2.5	17.5
L16_2_1	L13	14.03.2023	2.34	0.74	16.07	-	-
L16_2_2	L14	14.03.2023	2.08	1.95	426.18	2.3	17.7

L16_2_3	L15	14.03.2023	2.13	1.99	519.21	1.9	18.1
L16_2_4	L16	14.03.2023	2.1	1.92	192.36	5.2	14.8
L16_2_5	L17	14.03.2023	2.12	1.12	49.58	-	-
L16_2_6	L18	14.03.2023	2.08	1.02	42.18	-	-
L16_2_7	L19	14.03.2023	2.02	0.92	56.37	-	-
L16_2_8	L20	14.03.2023	2.08	1.03	61.93	-	-
L16_2_9	L21	14.03.2023	2.11	1.92	852.37	1.2	18.8
L16_2_10	L22	14.03.2023	2.12	2.12	1396.27	0.7	19.3
L16_2_11	L23	14.03.2023	2.07	1.41	83.64	12	8
L16_2_12	L24	14.03.2023	2.1	1.75	280.68	3.6	16.4
L8_2_1	L25	14.03.2023	2.12	1.68	103.54	9.7	10.3
L8_2_2	L26	14.03.2023	2.12	1.6	89.83	11.1	8.9
L8_2_3	L27	14.03.2023	2.15	1.78	135.95	7.4	12.6
L8_2_4	L28	14.03.2023	2.11	0.84	72.09	-	-
L8_2_5	L29	14.03.2023	2.1	1.31	61.85	-	-
L8_2_6	L30	14.03.2023	2.14	1.78	164.49	6.1	13.9
L8_2_7	L31	14.03.2023	2.13	1.42	64.85	-	-
L8_2_8	L32	14.03.2023	2.04	1.06	64.24	-	-
L8_2_9	L33	14.03.2023	2.09	1.49	128.58	7.8	12.2
L8_2_10	L34	14.03.2023	2.02	2.02	484.68	2.1	17.9
L8_2_11	L35	14.03.2023	2.13	1.83	229.82	4.4	15.6
L8_2_12	L36	14.03.2023	2.12	2.01	797.93	1.3	18.7
L16_3_1	L37	14.03.2023	2.13	1.74	537.98	1.9	18.1
L16_3_2	L38	14.03.2023	2.09	1.84	330.76	3	17
L16_3_3	L39	14.03.2023	2.12	2	881.59	1.1	18.9
L16_3_4	L40	14.03.2023	2.09	1.78	191.52	5.2	14.8
L16_3_5	L41	14.03.2023	2.11	1.85	289.73	3.5	16.5
L16_3_6	L42	14.03.2023	2.11	1.26	73.8	-	-
L16_3_7	L43	14.03.2023	2.12	1.65	205.84	4.9	15.1
L16_3_8	L44	14.03.2023	2.12	1.65	171.1	5.8	14.2
L16_3_9	L45	14.03.2023	2.12	1.65	200.64	5	15
L16_3_10	L46	14.03.2023	2.13	2.05	1198.36	0.8	19.2
L16_3_11	L47	14.03.2023	2.12	1.59	122.04	8.2	11.8
L16_3_12	L48	14.03.2023	2.1	1.32	90.95	11	9
L12_3_1	L49	14.03.2023	2.12	1.97	326.28	3.1	16.9
L12_3_2	L50	14.03.2023	2.17	1.94	186.11	5.4	14.6
L12_3_3	L51	14.03.2023	2.14	1.49	303.53	3.3	16.7
L12_3_4	L52	14.03.2023	2.14	1.81	518.8	1.9	18.1
L12_3_5	L53	14.03.2023	2.15	1.99	880.14	1.1	18.9

L12_3_6	L54	14.03.2023	2.15	1.85	167.64	6	14
L12_3_7	L55	14.03.2023	2.16	1.97	291.71	3.4	16.6
L12_3_8	L56	14.03.2023	2.15	1.89	272.51	3.7	16.3
L12_3_9	L57	14.03.2023	2.13	2.11	1546.22	0.6	19.4
L12_3_10	L58	14.03.2023	2.15	2.01	231.7	4.3	15.7
L12_3_11	L59	14.03.2023	2.12	1.95	340.76	2.9	17.1
L12_3_12	L60	14.03.2023	2.14	1.74	711.38	1.4	18.6
L8_3_1	L61	14.03.2023	2.15	2.12	1696.72	0.6	19.4
L8_3_2	L62	14.03.2023	2.16	2.06	1242.14	0.8	19.2
L8_3_3	L63	14.03.2023	2.14	1.99	326.57	3.1	16.9
L8_3_4	L64	14.03.2023	2.12	2	354.66	2.8	17.2
L8_3_5	L65	14.03.2023	2.12	2.03	986.73	1	19
L8_3_6	L66	14.03.2023	2.1	2.09	422	2.4	17.6
L8_3_7	L67	14.03.2023	2.14	1.97	1095.12	0.9	19.1
L8_3_8	L68	14.03.2023	2.08	2.03	445.41	2.2	17.8
L8_3_9	L69	14.03.2023	2.15	1.92	246.65	4.1	15.9
L8_3_10	L70	14.03.2023	2.14	1.95	734.34	1.4	18.6
L8_3_11	L71	14.03.2023	2.16	2.09	1305.2	0.8	19.2
L8_3_12	L72	14.03.2023	2.11	2.07	436.43	2.3	17.7

Appendix 6 – Volume used to dilute RNA concentrations using Biomek 4000 (Beckman Coulter INC, California, USA)

Appendix 6 Tabell 1 The RNA concentrations were diluted with nuclease free water to 50ng/µL using Biomek 4000 (Beckman Coulter INC, California, USA).

Stage	**Destwell**	**Volume**
M0_1	A1	61
M0_2	B1	74
M0_3	C1	50
M0_4	D1	63
M0_5	E1	77
M0_6	F1	49
M0_7	G1	73
M0_8	H1	72
M0_9	A2	77
M0_10	B2	82
M0_11	C2	79
M0_12	D2	71
L0_1	E2	7
L0_2	F2	83
L0_3	G2	7
L0_4	H2	0
L0_5	A3	25
L0_6	B3	9
L0_7	C3	14
L0_8	D3	2
L0_9	E3	11
L0_10	F3	1
L0_11	G3	1
L0_12	H3	0
M12_2_1	A4	26
M12_2_2	B4	22
M12_2_3	C4	45
M12_2_4	D4	16
M12_2_5	E4	16
M12_2_6	F4	17
M12_2_7	G4	21
M12_2_8	H4	13

M12_2_9	A5	24
M12_2_10	B5	19
M12_2_11	C5	22
M12_2_12	D5	14
M16_2_1	E5	13
M16_2_2	F5	12
M16_2_3	G5	7
M16_2_4	H5	10
M16_2_5	A6	21
M16_2_6	B6	18
M16_2_7	C6	16
M16_2_8	D6	23
M16_2_9	E6	16
M16_2_10	F6	27
M16_2_11	G6	21
M16_2_12	H6	3
M8_2_1	A7	27
M8_2_2	B7	30
M8_2_3	C7	5
M8_2_4	D7	4
M8_2_5	E7	18
M8_2_6	F7	22
M8_2_7	G7	0
M8_2_8	H7	18
M8_2_9	A8	19
M8_2_10	B8	12
M8_2_11	C8	25
M8_2_12	D8	18
M16_3_1	E8	32
M16_3_2	F8	15
M16_3_3	G8	1
M16_3_4	H8	24
M16_3_5	A9	17
M16_3_6	B9	23
M16_3_7	C9	12
M16_3_8	D9	25
M16_3_9	E9	12
M16_3_10	F9	31
M16_3_11	G9	14

M16_3_12	H9	13
M12_3_1	A10	10
M12_3_2	B10	32
M12_3_3	C10	38
M12_3_4	D10	12
M12_3_5	E10	21
M12_3_6	F10	11
M12_3_7	G10	16
M12_3_8	H10	3
M12_3_9	A11	22
M12_3_10	B11	8
M12_3_11	C11	16
M12_3_12	D11	12
M8_3_1	E11	19
M8_3_2	F11	23
M8_3_3	G11	17
M8_3_4	H11	19
M8_3_5	A12	41
M8_3_6	B12	39
M8_3_7	C12	21
M8_3_8	D12	8
M8_3_9	E12	16
M8_3_10	F12	36
M8_3_11	G12	16
M8_3_12	H12	9
L12_2_1	A1	16
L12_2_2	B1	17
L12_2_3	C1	8
L12_2_4	D1	58
L12_2_5	E1	42
L12_2_6	F1	6
L12_2_7	G1	5
L12_2_8	H1	18
L12_2_9	A2	7
L12_2_10	B2	93
L12_2_11	C2	27
L12_2_12	D2	70
L16_2_1	E2	0
L16_2_2	F2	75

L16_2_3	G2	94
L16_2_4	H2	28
L16_2_5	A3	0
L16_2_6	B3	0
L16_2_7	C3	1
L16_2_8	D3	2
L16_2_9	E3	160
L16_2_10	F3	130
L16_2_11	G3	7
L16_2_12	H3	46
L8_2_1	A4	11
L8_2_2	B4	8
L8_2_3	C4	17
L8_2_4	D4	4
L8_2_5	E4	2
L8_2_6	F4	23
L8_2_7	G4	3
L8_2_8	H4	3
L8_2_9	A5	16
L8_2_10	B5	87
L8_2_11	C5	36
L8_2_12	D5	150
L16_3_1	E5	98
L16_3_2	F5	56
L16_3_3	G5	166
L16_3_4	H5	28
L16_3_5	A6	48
L16_3_6	B6	5
L16_3_7	C6	31
L16_3_8	D6	24
L16_3_9	E6	30
L16_3_10	F6	110
L16_3_11	G6	14
L16_3_12	H6	8
L12_3_1	A7	55
L12_3_2	B7	27
L12_3_3	C7	51
L12_3_4	D7	94
L12_3_5	E7	166

L12_3_6	F7	24
L12_3_7	G7	48
L12_3_8	H7	45
L12_3_9	A8	145
L12_3_10	B8	36
L12_3_11	C8	58
L12_3_12	D8	132
L8_3_1	E8	160
L8_3_2	F8	115
L8_3_3	G8	55
L8_3_4	H8	61
L8_3_5	A9	187
L8_3_6	B9	74
L8_3_7	C9	100
L8_3_8	D9	79
L8_3_9	E9	39
L8_3_10	F9	137
L8_3_11	G9	120
L8_3_12	H9	77

Appendix 7 – Nanodrop readings of the new RNA samples

Appendix 7 Tabell 1 New RNA was made for all the tissue samples and measured in Nanodrop. Thereafter, diluted to 50 ng/µL.

Stage	Sample ID	Date	260/280	260/230	ng/mL	mL RNA	H2O to 50ng
L12_2_6	L6	30.03.2023			1000	1	19
L12_2_7	L7	30.03.2023	1.99	1.55	905	1.1	18.9
L16_2_1	L13	30.03.2023	1.93	0.61	84,4	11.8	8.2
L16_2_5	L17	30.03.2023	2.01	1.25	911	1.1	18.9
L16_2_6	L18	30.03.2023	1.94		618	1.6	18.4
L16_2_7	L19	30.03.2023	1.97		968	1	19
L16_2_8	L20	30.03.2023	1.99		940	1.1	18.9
L8_2_4	L28	30.03.2023	1.96		1021	1	19
L8_2_5	L29	30.03.2023	1.99		992	1	19
L8_2_7	L31	30.03.2023	1.94	0.67	940	1.1	18.9
L8_2_8	L32	30.03.2023	1.9		944	1.1	18.9
L16_3_6	L42	30.03.2023	2.00		1037	1	19
L0_4	L4	30.03.2023	1.96		1016	1	19
L0_8	L8	30.03.2023	1.88	0.84	420	2.4	17.6
L0_10	L10	30.03.2023	1.95		656	1.5	18.5
L0_11	L11	30.03.2023	1.83	0.78	842	1.2	18.8
L0_12	L12	30.03.2023	1.78		851	1.2	18.8
M16_2_12	M36	30.03.2023	2.18		106,8	9.4	10.6
M8_2_3	M39	30.03.2023	2.03		491	2	18
M8_2_4	M40	30.03.2023	2.00		422	2.4	17.6
M8_2_7	M43	30.03.2023	2.02		423	2.4	17.6
M16_3_3	M51	30.03.2023	2.00		734	1.4	18.6
M12_3_8	M68	30.03.2023	2.07		403	2.5	17.5

Appendix 8 – Primer and probes

Appendix 8 Table 1 Primers and probes (In name column; PP = Pleuronectes platessa, Fw = forward primer, Pb = probe, Rw = reverse primer).

Amplicon size	**Name**	**Sequence**	**Sense**	**Annealing temperature**	**GC content %**
130 bp	PP_Eef1a_NCBI_Fw	CTGAGAAAGCCCAGAAGAAGAA	(Sense)	62	45.5
	PP_Eef1a_ NCBI_Pb	AGGACACCCAGCAACAAGATGTGT	(Sense)	68	50
	PP_Eef1a_ NCBI_Rw	AGAGAGCATTGCCTCAGAATAG	(AntiSense)	62	45.5
99 bp	PP_Gapdh_ NCBI_Fw	CACCCACTCCTCCATCTTTG	(Sense)	62	55
	PP_Gapdh_ NCBI_Pb	TCGCCCTCAATGACCACTTTGTCA	(Sense)	68	50
	PP_Gapdh_ NCBI_Rw	TGGCTGTAGGCAAACTCATT	(AntiSense)	62	45
107 bp	PP_Igf1_Fw	CGTGTCTCAGCAGCTAAACT	(Sense)	62	50
	PP_Igf1_Pb	TCCCGATATGGAATGGTGCAGTGT	(Sense)	68	50
	PP_Igf1_Rw	GGGTTTGATGAGGGATCTTGT	(AntiSense)	62	47.6
119 bp	PP_Igf1R_Fw	AGGACAGCTTTGTGGTTTCT	(Sense)	62	45
	PP_Igf1R_Pb	CCTGCTCATTTGTGAGACCCTGGT	(Sense)	68	54
	PP_Igf1R_Rw	GGGTTGTTCTGTGGGAGATT	(AntiSense)	62	50
110 bp	PP_GhR_Fw	GACTCTGCCTCGTCAGTTAAT	(Sense)	62	47.6
	PP_GhR_Pb	TGGATGTTGGAGTTGACCGAACGT	(Sense)	68	50
	PP_GhR_Rw	CCACAGTCTAGGGCTGTTATG	(AntiSense)	62	52.4

Appendix 9 - 1:100 dilution of cDNA

Appendix 9 Table 1 A 1:100 dilution of cDNA for each gene at each stage.

Gene	Group	Slope	R^2	Efficiency (%)
eef1a	M0	-3.4	0.997	95
	$M8_{Oct}$	-3.4	0.982	109
	$M8_{Des}$	-3.4	0.998	96
	$M12_{Oct}$	-3.5	0.998	90
	$M12_{Des}$	-3.4	0.996	94
	$M16_{Oct}$	-3.5	0.996	90
	$M16_{Des}$	-3.3	0.995	98
gapdh	M0	-3.5	0.99	91
	$M8_{Oct}$	-3.3	0.99	100
	$M8_{Des}$	-3.4	0.99	94
	$M12_{Oct}$	-3.4	0.99	96
	$M12_{Des}$	-3.5	0.99	90
	$M16_{Oct}$	-3.5	0.99	90
	$M16_{Des}$	-3.6	0.99	89
ghr	M0	-3.7	0.997	85
	$M8_{Oct}$	-3.3	0.998	97
	$M8_{Des}$	-3.4	0.991	94
	$M12_{Oct}$	-3.4	0.989	93
	$M12_{Des}$	-3.4	0.996	95
	$M16_{Oct}$	-3.5	0.992	93
	$M16_{Des}$	-3.5	0.995	92
igf-1	M0	-3.5	0.98	90
	$M8_{Oct}$	-2.9	0.95	116
	$M8_{Des}$	-3.1	0.98	109
	$M12_{Oct}$	-3.4	0.99	93
	$M12_{Des}$	-3.2	0.94	104
	$M16_{Oct}$	-3.3	0.95	99
	$M16_{Des}$	-3.6	0.99	86
igf-1r	M0	-3.5	0.92	90
	$M8_{Oct}$	-3.4	0.97	95
	$M8_{Des}$	-3.3	0.97	99
	$M12_{Oct}$	-3.8	0.99	81.9
	$M12_{Des}$	-3.3	0.98	97
	$M16_{Oct}$	-3.7	0.98	85
	$M16_{Des}$	-3.5	0.98	89

Appendix 10 – Statistical tests

Shapiro-Wilk normality test

Appendix 10 Table 1 Shapiro-Wilk normality test results for normal distribution analysis. Data are presented in p-values.

Dataset	Sampling	W	p-value
Weight_data	1	0.94664	$1.657e^{-11}$
	2	0.97841	$3.469e^{-06}$
	3	0.97395	$3.519e^{-07}$
	4	0.96798	$< 2.2e^{-16}$
Length_data	1	0.97846	$4.021e^{-06}$
	2	0.98914	0.002167
	3	0.99528	0.1913
	4	0.99797	0.007026
Condition_factor_data	1	0.99565	0.2608
	2	0.99104	0.008394
	3	0.9835	$5.495e^{-05}$
	4	0.9788	$< 2.2e^{-16}$
GhR muscle data	1	0.86275	0.0625
	2	0.89226	0.002111
	3	0.74264	3.092e-06
igf-1r muscle data	1	0.87196	0.1053
	2	0.90069	0.006449
	3	0.96701	0.4213
GhR liver data	1	0.90422	0.1798
	2	0.75779	9.362e-06
	3	0.93693	0.0408
Igf-1 liver data	1	0.90631	0.1913
	2	0.92186	0.01824
	3	0.95779	0.2387
Deformity data: start-end	1	0.74115	2.411e-07
	2	0.73496	2.806e-16
≥1 deformed vertebra	1	0.7577	0.0007877
	2	0.84708	8.4e-12
>5 deformed vertebrae	1	0.88691	0.369
	2	0.89699	$1.147e^{-05}$

Levene's test

*Appendix 10 Table 2 Levene's Test results for Homogeneity of Variance (center = median). Data are presented in p-values. Significant codes: 0 '***', 0.001 '**', 0.01 '*', 0.05 '.', 0.1 ' ', 1. Df: degrees of freedom for the independent variable and the residuals. F value: the test statistic from the F test. Pr(>F): p value of the F statistic.*

Dataset	Sampling	Temp (°C)	Df	F value	Pr(>F)
Weight data	1		8	0.7058	0.6865
	2	16	2	0.1634	0.8494
		12	2	0.1788	0.8365
		8	2	0.5167	0.5976
	3	16	2	1.7901	0.1706
		12	2	0.7133	0.4917
		8	2	2.8444	0.06137
	4	16	2	0.0741	0.9286
		12	2	2.4932	0.08334
		8	2	7.0714	0.0009083 ***
Length data	1		8	0.6374	0.7463
	2	16	2	0.3507	0.7048
		12	2	0.4823	0.6183
		8	2	0.2238	0.7998
	3	16	2	1.8776	0.1566
		12	2	1.4103	0.2474
		8	2	2.1001	0.1261
	4	16	2	0.3359	0.7148
		12	2	0.0596	0.9422
		8	2	6.0338	0.002517 **
Condition factor	1		8	0.3752	0.9336
	2	16	2	2.7116	0.0698
		12	2	0.0717	0.9308
		8	2	1.1353	0.3242
	3	16	2	0.1399	0.8696
		12	2	2.7756	0.0656
		8	2	0.0262	0.9742
	4	16	2	1.4887	0.2264
		12	2	1.4541	0.2343
		8	2	1.7951	0.1668
GhR muscle	2	16	2	3.0965	0.09477
		12	2	0.5969	0.5709
		8	2	0.6516	0.5441
	3	16	2	0.6375	0.5509

		12	2	0.239	0.7946
		8	2	0.0538	0.9479
Igf-1r muscle	2	16	2	3.449	0.07728
		12	2	0.5369	0.6022
		8	2	0.4042	0.6875
	3	16	2	0.1811	0.8373
		12	2	0.7191	0.5249
		8	2	0.8615	0.4583
GhR liver	2	16	2	0.4636	0.6449
		12	2	1.9135	0.2415
		8	2	3.1909	0.08965
	3	16	2	0.252	0.7825
		12	2	0.0625	0.9398
		8	2	0.2831	0.7599
Igf-1 liver	2	16	2	0.3005	0.7495
		12	2	1.2809	0.324
		8	2	1.9305	0.2006
	3	16	2	2.6348	0.1403
		12	2	1.3845	0.3114
		8	2	0.5159	0.6136
Liver ghr with time	Sep-Oct	12	2	7,598	0,013
	Oct-Des	16	2	0,028	0,868
		12	2	2,147	0,16
		8	2	2,755	0,111
Liver igf-1 with time	Sep-Oct	12	2	0,458	0,506
	Oct-Des	16	2	3,47	0,079
		12	2	3,623	0,071
		8	2	4,112	0,055
Muscle ghr with time	Sep-Oct	12	2	1,169	0,292
	Oct-Des	16	2	37,016	<,001
		12	2	2,563	0,126
		8	2	1,954	0,176
Muscle igf-1r with time	Sep-Oct	12	2	26,624	<,001
	Oct-Des	16	2	0,023	0,88
		12	2	16,011	<,001
		8	2	5,87	0,027
≥1 deformed vertebra	2	16	2	0.392	0.6776
		12	2	0.0188	0.9814
		8	2	0.5377	0.5879

>5 deformed vertebrae	2	16	2	0.1963	0.8232
		12	2	0.7112	0.4997
		8	2	1.0671	0.3638

Two-way nested ANOVA

*Appendix 10 Table 3 Two-way nested ANOVA results. Data are presented in p-values. Significant codes: 0 '***', 0.001 '**', 0.01 '*', 0.05 '.', 0.1 ' ', 1. Df: degrees of freedom for the independent variable and the residuals. Sum Sq: sum of squares. Mean Sq: mean of the sum of squares. F value: the test statistic from the F test. Pr(>F): p value of the F statistic. As the ANOVA test is significant, it was computed a Tukey HSD (Tukey Honest Significant Differences) for performing multiple pairwise-comparison between the means of groups.*

Dataset	Sampling	Df	Sum Sq	Mean Sq	F value	Pr(>F)
Weight data	2	2	2573	1286.4	45.133	<2e-16 ***
	3	2	6989	3495	43.834	<2e-16 ***
	4	2	145005	72503	538.882	< 2e-16 ***
Length data	2	2	133.4	66.71	69.485	<2e-16 ***
	3	2	201.8	100.88	66.177	<2e-16 ***
	4	2	2396	1198.1	762.926	< 2e-16 ***
Condition factor	2	2	0.791	0.3957	16.498	1.24e-07 ***
	3	2	2.030	1.0151	43.470	< 2e-16 ***
	4	2	2.65	1.3261	55.61	< 2e-16 ***
GhR muscle	2	2	3.351	1.6757	3.341	0.05054
	3	2	2.750	1.3752	2.815	0.0628
Igf-1r muscle	2	2	17.22	8.611	3.644	0.0422 *
	3	2	0.233	0.1164	0.106	0.900
GhR liver	2	2	3.377	1.6884	11.086	0.000468 ***
	3	2	1.2352	0.6176	7.463	0.00263 **
Igf-1 liver	2	2	9.859	4.929	9.146	0.00104 **
	3	2	1.493	0.7467	4.144	0.029 *

One-way ANOVA

Appendix 10 Table 4 One-way ANOVA results. Data are presented in p-values. Df: degrees of freedom for the independent variable and the residuals. Sum Sq: sum of squares. Mean Sq: mean of the sum of squares. F value: the test statistic from the F test. Pr(>F): p value of the F statistic.

Dataset	Df	Sum Sq	Mean Sq	F value	Pr(>F)
Deformity data: start-end	3	1048	349.2	7.279	0.000128 ***
≥1 deformed vertebra	2	83	41.67	0.983	0.377
>5 deformed vertebrae	2	286.7	143.35	4.420	0.0156 *

Tukey HSD

Appendix 10 Table 5 Tukey HSD (Tukey Honest Significant Differences) results for performing multiple pairwise-comparison between the means of groups. 95% family-wise confidence level. diff: difference between means of the two groups. lwr, upr: the lower and the upper end point of the confidence interval at 95% (default). p adj: p-value after adjustment for the multiple comparisons.

Dataset	Sampling	temp	diff	lwr	upr	p adj
Weight data	2	8-12	4.388591	2.9254395	5.851742	<0.0001
		8-16	5.592532	4.1318219	7.053243	<0.0001
		12-16	1.198032	-0.2590605	2.655124	0.1305019
	3	8-12	7.685333	5.263083	10.107584	<0.0001
		8-16	8.924667	6.502416	11.346917	<0.0001
		12-16	1.268291	-1.160385	3.696966	0.4372102
	4	8-12	12.06379	10.642453	13.485121	<0.0001
		8-16	19.79161	18.367850	21.215365	<0.0001
		12-16	7.72782	6.304545	9.151096	<0.0001
Length data	2	8-12	0.8986577	0.6318286	1.1654868	<0.0001
		8-16	1.3047338	1.0383498	1.5711178	<0.0001
		12-16	0.4060761	0.1396921	0.6724601	0.0010903
	3	8-12	1.0860000	0.7509953	1.4210047	<0.0001
		8-16	1.6066667	1.2716619	1.9416714	<0.0001
		12-16	0.5206667	0.1856619	0.8556714	0.0008403
	4	8-12	1.5435059	1.3896656	1.697346	<0.0001
		8-16	2.5298423	2.3757397	2.683945	<0.0001
		12-16	0.9863364	0.8322859	1.140387	<0.0001
Condition factor	2	8-12	-0.01351710	-0.05571208	0.02867788	0.7317472
		8-16	-0.09544279	-0.13770899	-0.05317659	<0.0001
		12-16	-0.08192569	-0.12419189	-0.03965949	<0.0001
	3	8-12	-0.01481401	-0.05638033	0.02675231	0.6795191
		8-16	-0.14937249	-0.19086924	-0.10787574	<0.0001
		12-16	-0.13455848	-0.17612480	-0.09299216	<0.0001
	4	8-12	-0.02089255	-0.03979826	-0.00198684	0.0260064
		8-16	-0.08213823	-0.10110911	-0.06316736	<0.0001
		12-16	-0.06124569	-0.08021656	-0.04227481	<0.0001
Igf-1r muscle	2	8-12	-1.594588	-3.351866	0.16268958	0.0801834
		8-16	-1.774667	-3.531945	-0.01738946	0.0474692
		12-16	0.180079	-1.391678	1.75183597	0.9557191
GhR liver	2	8-12	0.67456396	0.2270946	1.1220333	0.0027960
		8-16	0.67977607	0.2705523	1.0889998	0.0011075
		12-16	-0.00521211	-0.4607446	0.4503204	0.9995446

	3	8-12	0.2204822	-0.07070232	0.51166677	0.1646200
		8-16	0.4536717	0.16248718	0.74485628	0.0017813
		12-16	-0.2331895	-0.52437406	0.05799504	0.1351056
Igf-1 liver	2	8-12	0.5387351	-0.2077739	1.28524405	0.1909448
		8-16	1.3417148	0.5587695	2.12465998	0.0007020
		12-16	-0.8029797	-1.5859249	-0.02003447	0.0436318
	3	8-12	-0.4730755	-0.9282190	-0.01793199	0.0405962
		8-16	-0.4141600	-0.8693035	0.04098352	0.0791806
		12-16	-0.0589155	-0.5342974	0.41646639	0.9484034
Deformity data: start-end	1-2	Start-8	-3.5723069	-7.448669	0.3040551	0.0826363
		Start-12	-5.7118418	-9.588204	-1.8354798	0.0010537
		Start-16	-6.3009890	-10.177351	-2.4246271	0.0002337
>5 deformed vertebrae	2	8-12	0.8328446	-2.96989943	4.635589	0.8595841
		8-16	4.5309091	0.54324170	8.518576	0.0221110
		12-16	3.6980645	0.03120303	7.364926	0.0476303

T-test

Appendix 10 Table 6 T-test for equality of means results. 95% family-wise confidence level. SE diff.: Std. Error Difference.

Dataset	Sampling	Temp (°C)	Mean Difference	SE diff.	t-value	p-value
Liver ghr with time	Sep-Oct	12	0,71403263	0,20540861	3,476	0,001
	Oct-Des	16	-0,06582651	0,08536301	-0,771	0,225
		12	-0,2938039	0,08422095	-3,488	0,001
		8	0,16027783	0,22658788	0,707	0,243
Liver igf-1 with time	Sep-Oct	12	-0,55958354	0,20579161	-2,719	0,006
	Oct-Des	16	-1,42649088	0,17286278	-8,252	<,001
		12	-0,68242669	0,19268406	-3,542	0,001
		8	0,32938388	0,3315097	0,994	0,166
Muscle ghr with time	Sep-Oct	12	-0,57152843	0,32551024	-1,756	0,047
	Oct-Des	16	-1,32252306	0,66575343	-1,987	0,03
		12	0,67366887	0,33179556	2,03	0,028
		8	0,28523438	0,45826838	0,622	0,27
Muscle igf-1r with time	Sep-Oct	12	-0,57152843	0,32551024	-1,756	0,047
	Oct-Des	16	0,5942269	0,57522641	1,033	0,156
		12	0,53483664	0,78971864	0,677	0,253
		8	-0,98082025	0,35276353	-2,78	0,006

Appendix 11 Types of deformities in the vertebral column of Atlantic salmon described by Witten et al. (2009)

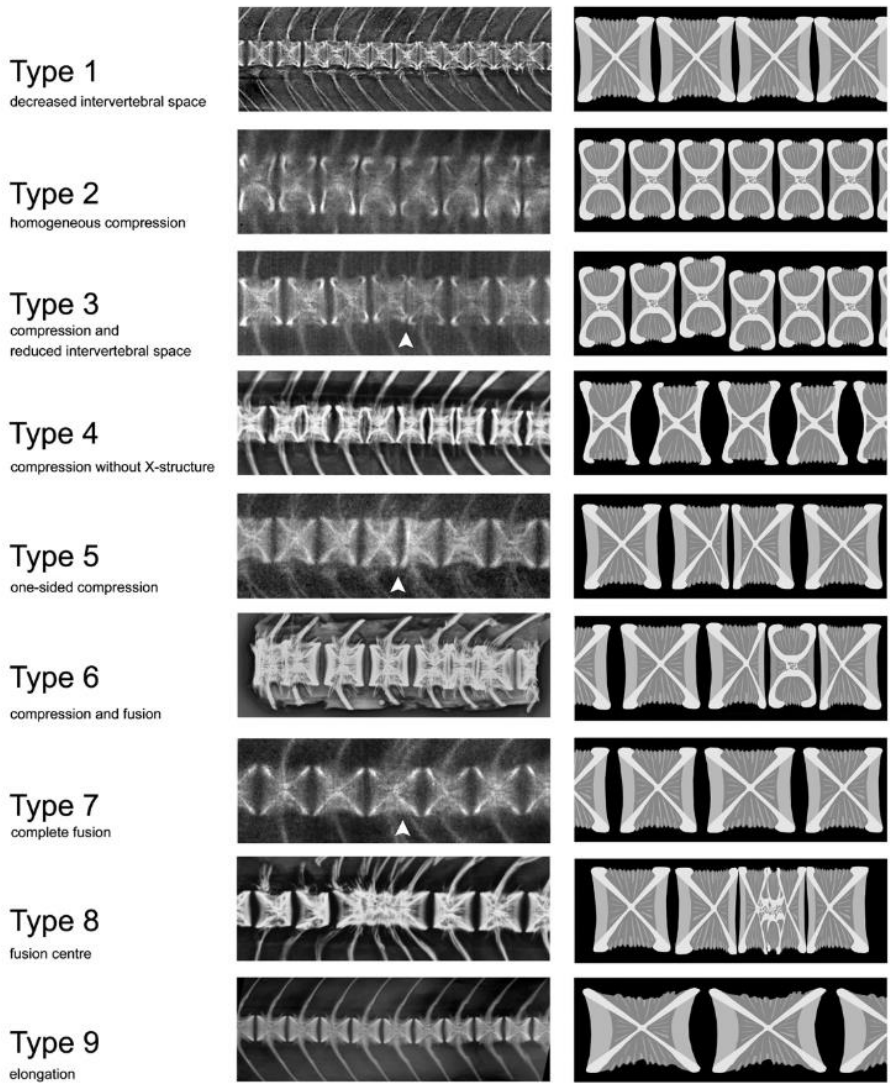

Fig. 2. Radiographs and schematic representations of vertebral body malformations in Atlantic salmon. Type 1—decreased intervertebral space. Intervertebral spaces are reduced without vertebral fusion (commonly related to platyspondyly). The width of the radiograph is equal to 91 mm. Type 2—homogeneous compression. Homogeneously and two-sided compressed vertebrae with shape alteration of the vertebral end plates (commonly related to platyspondyly). The width of the radiograph is equal to 57 mm. Type 3—compression and reduced intervertebral space (white arrowhead). Type 1 and Type 2 characters (commonly related to platyspondyly), combined in this case with dorso-ventral shift of vertebrae. The width of the radiograph is equal to 59 mm. Type 4—compression without X-structure. Anteriorly posteriorly compressed vertebrae with straight (non-funnel-shaped) vertebral end plates and possible calcification of the intervertebral tissue (commonly related to platyspondyly and/or to vertebral fusion). The width of the radiograph is equal to 75 mm. Type 5—one-sided compression (white arrowhead). Opposing, one-sided compressed vertebrae also referred to as K-vertebrae (commonly related to vertebral fusion). The width of the radiograph is equal to 45 mm. Type 6—compression and fusion. Anterior-posterior compression, reduced intervertebral space and intervertebral calcification (commonly related to subsequent vertebral fusion). The width of the radiograph is equal to 89 mm. Type 7—complete fusion (white arrowhead). Complete fusion and remodelling of vertebral centra, indicated by the multiple pairs of haemal and neural arches (vertebral fusion proper). The width of the radiograph is equal to 63 mm. Type 8—fusion centre. Multiple vertebral fusion with partial remodelling. Vertebrae adjacent to the fusion centre display Type 5 pathology (one-sided compression). The width of the radiograph is equal to 49 mm. Type 9—elongation. Anteriorly posteriorly elongated vertebrae. Elongated vertebrae are common in spines with partial compression and/or fusion, see e.g. in Type 8 (commonly related to platyspondyly and/or vertebral fusion). The width of the radiograph is equal to 74 mm.

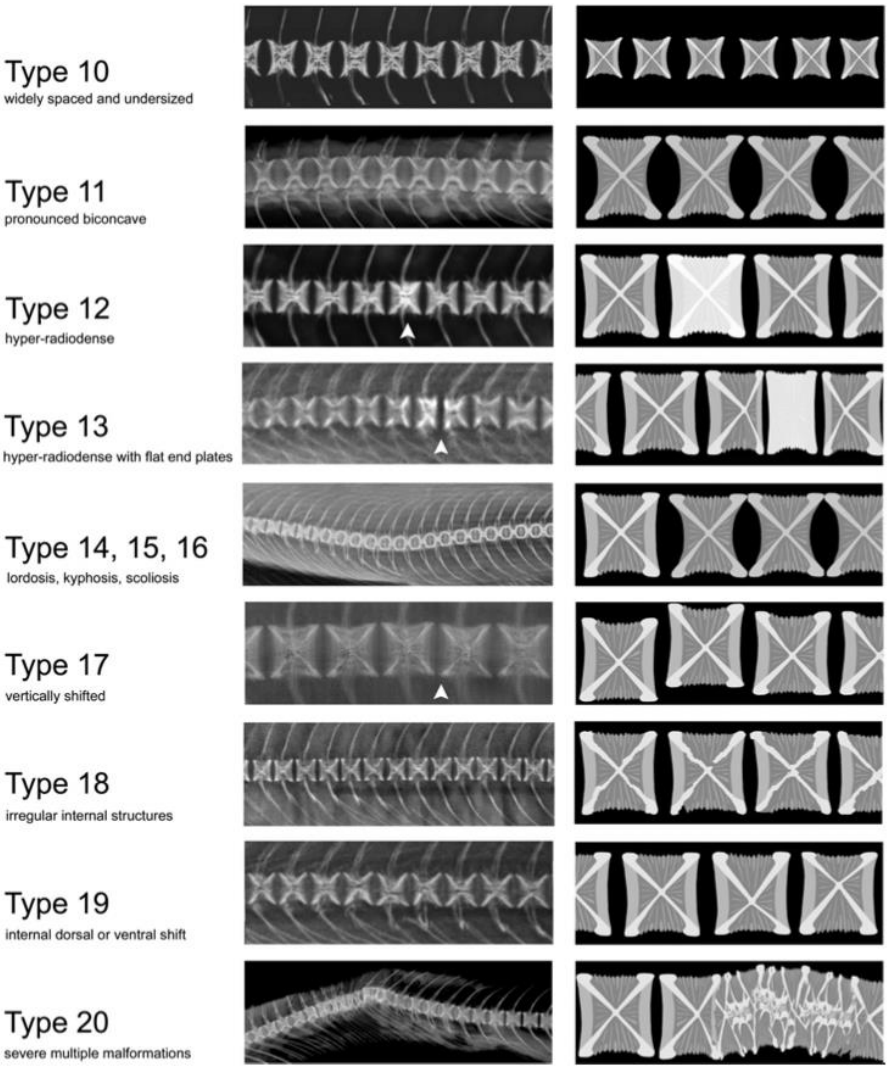

Fig. 3. Radiographs and schematic representations of vertebral body malformations in Atlantic salmon. Type 10—widely spaced and undersized. Small-sized vertebral bodies and widened intervertebral space. The dwarf-like size of the vertebral bodies and the appearance of widened intervertebral spaces can be an X-ray artefact, caused by the undermineralisation of vertebral bodies (commonly related to osteopenia). The width of the radiograph is equal to 56 mm. Type 11—pronounced biconcave. Biconcave vertebral bodies (commonly related to osteopenia). Notice that the analogue high resolution X-ray displays unmineralised bone tissue that would not be visualised by the digital X-ray (compare with the X-ray of Type 10). The width of the radiograph is equal to 48 mm. Type 12—hyper-radiodense (white arrowhead). Increased radiodensity of a single vertebral body. The deep notches that appear dorsally and ventrally on each of the non-affected vertebral bodies represent a digital X-ray artefact. The width of the radiograph is equal to 26 mm. Type 13—hyper-radiodense with flat end plates (white arrowhead). Increased radiodensity of a single vertebral body together with increased one-sided radiodensity of the adjacent vertebrae (has been observed to be related to heterotopic cartilage development in the bone marrow). The width of the radiograph is equal to 38 mm. Types 14– 16—lordosis, kyphosis, scoliosis. Lordotic (ventral spine curvature, Type 14) and kyphotic (dorsal spine curvature, Type 15) curvatures are easily recognised on lateral X-rays. We here show a scoliotic bending (lateral curvature), Type 16. Scoliosis may be visible on X-rays by the sudden transition from non-altered to pronounced biconcave vertebrae. This alteration is caused by the change of the angle between the bent spine and the X-ray beam (see description of X-ray artefacts). The width of the radiograph is equal to 36 mm. Type 17—vertically shifted (white arrowhead). Dorso-ventral shift of undeformed vertebral bodies. Dorso-ventral shifts are also observed connected to deformations of vertebral bodies, see, e.g., Type 3. The width of the radiograph is equal to 58 mm. Type 18—irregular internal structures. Various internal shape variations. No particular type of deformity can be assigned to this phenotype. At the same time, none of the vertebral bodies displays a symmetrical and smooth internal X-structure. The width of the radiograph is equal to 56 mm. Type 19—internal dorsal or ventral shift. The very central part of vertebral bodies is shifted with approximate preservation of the external shape. The width of the radiograph is equal to 24 mm. Type 20—severe multiple malformations. A combination of different pathologies that may also include vertebral body fractures. The width of the radiograph is equal to 96 mm.